



# VCU

Virginia Commonwealth University  
VCU Scholars Compass

---

Theses and Dissertations

Graduate School


---

2015

## Role of Extracytoplasmic RNA Polymerase Sigma 70 Factor, PG0214, in The Survival of *Porphyromonas gingivalis* and in Adaptation to Environmental Stress.

David M. Smith  
*Virginia Commonwealth University*

Follow this and additional works at: <https://scholarscompass.vcu.edu/etd>

 Part of the [Bacteriology Commons](#), [Microbial Physiology Commons](#), and the [Other Microbiology Commons](#)

© The Author

---

Downloaded from

<https://scholarscompass.vcu.edu/etd/4046>

This Thesis is brought to you for free and open access by the Graduate School at VCU Scholars Compass. It has been accepted for inclusion in Theses and Dissertations by an authorized administrator of VCU Scholars Compass. For more information, please contact [libcompass@vcu.edu](mailto:libcompass@vcu.edu).

©David Smith 2015

All Rights Reserved

Role of Extracytoplasmic RNA Polymerase Sigma 70 Factor, PG0214, in The Survival of  
*Porphyromonas gingivalis* and in Adaptation to Environmental Stress.

A thesis submitted in partial fulfillment of the requirements for the degree of Masters of  
Science in Physiology and Biophysics at Virginia Commonwealth University

By

DAVID SMITH

B.S. in Biology, Christopher Newport University, 2011

M.S. in Physiology and Biophysics, Virginia Commonwealth University, 2015

Director: **JANINA P. LEWIS**, Ph.D, Professor  
The Philips Institute for Oral Health Research, School of Dentistry, Virginia  
Commonwealth University

Virginia Commonwealth University  
Richmond, Virginia  
December 2015

## Acknowledgements

First of all, I would like to express my gratitude and appreciation to my faculty advisor, Dr. Janina Lewis. Thank you for all of the advice, training, and time that you have given me. Thank you for allowing me to work in your lab and for exposing me to the world of research. Your dedication to science and research is inspiring and working with you has been one of the most influential experiences I have ever had.

I would also like to thank my committee members Dr. Roland Pittman and Dr. Liya Qiao for their patience, guidance, and expertise throughout this project. Additional thanks to Dr. Ian Morgan, Dr. Todd Kitten, Dr. Andrew Yeudall, Dr. Myrna Serrano, and Mr. Rennie Berry for their instruction and use of their facilities and laboratory equipment.

Thank you to my colleagues for your time, advice, laughter, and support throughout my journey, especially Dr. Justin Hutcherson, Chris Wunsch, Ross Belvin, Nicaï Zollar, Chris Pham, and Kathryn Sinclair.

I would not be here without the love and support of my wonderful parents, Dr. Fred and Judy Smith. Your faith and encouragement is unmatched and I cannot thank you enough for everything you have done for me.

Finally I would like to thank my best friend and fiancée, Melissa Farmer. You are a testament to strength and perseverance and have been the inspiration for me to set and achieve my goals.

## List of Tables

Table 1. Functions of *Porphyromonas gingivalis* proteases.

Table 2: Bacterial strains used in this study.

Table 3. The Most Differentially Regulated Genes for W83 vs W83 + DP.

Table 4. DAVID Functional Annotation Clustering for W83 vs W83 + DP.

Table 5. The Most Differentially Regulated Genes for W83 vs W83 6%O<sub>2</sub>.

Table 6. DAVID Functional Annotation Clustering for W83 vs W83 6%O<sub>2</sub>.

Table 7. The Most Differentially Regulated Genes for 77 vs 77 + DP.

Table 8. DAVID Functional Annotation Clustering for 77 vs 77 + DP.

Table 9. The Most Differentially Regulated Genes for 77 vs 77 6%O<sub>2</sub>.

Table 10. DAVID Functional Annotation Clustering for 77 vs 77 6%O<sub>2</sub>.

Table 11. The Most Differentially Regulated Genes for W83 vs V0214.

Table 12. DAVID Functional Annotation Clustering for W83 vs V0214.

Table 13. The Most Differentially Regulated Genes for W83 + DP vs V0214 + DP.

Table 14. DAVID Functional Annotation Clustering for W83 + DP vs V0214 + DP.

Table 15. The Most Differentially Regulated Genes for W83 6%O<sub>2</sub> vs V0214 6%O<sub>2</sub>.

Table 16. DAVID Functional Annotation Clustering for W83 6%O<sub>2</sub> vs V0214 6%O<sub>2</sub>.

Table 17. The Most Differentially Regulated Genes for W83 + DP 6%O<sub>2</sub> vs V0214 + DP 6%O<sub>2</sub>.

## List of Figures

Figure 1. Biofilm formation and communication in the oral cavity.

Figure 2. Illustration of potential pathways by which *Porphyromonas gingivalis* invades and regulates gene expression of host cells.

Figure 3. Schematic representation of hemin uptake mechanisms present in *Porphyromonas gingivalis*.

Figure 4. Conserved regions of sigma factors.

Figure 5: Ovation Complete cDNA Library Generation Workflow.

Figure 6. Denaturing RNA gel for confirmation of RNA isolates.

Figure 7. Electropherogram results from bioanalyzer of cDNA from 5.26.15.

Figure 8. KEGG Ribosomal Pathway for W83 vs W83 + DP.

Figure 9. KEGG Ribosomal Pathway for W83 vs W83 6%O<sub>2</sub>.

Figure 10. KEGG Thiamine Metabolism Pathway for 77 vs 77 + DP.

Figure 11. KEGG Ribosomal Pathway for 77 vs 77 6%O<sub>2</sub>.

Figure 12. Characteristics of *Porphyromonas gingivalis* PG0214.

Figure 13. KEGG Ribosomal Pathway for W83 vs V0214.

Figure 14. KEGG Ubiquinone and Other Terpenoid-quinone Biosynthesis Pathway for W83 6%O<sub>2</sub> vs V0214 6%O<sub>2</sub>.

Figure 15. Protein Gel for Protease Assay.

Figure 16. Protein ID results for W83 and V0214 under normal and iron-deficient conditions.

Figure 17. Interaction of *P. gingivalis* W83 and V0214 Strains Into Eukaryotic Cells.

Figure 18. Invasion of *P. gingivalis* W83 and V0214 Strains Into Eukaryotic Cells.

Figure 19. Arginine Protease Activity Assay.

Figure 20. Arginine Protease Activity Assay, Iron-Stress.

Figure 21. Arginine Protease Activity Assay, Oxygen-Stress.

Figure 22. Arginine Protease Activity Assay, Iron- and Oxygen-Stress.

Figure 23. Lysine Protease Activity Assay.

Figure 24. Lysine Protease Activity Assay, Iron-Stress.

Figure 25. Lysine Protease Activity Assay, Oxygen-Stress.

Figure 26. Lysine Protease Activity Assay, Iron- and Oxygen-Stress

**List of Abbreviations**

A or $\alpha$	Alpha
$\beta$	Beta
$\mu$ l	Microliter
$\mu$ M	Micromolar
$^{\circ}$ C	Degree Celsius
$\sigma$	Sigma
BHI	Brain Heart Infusion
cDNA	Complementary DNA
CFU	Colony forming unit
CO <sub>2</sub>	Carbon dioxide
DNA	Deoxyribonucleic acid
DNase	Deoxyribonuclease
DP	2,2,-dipyridyl
ECF	Extracytoplasmic function
ES	Enrichment Score
HUVEC	Human umbilical endothelial cells
LPS	Lipopolysaccharide
mL	Milliliter
MOI	Multiplicity of infection
OD	Optical density
PBS	Phosphate-buffered saline



<i>P. gingivalis</i> or <i>Pg</i>	<i>Porphyromonas gingivalis</i>
RNA	Ribonucleic acid
RPKM	Reads by kilobase per million
S1	V0214, PG0214-deficient mutant strain
SDS	Sodium dodecyl sulfate
TLR	Toll-like receptor
TNF	Tumor-necrosis factor
VCU	Virginia Commonwealth University
V0214	PG0214-deficient mutant strain
W77 or 77	Wild-type, nonencapsulated strain of <i>Pg</i>
W83	Wild-type strain of <i>Pg</i>
WT	Wild-type
UV	Ultraviolet

## Table of Contents

		Page
	Acknowledgements	3
	List of Tables	4
	List of Figures	5
	List of Abbreviations	7
	Abstract	11
Chapter		
1	Introduction	13
1.1	Periodontal Disease	13
1.1.1	General	13
1.1.2	Initiation and Progression	13
1.1.3	Prevention and Treatment	18
1.2	<i>Porphyromonas gingivalis</i>	19
1.2.1	Virulence Mechanisms of <i>P.g.</i>	24
1.2.2	Virulence Factors of <i>P.g.</i>	24
1.2.2.1	Fimbriae	25
1.2.2.2	Gingipain Proteases	26
1.2.2.3	Lipopolysaccharides	29
1.2.2.4	Capsular Polysaccharides	30
1.2.2.5	Hemagglutinins	30
1.2.3	Importance of Metals	31
1.2.3.1	Iron	31
1.2.3.2	Iron Regulation and Uptake	32
1.2.4	Role of Oxygen/ Oxidative Stress Mechanism	34
1.2.5	Sigma Factors and Their Significance	35
1.2.5.2	RNA Polymerase (RNAP)	35
1.2.5.3	Extracytoplasmic Function Sigma Factors (ECF- $\sigma$ )	36
1.2.6	Regulation of Activity of ECF Sigma Factors	38
1.2.7	ECF Sigma Factors of <i>P. gingivalis</i>	38
1.2.8	Genes of Interest	39
2	Hypothesis and Aims	40
2.1	Hypothesis	40
2.2	Research Objective and Aims	40
3	Materials and Methods	42
3.1	Bacterial Strains	42
3.2	Media Growth Conditions	42
3.2.1	<i>Porphyromonas gingivalis</i>	42
3.2.2	Endothelial Cells	43
3.3	Cell Culture Preparation	43

3.3.1	<i>Porphyromonas gingivalis</i>	43
3.3.2	Endothelial Cells	44
3.4	RNA Sequencing and Library Generation	45
3.4.1	Transcriptome Preparation	45
3.4.2	RNA Isolation	45
3.4.3	Denaturing RNA Gel	47
3.4.4	Library Generation	58
3.5	Proteomics	51
3.5.1	Proteome Preparation	51
3.5.2	Tryptic Digestion	52
3.6	Antibiotic Resistance Assay	53
3.6.1	Endothelial Cell Preparation	53
3.6.2	Bacterial Culture Preparation	53
3.6.2	Infection	54
3.6.3	Interaction	54
3.6.4	Invasion	55
3.7	Protease Activity Assay	56
3.7.1	Arg-X Activity Assay	57
3.7.2	Lys-X Activity Assay	57
4	Results	59
4.1	RNA Sequencing	59
4.1.1	RNA Isolation	59
4.1.2	RNA Library Generation	61
4.1.2.1	Validation of cDNA Library	61
4.1.3	RNA Sequencing of RNA Libraries	63
4.1.4	Statistical Analysis	63
4.2	Bioinformatic Characterization of <i>P. gingivalis</i> V0214	100
4.2.1	Statistical Analysis of Transcriptome of V0214	102
4.3	Proteomics	131
4.4	Interaction and Invasion of <i>P. gingivalis</i> with Eukaryotic Cells	135
4.5	Arg-X and Lys-X Protease Activity	140
5	Discussion	150
	Conclusion	161
	Literature Cited	163

## Abstract

### **Role of Extracytoplasmic RNA Polymerase Sigma 70 Factor, PG0214, in The Survival of *Porphyromonas gingivalis* and in Adaptation to Environmental Stress.**

A thesis submitted in partial fulfillment of the requirements for the degree of Masters of Science in Physiology and Biophysics at Virginia Commonwealth University

By David Smith, MS

Virginia Commonwealth University, 2015

Major Director: Janina P. Lewis, Ph.D., Professor

The Philips Institute for Oral Health Research, School of Dentistry, Virginia Commonwealth University

*Porphyromonas gingivalis*, a gram-negative anaerobic, pathogenic bacterium is a major etiological agent in the initiation and progression of periodontal disease. Due to the ever-changing environment of the oral cavity, inhabitants like *Porphyromonas gingivalis* must possess the ability to adapt to changes in environmental conditions like pH, temperature, oxygen tension, and metal concentration. *P. gingivalis* should therefore have an efficient regulatory system in order to adapt and survive in the oral cavity. This response adaptation occurs at the transcriptional level, which involves alternative sigma factors. Extracytoplasmic function sigma (ECF- $\sigma$ ) factors are the largest group of alternative sigma factors that play a role in the bacterial response to environmental stress

conditions. Here we analyze the  $\sigma$ -70 factor gene, PG0214, an extracytoplasmic function sigma factor encoded in the *P. gingivalis* genome, and examine its role in the bacterial response to environmental stress and virulence.

Our results show similar findings to recent studies on the effect of oxidative- and iron-stress on *Porphyromonas gingivalis* (Lewis *et al.* 2009 and Anaya-Bergman *et al.* 2015). Our findings indicate that the PG0214 gene is important in regulating major functional gene groups and pathways in the *P. gingivalis* genome. Strains deficient in the PG0214 gene were analyzed and shown to have decreased protease activity, as well as reduced survivability and invasion rates in eukaryotic host cells when compared against wild-type W83 and ATCC 33277 strains.

Several biostatistical and molecular biology techniques were learned and used for this study including proteomic studies, antibiotic protection assays, protease assays, RNA isolation and sequencing, bioinformatics analysis, functional gene clustering, and gene pathway generation. Using these techniques we were able to learn the tools necessary to identify the biological function of a bacterial gene. Collectively our studies demonstrate that the PG0214 gene is a positive regulator of gene expression for the survival and virulence of *P. gingivalis* in the presence of oxidative- and iron-stress, although further study is needed to fully characterize the gene and determine its specific function.

## **CHAPTER 1: INTRODUCTION**

### **1.1 Periodontal Disease**

#### **1.1.1 General**

The oral cavity is an ever-changing environment that is host to a myriad of oral flora. The microbes work in concert to protect and support homeostasis in the oral environment. When the ecological balance between host and bacteria is disturbed, a healthy mouth can quickly turn to a diseased state resulting in various forms of periodontal disease.

Periodontal disease is a bacterially induced, chronic, inflammatory disease that affects the gingiva and the supporting structures of the periodontium. It can range in severity from reversible redness and inflammation of gingival tissue to bone resorption and eventual exfoliation of teeth, and is the most common cause of tooth loss worldwide (Darveau, 1997). Periodontal disease affects over 743 million people worldwide and approximately 47% of those surveyed in a recent national health and nutrition survey exhibited some form of the disease, although only approximately 10% exhibited the more severe forms (Kassebaum et al., 2014 and Eke et al., 2012). While not typically fatal, periodontal disease is a great cause for concern as it can reduce the quality of life for afflicted patients and has been shown to have associations with systemic diseases such as diabetes, coronary heart disease, and cardiovascular disease (Seymour et al., 2007).

#### **1.1.2 Initiation and Progression**

While each person hosts their own unique compilation, over 700 different bacterial species can be found in the oral cavity (Aruni et al., 2015 and Moore et al.,

1994). In a healthy mouth these bacteria adhere to and associate with one another in what is known as a biofilm. Each bacterium in the biofilm has a unique role ranging from communication and attachment to protection and nutrient uptake, but each works to promote the survival of the community as a whole (Stoodly et al., 2002). These biofilms serve as a first line of defense for the oral environment and promote environmental homeostasis. Biofilm development starts with the attachment of early colonizers such as *Actinomyces* species and oral streptococci on the acquired pellicle and on tooth enamel. As illustrated in figure 1, these bacteria not only adhere to tooth surface but also interact with each other laying a foundation for attachment of bridging colonizers such as *Fusobacterium nucleatum* followed by late colonizers including the red complex species which will be discussed later (Aruni et al., 2015). The tooth pellicle consists of proteins and glycoproteins found in saliva and gingival crevicular fluid and once attached, bacterial biofilms form what has been termed dental plaque (Darveau et al., 1997). Dental plaque is often helpful for the host by colonizing tooth surfaces thus preventing colonization of periopathogens and other harmful species. In a healthy mouth bacterial composition remains relatively stable despite regular exposure to environmental perturbations and changes. This stability is largely due to the homeostatic nature of the microbial interactions and the equilibrium they provide with the innate host defense system.

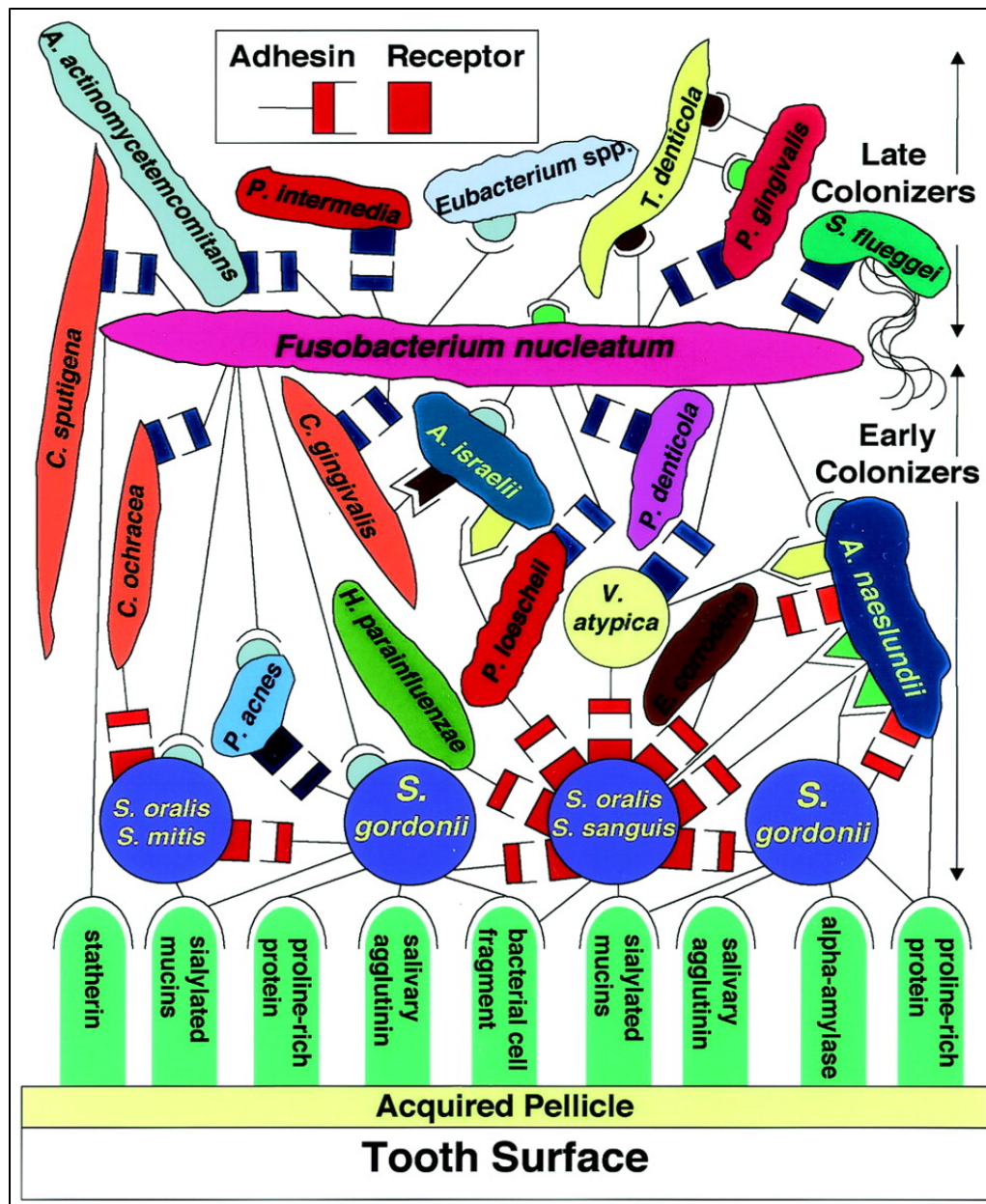


**Figure 1. Biofilm formation and communication in the oral cavity.**

This figure depicts the coaggregation and communication among early and late colonizing bacteria in the oral cavity. Used with permission from Kolenbrander et al. 2002. Communication among Oral Bacteria. *Microbiology and Molecular Biology Reviews*. 66(3):486-505.



Homeostasis can, however break down due to a variety of reasons, leading to shifts in the balance of the microflora, thereby predisposing sites to disease. As the biofilm progresses from supragingival sites to subgingival sites, the environment changes from aerobic to anaerobic creating a new environmental niche for bacteria (Aruni et al., 2015). Periodontal disease has been characterized as a 'microbial-shift disease' meaning a shift from healthy numbers of certain bacteria to an unhealthy population can initiate the disease (Darveau, R., 2010). Studies have shown that during disease progression the subgingival microflora shifts from being mainly Gram-positive to being comprised of increased levels of obligately anaerobic, asaccharolytic Gram-negative organisms (Marsh, P., 1994). These Gram-negatives proliferate in dental plaques leading to inflammation and host response increasing the flow of gingival crevicular fluid. This increase in GCF secretion changes the nutrient profile of the gingival crevice and can lower the redox potential of the site as well as raise the pH, further enriching the environment for obligately anaerobic and asaccharolytic Gram-negative bacteria (Marsh, P., 1994).

During the transition from a healthy site to gingivitis, the chronic inflammation of the gingiva and surrounding tissue, the bacterial load has been shown to shift from a relatively low state ( $10^2$ - $10^3$  isolates) comprised of about 15% Gram-negative rod shaped bacteria to much higher microbial load ( $10^4$ - $10^5$  organisms) of which 15-50% are Gram-negative (Darveau et al., 1997). As the microbial load increases, space in the sub-gingival region becomes increasingly scarce, and bacterial growth occurs apically between the

tooth surface and gingival epithelium, further separating the two leading to tissue damage and bleeding. This deeper subgingival environment, referred to as the periodontal pocket, provides a gradient of environmental conditions including variable concentrations of oxygen, pH, and temperature (Tribble et al., 2013). The deeper regions of the pocket are rich in blood and serum protein, low in oxygen, and have a more stable pH providing ideal conditions for the growth of obligate anaerobes while restricting the growth of the early Gram-positive facultative aerobes (Tribble et al., 2013 and Aruni et al., 2015).

As the disease progresses from the moderate gingivitis to periodontitis, the total microbial load further increases ( $10^5$ - $10^6$ ) and an increase in Gram-negative bacterium is again seen. A study involving subjects with abundant plaque found that elevated levels of a particular pathogen, *Porphyromonas gingivalis*, markedly differentiated periodontitis from gingivitis (Dahlen et al., 1992). While the cause of periodontitis cannot be confined to a single pathogen, three Gram-negative bacterial species – *Porphyromonas gingivalis*, *Tannerella forsythia*, and *Treponema denticola* - termed the “red complex”, have been identified as strongly associated with one another and as potential causative agents for the disease (Socransky et al., 1998). These bacteria tend to be more virulent and can proliferate in higher number further promoting disbiosis in the oral cavity. Once pathogenic colonization has occurred in the subgingival region, select organisms, including *P. gingivalis* shed from the biofilm and interact with host epithelial cells followed by host cell invasion. *P. gingivalis* and other red complex pathogens have a unique ability to inhibit host defense functions and suppress the immune system by inhibiting or degrading constitutive IL-8 secretion through various mechanisms and by production of a lipid A structure that acts as a TLR4 antagonist in the host cell (Ji et al.,

2007 and Coats et al., 2007). These pathogens employ a variety of virulence factors that can degrade host tissues and promote bacterial survival (Jandik et al., 2008).

Ultimately the more virulent bacteria invade host cells. Invasion is followed by host tissue destruction and bone resorption. This is known as severe periodontitis and is not easily reversed. If left untreated, this level of disease results in sepsis, tooth loss, and other medical complications.

### **1.1.3 Prevention and Treatment**

Prevention of periodontal disease starts with proper diet, lifestyle, and oral hygiene consisting of regular brushing and flossing. The physical removal of bacteria from the teeth and gums can help to prevent bacterial biofilms from residing on surfaces long enough to have a disbiotic microbial shift. Additionally, antimicrobial agents such as chlorhexidine mouthwash have been shown to assist mechanical modes of cleaning by absorption into the pellicle-coated enamel surface thus inhibiting plaque formation (Jenkins et al., 1998). Fluoride treatments have also showed promise due to their ability to increase resistance of enamel to demineralization and to promote remineralization. These preventative measures are crucial for the prevention of all oral diseases ranging from minor dental caries and cavities to gingivitis, and periodontitis.

The goal of periodontal treatment is to restore the homeostatic relationship between periodontal tissue and its polymicrobial dental-plaque community. The most effective and most widely used treatment is physical removal of the pathogenic dental-plaque biofilm via scaling and root planing by a periodontist (Darveau R., 2010).

Following treatment, the homeostatic relationship is restored through commensal microbial recolonization and tissue healing. Periodontists check clinical attachment levels, bleeding upon probing, and pocket depth to determine disease progression and regression. In conjunction with antibiotics and anti-inflammatory agents, regular clinical visits have shown promise in the treatment and improvement of the disease. In more severe cases, gum and tooth surgeries may be required but are typically followed with the clinical treatments mentioned above.

### ***1.2 Porphyromonas gingivalis***

*Porphyromonas gingivalis* is a non-motile, Gram-negative, rod-shaped, oral bacterium that forms black colonies on blood agar plates. It requires anaerobic conditions for growth and sustains itself by feeding on heme and vitamin K found in the saliva, blood, and gingival crevicular fluid. Metabolically, it gains energy by fermenting and/or breaking down amino acids and peptides rather than sugars. This is critical for survival of the asaccharolytic and proteolytic bacterium as sugars are scarce in deep periodontal pockets. It is a pathogenic bacterium and is identified as a major etiological agent for the initiation and progression of periodontal disease, where it is found in up to 85% of diseased sites (Yang et al., 2004). *P. gingivalis* is predominantly located in the oral cavity but has also been observed in the respiratory tract, gastrointestinal tract, and colon. It is an excellent model organism, has a well-characterized population structure and is the easiest of the 3 red complex bacteria to grow and genetically manipulate, subsequently making it the most well-studied pathogen in the oral microbiome (Darveau et al., 2012).

*P. gingivalis* is known as a keystone species, meaning it has a disproportionately large effect on the oral community, even in low numbers. It has been further characterized as a keystone pathogen because of its ability to remain quiescent for long periods of time before expressing pathogenicity, thus disrupting host-microbe homeostasis via molecular manipulation of select host protective mechanisms, ultimately leading to disease (Hajishengallis et al., 2011). *P. gingivalis* colonization elevates the virulence of the entire biofilm community following interactive communication with accessory pathogens. Initially, the host immune surveillance is impaired allowing the disbiotic bacterial community to increase in number. This is followed by the community proteoactively inducing inflammation to sustain itself with derived nutrients which gives rise to an inflammophilic community (Hajishengallis and Lamont, 2014). While *P. gingivalis* is not the only pathogenic bacterium at play in periodontal disease, the timing, location, and context of immune suppression has a major significance in the progression of the inflammatory disease.

*P. gingivalis* invades the periodontal pockets and colonizes in gingival crevices and the sub-gingival region. As a late colonizer, *P. gingivalis* adheres to many early plaque colonizers such as those in the oral streptococci family and *Actinomyces naeshundii* as well as later colonizers such as *Fusobacterium nucleatum*, *Treponema denticola*, and *Bacteriodes forsythus*. These attachments lead to interactions via fimbriae and outer membrane proteins that not only favor colonization, but also promote nutritional interrelationships and intercellular signaling mechanisms (Lamont and Jenkinson, 1998). During initial colonization of the subgingival area, *P. gingivalis* persists by disabling innate and adaptive immunity by its ability to degrade human

defensins, its resistance to oxidative burst-killing by polymorphonuclear neutrophils (PMNs), and its ability to inhibit the production of proinflammatory cytokines (Bostanci and Belibasakis, 2012). *P. gingivalis* also possesses the somewhat paradoxical ability to stimulate or inhibit interleukin (IL)-8 production, a major proinflammatory cytokine. This allows the bacterium to essentially control the immune response at will and during inhibition of IL-8, PMN chemotaxis is hindered resulting in a phenomenon known as ‘chemokine paralysis’ (Darveau et al., 1998).

The reduced immune surveillance begins to benefit the entire biofilm community resulting in local overgrowth of organisms that overwhelms the structural integrity of the tissues leading to inflammation and bleeding. Destruction of the tissues releases peptides and heme-containing compounds, which stimulate the growth of *P. gingivalis* (Hajishengallis and Lamont, 2014). This is a favorable environment for the proteolytic bacterium, which leads to increased proliferation followed by host cell invasion.

*P. gingivalis* has the unique ability to invade gingival epithelial cells where it can maintain viability and replicate thus evading immune surveillance by the host (Bostanci and Belibasakis, 2012). One proposed mechanism of *P. gingivalis* invasion is its fimbrial interaction with gingival epithelial cell B1 integrin receptors (Lamont and Yilmaz, 2002). This interaction, illustrated in figure 3, leads to the engulfment of the bacterial cells. *P. gingivalis* has also been shown to secrete novel proteins when in close proximity to epithelial cells (Lamont and Jenkinson, 2000). While the mechanism is not fully understood, it is hypothesized that these proteins may induce bacterial uptake by the host cells.

Once inside the host cell *P. gingivalis* actively secretes an ATP-hydrolyzing enzyme that suppresses ATP-dependent apoptosis of the host cell. *P. gingivalis* invasion also induces the release of  $\text{Ca}^{2+}$  ions from intracellular stores and phosphorylation of MAP-kinase family proteins which down-regulates interleukin-8 (IL-8) secretion and apoptotic proteins (Lamont and Yilmaz, 2002). This coupled with its ability to disseminate from cell to cell via actin cytoskeleton bridges without causing cell death allows the bacteria to spread and thrive without triggering immune surveillance and response (Yilmaz et al., 2008). Once it is established in the cell, *P. gingivalis* employs a variety of virulence mechanisms to further progress the disease.

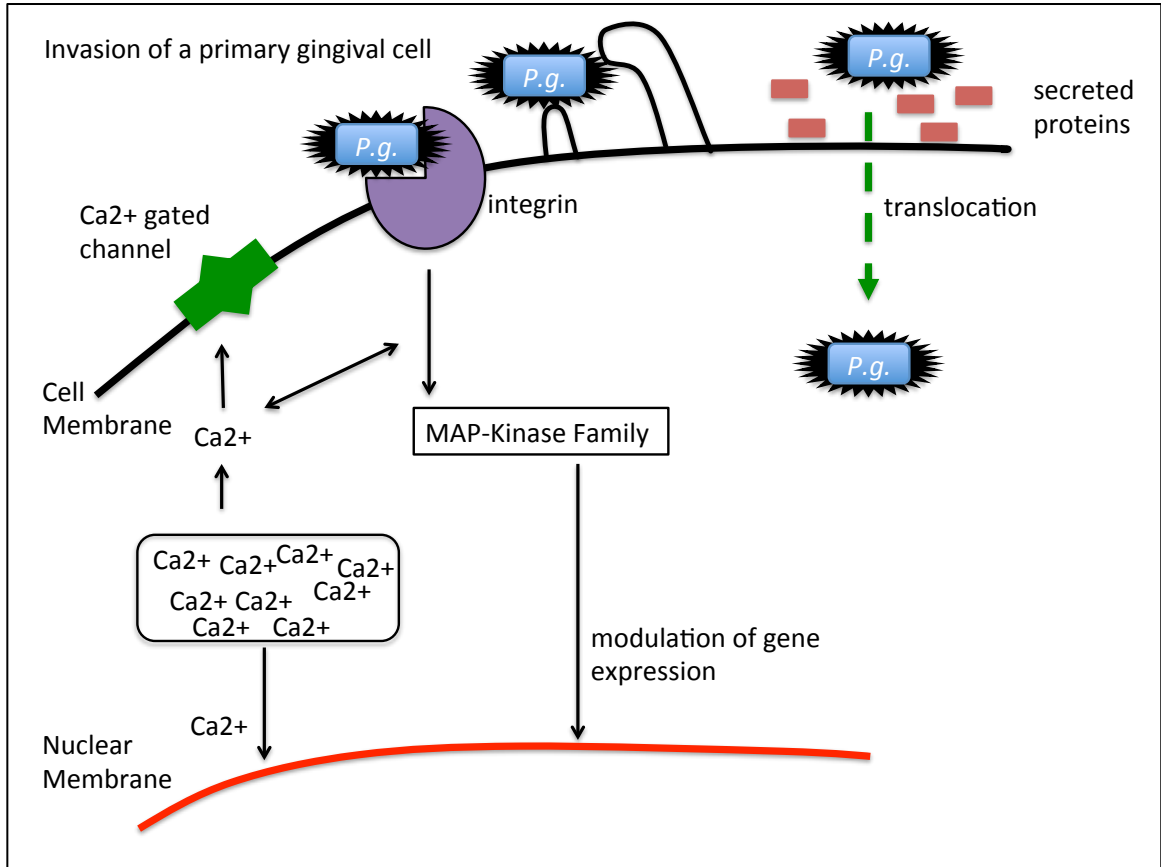


**Figure 2. Illustration of potential pathways by which *P. gingivalis* invades and regulates gene expression of host cells.** Adapted with permission from Lamont RJ and Jenkinson HF. 1998. Life Below The Gum Line: Pathogenic Mechanisms of *Porphyromonas gingivalis*. *Microbiology and Molecular Biology Reviews*. 62(4): 1244-1263.



### **1.2.1 Virulence Mechanisms of *Porphyromonas gingivalis***

Long-term survival of *P. gingivalis* requires the bacteria to successfully evade the host immune response. In addition, *P. gingivalis* must simultaneously adapt to the changing physiology of the host and to alterations in the plaque biofilm (Tribble et al., 2013). Different regions of the oral cavity provide a gradient of environments, each of which can quickly and constantly change. Temperature, pH, nutrient concentration, and oxygen tension can vary greatly between areas in the mouth that bacteria inhabit (Dou et al., 2010). In reflection of this highly variable niche, *P. gingivalis* has adapted a set of highly evolved virulence mechanisms that allow it to survive and thrive. *P. gingivalis* is a highly diverse species that has perfected adaptive self-modifications in genetic content in response to environmental variations. Differential gene expression at the level of transcription initiation is the main mode of environmental adaptation in *P. gingivalis*. These modification methods not only aid *P. gingivalis* in survival, but also have been shown to improve its virulence and pathogenic potential.

### **1.2.2 Virulence Factors of *Porphyromonas gingivalis***

As an opportunistic pathogen, *P. gingivalis* is host to an arsenal of various virulence factors. Many of these ‘weapons of survival’ assist in colonization of and immune disruption of the host, while others are important in communication, nutrient uptake, cell proliferation, and tissue destruction. The main virulence factors used by *P. gingivalis* are fimbriae, gingipain proteases, lipopolysaccharides, exopolysaccharides, and hemagglutinins.

### 1.2.2.1 Fimbriae

Like many other gram-negative bacteria *P. gingivalis* possesses numerous, thin, straight appendages protruding from the cell surface. These structures are referred to as fimbriae due to their hair-like, thin stranded character (Holt et al., 2007). The fimbriae facilitate *P. gingivalis*' adherence to salivary proteins, extracellular matrix, eukaryotic cells, and bacteria of the same or different species (Bostanci and Belibasakis, 2012). This adherence ability is critical for the attachment to early colonizing bacteria, allowing *P. gingivalis* to participate in the development of the biofilm. There are two types of fimbriae found on *P. gingivalis* and are referred to as major and minor fimbriae. Major fimbriae are longer and are composed of a fimbrillin monomer subunit that varies in size between 41-49 kDa depending on the strain (Lamont and Jenkinson, 1998). Minor fimbriae are composed of a 67 kDa protein that is antigenically distinct from the fimbrillin, called *mfa1* (Lamont and Jenkinson, 1998). The gene that codes for fimbrillin is *fimA* and it can be found in on the chromosome in a single copy in all fimbrial strains of *P. gingivalis*. Major fimbriae are found have roles in colonization and invasion while minor fimbriae work more in a proinflammatory capacity (Lamont and Jenkinson, 1998). Fimbriae have also been shown to be involved in periodontal bone loss. An animal study using a *fimA*-knockout strain of *P. gingivalis* resulted in markedly reduced bone loss in the gnotobiotic rats infected with the knockout when compared to those infected with the wild-type strain (Evans et al., 1992). Fimbriae also have the ability to directly induce signaling through TLR2 and TLR4 host pathways that can mediate production of proinflammatory cytokines like IL-6 and TNF- $\alpha$  as well as mediate the expression of cell adhesion molecules such as ICAM-1 (Bostanci and Belibasakis, 2012). Major fimbriae

can also exploit TLR2 signaling in order to interact with complement receptor 3 in a novel ‘inside-out’ signaling pattern. This activates the binding capacity of CR3 and allows for internalization of *P. gingivalis* into macrophages as well as reducing IL-12 production, which collectively allows *P. gingivalis* to avoid bacteria clearance (Wang et al., 2007).

#### 1.2.2.2 Gingipain Proteases

*P. gingivalis* is an asaccharolytic bacterium that secretes a variety of cysteine proteases primarily to break down erythrocytes providing peptides and heme for growth. These cell surface proteases are referred to as gingipains and account for 85% of the total proteolytic activity of *P. gingivalis* (Potempa and Travis, 1997). Gingipains are characterized based on their substrate specificity and have been divided into arginine-specific (Arg-X) and lysine-specific (Lys-X) gingipains. The Arg-X group of gingipains have trypsin-like activity and degrade extracellular matrix components including integrin-fibronectin binding, cytokines, immunoglobulins and complement factors. This group is further broken down into two types of gingipains: RgpA and RgpB. Both types are encoded by the *rgp* gene and contain proteolytic domains while RgpA also contains an adhesion domain. There is only one type of Lys-X gingipain, known as Kgp, which contains an adhesion and proteolytic domain and is encoded by *kgp* (Lewis et al., 1999).

Gingipains have a variety of functions in the survival and virulence of *P. gingivalis* including adherence to and colonization of epithelial cells, haemagglutination and hemolysis of erythrocytes, disruption and manipulation of the inflammatory response, and degradation of host proteins and tissues (Li and Collyer,

2011). Additional functions of *P. gingivalis* gingipain proteases are summarized in Table 1.

**Table 1. Functions of *Porphyromonas gingivalis* proteases.** Adapted with permission from Lamont RJ and Jenkinson HF. 1998. Life Below The Gum Line: Pathogenic Mechanisms of *Porphyromonas gingivalis*. *Microbiology and Molecular Biology Reviews*. 62(4): 1244-1263.

<b>Impairment of tissue integrity</b>	<b>Perturbation of host defenses</b>	<b>Bacterial function</b>
Degradation of extracellular matrix proteins (fibronectin, laminin)	Degradation of immunoglobulins	Release of hemin and iron from host proteins
Hydrolysis of collagens I, III, IV, and V	Inactivation or activation of complement components	Exposure of host and bacterial cryptitopes
Degradation of fibrinogen	Destruction of cytokines and chemokines	Posttranslational processing of proteases, fimbriin, and outer membrane proteins
Inactivation of tissue and plasma protease inhibitors	Cleavage of leukocyte surface receptors	Involvement in intracellular invasion
Activation of MMPs and the kallikrein/kinin cascade	Degradation of antimicrobial peptides	

### 1.2.2.3 Lipopolysaccharides

All Gram-negative bacterial species, including *P. gingivalis* are sheathed by a lipopolysaccharide (LPS), which is an outer membrane component of the bacteria. LPS is a large molecule consisting of a lipid and a polysaccharide composed of O-antigen, outer core and inner core joined by a covalent bond. The LPS is recognized by the host and can trigger intracellular signaling events. The *P. gingivalis* LPS has been shown in experimental animal models as a stimulator of proinflammatory responses and bone resorption (Nishida et al., 2001). It also can release prostaglandin E<sub>2</sub> and stimulates proinflammatory cytokine production of IL-1 $\alpha$ , IL-1 $\beta$ , IL-6, IL-8, IL-18m and TNF- $\alpha$ , *in vivo* (Bostanci and Belibasakis, 2012). These compounds are potent local mediators of bone resorption and can inhibit collagen synthesis by osteoblasts and induce the production of MMPs that destroy connective tissue and bone (Lamont and Jenkinson, 1998). Structurally, the LPS of *P. gingivalis* differs from other species and even among strains in its O-antigen and lipid A component. The lipid A in most Gram-negative species is a strong activator of TLR4, but in *P. gingivalis* it has been shown to predominately activate TLR2 and may even act as a TLR4 antagonist, thus dampening the immune response (Darveau et al., 2004). The lipid A acylation patterns can be found in two forms: the tetra-acylated and penta-acylated forms. The penta-acylated lipid A acts as a TLR4 agonist while the tetra-acylated lipid A is a TLR4 antagonist (Darveau et al., 2004). These forms elicit opposing host immune responses and are dependent on microenvironmental conditions, namely hemin availability. By modifying its lipid A structure based on environmental conditions, *P. gingivalis* may modulate the binding

affinity of its LPS to the host TLR receptors, thus selecting how to affect downstream host immune signaling (Bostanci and Belibasakis, 2012).

#### **1.2.2.4 Capsular Polysaccharides (CPS)**

*P. gingivalis* exhibits an array of differences between strains. One major difference is the presence or lack of a capsular polysaccharide (CPS), also known as a K-antigen, external to the outer membrane. The protective capsule is a major defensive trait for most strains of the bacterium and can be found as either an amorphous or a fibrous layer (Lamont and Jenkinson, 1998). Encapsulated strains of *P. gingivalis* are more resistant to phagocytosis by polymorphonuclear leukocytes and have been shown to be highly invasive, causing spreading infection in a murine model versus only local abscesses caused by nonencapsulated strains (Sundqvist et al., 1991 and Laine and van Winkelhoff, 1998). Differences in the CPS serotypes can result in differential capacities in chemokine stimulation by macrophages and cytokine expression in dendritic cells (d'Empaire et al., 2006 and Vernal et al., 2009). While the association between the presence of a capsule and the virulence of the strain is highly debated, it is apparent that the capsule is a useful component of the cell surface providing protection from host defenses.

#### **1.2.2.5 Hemagglutinins**

Hemagglutinins are proteins that, when expressed, may promote colonization by mediating the binding of bacteria to receptors on human erythrocytes. Since *P. gingivalis* utilizes heme for growth, binding of bacterial cells to erythrocytes may also serve a

nutritional function as hemolysis provides the essential nutrients hemin and vitamin K (Lepine and Progulske-Fox, 1996). *P. gingivalis* produces at least 5 known hemagglutinating molecules encoded by the *hagA*, *hagB*, *hagC*, *hagD*, and *hagE* genes. Hemagglutinin activities have been linked to other factors in *P. gingivalis* including LPS and lipid on the cell surface and the hemagglutinins encoded by *hagA*, *hagD*, and *hagE* possess a 90% sequence similarity to RgpA family of cysteine proteases (Lamont and Jenkinson, 1998).

### 1.2.3 Importance of Metals

#### 1.2.3.1 Iron

Iron is an essential nutrient for almost all living organisms. It is a particularly important factor in the growth, virulence, and survival of gram-negative bacteria like *P. gingivalis*. Free iron is found in low abundance in the oral cavity, forcing *P. gingivalis* and other bacteria to acquire it in the form of hemin. Hemin can be acquired by proteolytic processing from a number of host iron-binding proteins and compounds (Lamont and Jenkinson, 1998). *P. gingivalis* gets its black pigmentation from storing hemin on its cell surface. Iron has the ability to be readily oxidized and reduced, and when free, can catalyze the conversion of hydrogen peroxides to harmful free radicals (Lewis, J., 2011). This reaction is known as the Fenton reaction:





These free radicals can lead to oxidative stress in *P. gingivalis*. Therefore free iron must be readily acquired and stored by the bacteria's iron regulation and uptake mechanisms.

### 1.2.3.2 Iron Regulation and Uptake

*P. gingivalis* acquires iron through a variety of iron-binding proteins of host cells. It does so by binding heme acquired by proteolytic processing of host compounds like hemoglobin, haptoglobin, myoglobin, hemopexin, mathemoglobin, oxyhemoglobin, albumin, lactoperoxidase, catalase, and cytochrome c (Lamont and Jenkinson, 1998). Nonheme sources of iron such as ferric, ferrous, and inorganic iron, as well as transferrin and lactoferrin can also support *P. gingivalis* growth (Bromanti and Holt, 1991 and Tazaki et al., 1995). Once the heme/ iron is released from the host proteins with the help of gingipains and hemagglutinins, *P. gingivalis* utilizes several gene clusters that have been shown to uptake heme. The first locus is termed *ihABCDEF*, is composed of five open reading frames, and is used for iron-heme transport (Dashper et al., 2000). The other loci are designated *tlr* or TonB-linked receptor and *hmu*, both of which are directly involved in heme uptake (Slakeski et al., 2000 and Lewis et al., 2006). These mechanisms are summarized in figure 4.

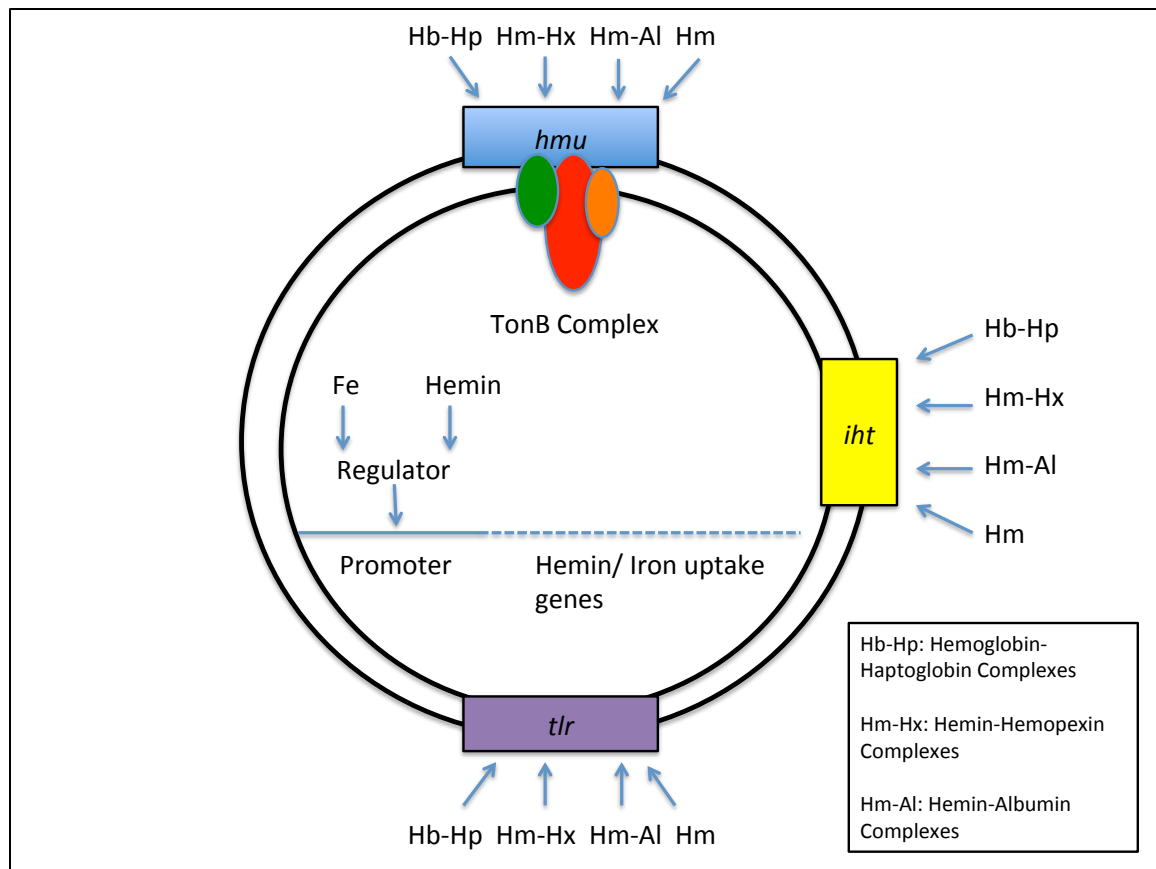


**Figure 3. Schematic representation of heme uptake mechanisms present in *Porphyromonas gingivalis*.** Adapted with permission from Lewis, J.P. 2010. Metal uptake in host-pathogen interactions: Role of iron in *Porphyromonas gingivalis* interactions with host organisms. *Periodontology* 2000. (52) 94-116.

#### 1.2.4 Role of Oxygen/ Oxidative Stress Mechanism

While *P. gingivalis* is an obligate anaerobe, it has developed a mechanism of aerotolerance that allows it to protect itself against oxidative stress. Pro-oxidants, or reactive oxygen species (ROS), such as the superoxide radical ( $O_2^-$ ), hydroxyl radical ( $HO^\cdot$ ), and hydrogen peroxide ( $H_2O_2$ ) are a significant threat to cellular integrity causing damage to proteins, lipids, RNA, and DNA (Strand et al., 2010). Although *P. gingivalis* typically resides in anaerobic periodontal pockets, it is still exposed to atmospheric oxygen and intracellular ROS. In order to survive in this oxidatively stressed environment, *P. gingivalis* has had to develop efficient oxidative stress protection mechanisms. Several genes involved in oxidative stress protection have been identified in *P. gingivalis*; *rprT*, *ahpC-F*, *bcp*, *tpx*, and *dps* (Henry et al., 2012). Many of these genes and enzymes are regulated by or dependent on the redox-sensitive protein OxyR. *P. gingivalis* also possesses the *sod* gene encoding Fe/Mn-containing SOD, which contributes to the relatively high aerotolerance of the bacterium, and is also under OxyR control (Ohara et al., 2006). While OxyR plays an important role in oxidative stress protection, it is not the sole regulator of genes involved in oxidative stress resistance. Extracytoplasmic function (ECF)- $\sigma$  factors have also been shown to play a role in oxidative stress resistance by modulating the virulence potential of the organism.

## 1.2.5 Sigma Factors and Their Significance

### 1.2.5.2 RNA Polymerase (RNAP)

RNA Polymerase (RNAP) is an enzyme responsible for producing primary transcript RNA. The bacterial core RNA polymerase complex consists of five subunits;  $\beta$ -subunit,  $\beta'$ -subunit,  $\alpha^I$ -subunit,  $\alpha^{II}$ -subunit, and  $\omega$ -subunit. This core is sufficient for transcription elongation and termination, but is unable to initiate transcription (Paget and Helmann, 2003). Transcription initiation from promoter elements requires a sixth, dissociable specificity subunit known as a sigma ( $\sigma$ ) factor. These sigma ( $\sigma$ ) factors reversibly associate with the core RNA polymerase complex to form what is termed the holoenzyme.

There are two major families of bacterial sigma ( $\sigma$ ) factors; the  $\sigma^{70}$  and  $\sigma^{54}$ . The  $\sigma^{54}$  promoters are highly conserved, short sequences that are located at positions -24 and -12 upstream of the transcription initiation site, whereas  $\sigma^{70}$  promoter sites are typically located at -35 and -10 upstream (Kazmierczak et al., 2005). These families are comprised of proteins that are functionally similar but structurally distinct from one another and the vast majority of sigma ( $\sigma$ ) factors belong to the  $\sigma^{70}$  family. The  $\sigma^{70}$  family is further broken down into 4 subfamilies, or groups. Group 1 contains primary or housekeeping sigma ( $\sigma$ ) factors that are found in all bacteria and are essential for basal transcription of important genes and expression of genes required for cell viability. Group 2 sigma ( $\sigma$ ) factors are the non-essential paralogues of the essential primary sigma ( $\sigma$ ) factors, which are found in group 1. Group 3  $\sigma^{70}$  proteins include flagellar, heat shock, and sporulation  $\sigma$  factors. The largest and most diverse subfamily of  $\sigma^{70}$  proteins is group 4, which is

known as the extracytoplasmic function (ECF)  $\sigma$  family (Staron et al., 2009). These alternative sigma factors direct RNAP to transcribe genes in response to environmental stimuli.

### 1.2.5.3 Extracytoplasmic Function Sigma Factors (ECF- $\sigma$ )

Extracytoplasmic function sigma (ECF- $\sigma$ ) factors regulate functions related to sensing and responding to changes and signals in the bacterial periplasm and extracellular environment. The ECF- $\sigma$  factors are numerically the largest and most diverse group in the  $\sigma^{70}$  family at the primary sequence level and have biological roles that include envelope maintenance and stress response, synthesis of exopolysaccharides, and extracellular proteases, iron transport, and oxidative stress response (Paget, M., 2015 and Bashyam and Hasnain, 2004). Sequence alignments of the  $\sigma^{70}$  family reveal four conserved regions ( $\sigma_1$ - $\sigma_4$ ), each differing in function. ECF  $\sigma$  factors only contain regions 2 and 4 which are well conserved in all members of the  $\sigma^{70}$  family (Staron et al., 2009). These two regions include subregions involved in binding to the core RNA polymerase complex, recognition of the -10 and -35 promoter, and promoter melting (Paget and Helmann, 2003). Specifically, region 2 is essential in the core-binding and recognizing the -10 promoter element while region 4 is the Carboxy terminal region which recognizes the -35 promoter element (Murakami and Darst, 2003). ECF  $\sigma$  factors are responsible for promoter recognition and transcription initiation before they are dissociated from the RNA polymerase holoenzyme. Following dissociation, the core enzyme goes through the elongation and termination phases of transcription.

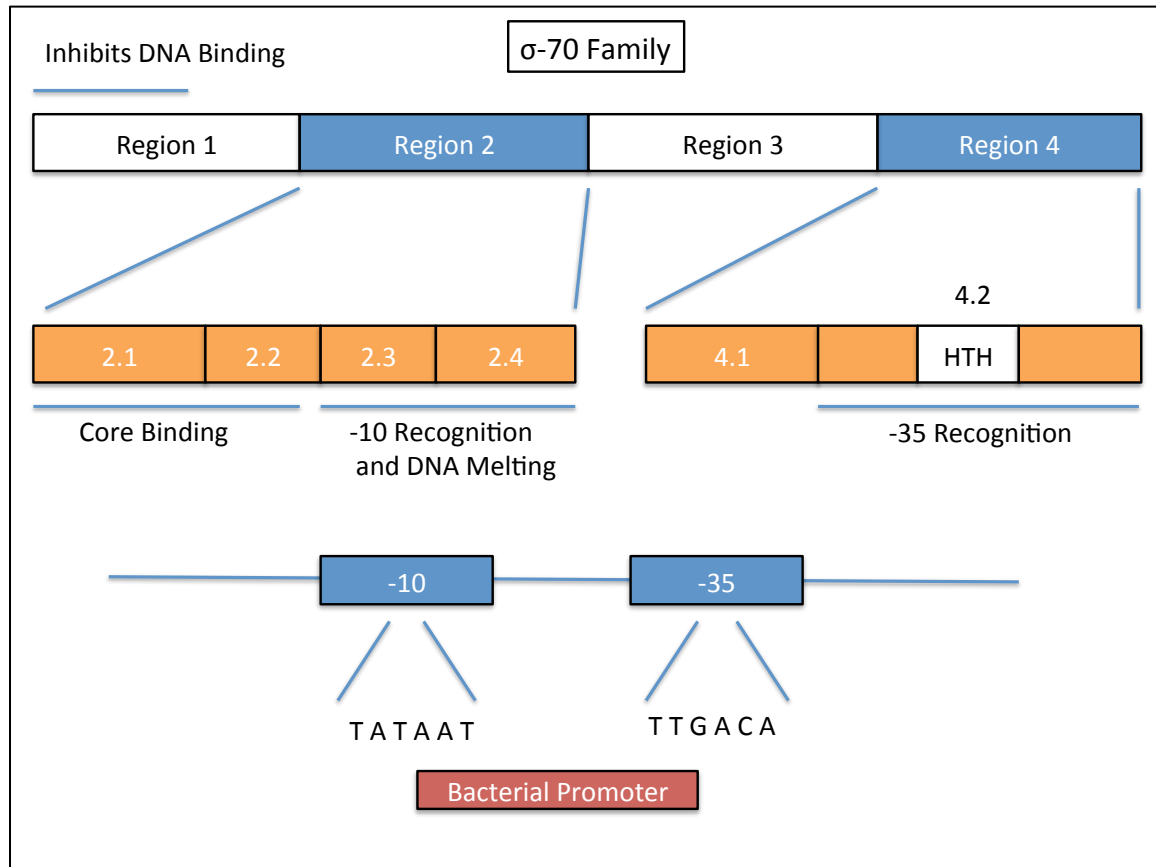


**Figure 4. Conserved regions of sigma factors.** Adapted with permission from Helmann, J.D. 2001. Sigma factors in gene expression. *Enc. Life. Sci.* 4(19): 1-7. Copyright © 2001 John Wiley & Sons, Ltd. All rights reserved.

### 1.2.6 Regulation of Activity of ECF Sigma Factors

Sigma factors are essential for the response of the bacteria to environmental stress conditions. However, these conditions can change abruptly requiring the bacteria to contain an inhibitory switch for sigma factors. Alternative sigma factors are typically cotranscribed with one or more negative regulators. These regulators are specific anti- $\sigma$  proteins localized in the cytoplasmic membrane that can directly bind or release  $\sigma$  factors (Helmann, J., 2002). This control can impede RNA polymerase binding with cognate  $\sigma$  factors and inhibit transcription until an environmental stress is present. Anti- $\sigma$  factors are often modular and consist of a  $\sigma$ -binding domain and a sensory domain that responds to signals inside or outside of the cell (Paget, M., 2015). Once an environmental stress cue is perceived by the sensory protein, the anti- $\sigma$  dissociates from its sensory domain and degrades. This releases and activates the sigma ( $\sigma$ ) factor, allowing it to competitively bind to RNAP, thus initiating transcription of the stimulus-responsive gene(s) (Helmann, J., 2002).

### 1.2.7 ECF Sigma Factors of *P. gingivalis*

ECF sigma factors are involved in virulence regulation in many pathogenic bacteria including *Mycobacterium tuberculosis*, *Staphylococcus aureus*, *Pseudomonas aeruginosa*, *Enterococcus faecalis*, and *Porphyromonas gingivalis* (Dou et al., 2015). The genome of *P. gingivalis* strain W83 encodes eight putative sigma factors, six of which fall into the ECF sigma factor subfamily (PG0162, PG0214, PG0985, PG1318, and PG1827) (Nelson et al., 2003 and Dou et al., 2015). Previous studies have demonstrated the roles of these ECF sigma factors for survival of *P. gingivalis* in the presence of

oxygen, hydrogen peroxide, and thiol-induced stress as well as positive regulation of hemin uptake and virulence regulation (Yanamandra et al., 2012).

While previous studies have sought to identify and characterize several of the ECF sigma factors, there is still a gap in our comprehensive understanding of the functional role of many of these ECF sigma factors in the response of *P. gingivalis* to environmental stress. Studies have been published analyzing genes such as PG0162 and PG1827, but more work is needed to characterize the remaining genes and to better understand the group as a whole.

### **1.2.8 Genes of Interest**

Our goal was to characterize one of the lesser studied extracytoplasmic function (ECF) sigma factor genes, PG0214, and better understand its role in survival and environmental stress response. Specifically we worked with comparing a mutant PG0214-deficient strain of *P. gingivalis* W83 (termed V0214) against wild-type strains W83 and ATCC 33277. We analyzed the RNA regulation, interaction and invasion of host endothelial cells, protease activity, and the proteome between the 3 strains under normal conditions and compared against oxidative- and iron-stress conditions.



## CHAPTER 2: HYPOTHESIS AND AIMS

### 2.1 Hypothesis

We hypothesize the sigma factor 70 gene, PG0214, of *Porphyromonas gingivalis* is required for survival in environmental stress conditions and virulence within cell culture model.

### 2.2 Research Objective and Aims

The main objective of this research is to investigate the importance of the PG0214 gene in *Porphyromonas gingivalis* in response of the bacteria to environmental stress as well as its role in eukaryotic cell interaction.

**Aim 1:** Identify the changes in the transcriptome of *P. gingivalis* in response to environmental stress and compare between strains. This will involve:

- I. Isolation of RNA
- II. cDNA library construction
- III. High throughput RNA sequencing, RNA library generation, and data analysis

**Aim 2:** Determine the role of PG0214 in response to environmental stress. This will involve:

- I. Bioinformatic characterization of gene
- II. Isolation of RNA
- III. cDNA library construction

IV. High throughput RNA sequencing, RNA library generation, and data analysis

V. Proteome preparation, mass spectrometry, and analysis

**Aim 3:** Observe interaction and invasion of wild-type and mutant strains of *P. gingivalis* with host cells in multiple environmental conditions using:

I. Antibiotic protection assay

II. Colony counting and data analysis

**Aim 4:** Determine the potential role of PG0214 in response to environmental stress by observing protease activity using:

I. Arg-X and Lys-X protease activity assay

## CHAPTER 3: MATERIALS AND METHODS

### 3.1. Bacterial Strains

The bacterial strains used in this study are listed in table 2.

**Table 2: Bacterial strains used in this study.**

<b>Bacteria</b>	<b>Strain</b>	<b>Description</b>	<b>Reference</b>
<i>P. gingivalis</i>	W83	Wild-type clinical strain	Lewis and Macrina, 1998.
<i>P. gingivalis</i>	ATCC 33277	Wild-type, Non-encapsulated strain	Schenkein, H.
<i>P. gingivalis</i>	V0214	PG0214 Knockout in W83	Lewis, J. P. (unpublished)

### 3.2 Media Growth Conditions

#### 3.2.1 *Porphyromonas gingivalis*

Bacterial strains used in this study are listed in table 2. *Porphyromonas gingivalis* strains W83, ATCC 33277, and V0214 were cultured in a vinyl anaerobic chamber with an atmosphere of 10% H<sub>2</sub>, 10% CO<sub>2</sub>, and 80% N<sub>2</sub> at 37°C. Bacteria were maintained on either blood agar plates (TSA II, 5% sheep blood; BBL, Sparks, MD) or liquid cultures

prepared in Brain-Heart Infusion broth (BHI: Difco Laboratories, Detroit, MI) supplemented with Hemin (5 µg/ml; Sigma, St. Louis, MO), yeast extract (5 mg/ml), cysteine (1 mg/ml; Sigma, St. Louis, MO) and Vitamin K3 (1 µg/ml; Sigma, St. Louis, MO) in sterile 15mL falcon conical tubes (Thermo Fisher Scientific Waltham, MA).

### **3.2.2 Endothelial Cells**

Pooled primary human umbilical vein endothelial cells (HUVECs: Lifeline Cell Technologies; Frederick, MD) were grown in VascuLife Basal Medium containing vascular endothelial growth factors (VEGF: Lifeline; Frederick, MD) at 37°C in 5% CO<sub>2</sub> according to the manufacturers instructions. Cells were seeded in T-75 flasks (Thermo Fisher Scientific Waltham, MA) at 2.5x10<sup>5</sup> cells/flask in 15 mL VEGF media. VEGF media was replaced every 2 days until cells were ready for experimental use.

## **3.3 Cell Culture Preparation**

### **3.3.1 *Porphyromonas gingivalis***

*P. gingivalis* wild-type and mutant strains were spread onto and blood agar plates and grown anaerobically at 37°C. Once individual colonies could be observed, a sterile inoculating loop was used to scrape a single colony from the plate, inoculated in 3 mLs of BHI broth, and incubated overnight at 37°C. Subsequent daily dilutions were performed to ensure continued viability and to keep the bacteria in logarithmic phase of growth. For environmental stress studies bacterial cultures were grown in BHI medium broth anaerobically and micro-aerophilically, in the presence of 6% oxygen (7.2% H<sub>2</sub>, 7.2% CO<sub>2</sub>, 79.7% N<sub>2</sub>, 6% O<sub>2</sub>; Lewis et al. 2009) as well as with or without the addition of 2,2'-

Dipyridyl (10 mg/ml DP: Sigma, St. Louis, MO), a high-affinity iron chelator. Cultures to be used for harvesting of cells for transcriptomic, proteomic, and protease studies were inoculated in BHI to an optical density of 0.1 at 660 nm ( $OD_{660}$ ). One of the aliquots was incubated at 37°C anaerobically while the other was grown in the presence of 6% oxygen at 37°C. Aliquots from each aerobic condition were supplemented with DP to simulate an iron deficient environment. Cultures were grown until they reached mid-logarithmic phase and an optical density,  $OD_{660}$ , of 0.5 and were then pelleted and stored at -20°C until needed.

### **3.3.2 Endothelial Cells**

Endothelial cell culturing was performed separately from bacterial cultures in a sterile cell culture fume hood that was ultraviolet light-sterilized daily. Pooled primary human umbilical vein endothelial cells (HUVECs: Lifeline Cell Technologies; Frederick, MD) were grown in Vasculife Basal Medium containing vascular endothelial growth factors (VEGF: Lifeline; Frederick, MD) and were incubated at 37°C in 5% CO<sub>2</sub> according to the manufacturers instructions. Cells were seeded in T-75 flasks at  $2.5 \times 10^5$  cells/flask in 15 mL VEGF media. Following seeding, cell viability was checked via a 1:1 dilution with 4.0% trypan blue dye (Thermo Fisher Scientific Waltham, MA) which stains a blue color in cells with compromised membranes. For each seeding, 100 cells were observed under a microscope to ensure at least 80% cell viability. Cell growth was observed daily and media was aspirated and replaced with fresh, pre-warmed VEGF media every 2 days. Approximately 5-6 days after initial seeding, cell concentration was

determined using a hemocytometer cell counting device. Once the cells reached approximately 80% confluency they were ready for experimental use.

### **3.4 RNA Sequencing and Library Generation**

#### **3.4.1 Transcriptome Preparation**

From an overnight culture, wild-type and mutant strains were diluted using 500 $\mu$ l of bacterial culture and 4.5ml of BHI media. DP positive and negative samples were created by the addition of 20 $\mu$ l DP (10 mg/ml) to half of the cultures for each strain. A DP positive and negative sample from each strain was incubated anaerobically while a duplicate sample set was incubated in 6% oxygen using airtight jars sealed with an anoxomat aerobic machine (Mart Microbiology: Drachten, The Netherlands), both at 37°C. Cultures were grown for 4-6 hours until the OD<sub>660</sub> reached 0.5. Once the cultures reached mid-logarithmic phase of growth they were centrifuged to pellet, and stored at -20°C for RNA isolation.

#### **3.4.2 RNA Isolation**

Prior to isolation, the lab benchtop, pipettors, tube and pipette racks, and buffer bottles were sterilized with 70% ethanol followed by RNaseZap RNase decontamination solution (Life Technologies: Catalog No. AM9780). Sealed boxes of pipette tips and unopened bottles of nuclease free water were used for each experiment. 1.5mL eppendorf tubes were autoclave sterilized prior to use. Gloves were sprayed with 70% ethanol and RNaseZap periodically throughout the protocol and all steps of the protocol were performed alongside an open flame to further prevent DNA/ RNA contamination.

Samples were removed from -20°C storage, thawed, and resuspended in 500µL of buffer RLT containing Beta-merceptoethanol (RNeasy Mini Kit, Qiagen, Catalog No. 74104). They were then vortexed and transferred to 2mL lysing matrix B tubes containing 0.1mm silica beads (MP Biomedicals; Catalog No. 116911050). In a laminar flow hood, 500µL of acid phenol:chloroform, pH 4.5 (Sigma, Catalog No. P1944) was added to each sample tube. Samples were then shaken in a bead beater machine at 6.0 M/S for 45 seconds and incubated on ice for 5 minutes. Following cooling, samples were spun down in a temperature-specific centrifuge at 13,000 rpm for 10 minutes, 4°C. In the flow hood, approximately 600µL of supernatant was removed from each sample and pipetted into fresh 1.5mL eppendorf tubes containing 400µL of 100% ethanol. Mixtures were transferred to RNeasy spin columns, centrifuged, and the flowthrough was discarded. 600µL of RW1 buffer was then added to each column, followed by centrifugation and disposal of flowthrough. A master mix containing 70µL of buffer RDD and 10µL of DNase enzyme (RNase-Free DNase Set, Qiagen, Catalog No. 9254) for each sample was created and 80µL of the mixture was added to the center of each column. Samples were incubated at room temperature for 30 minutes.

Following incubation, 250µL of buffer RW1 (RNeasy Mini Kit, Qiagen, Catalog No. 74104) was added to the columns containing RNA samples. Samples were centrifuged and flowthrough was discarded. Next, 500µL of buffer RPE was added to each column, centrifuged, and flow-through disposed of. This step was repeated to ensure samples were properly washed. Residual wash buffer was removed via a 2 minute centrifugation and columns were transferred to clean 1.5mL eppendorf tubes. 50µL of

nuclease-free water was added to the center of each column followed by a one minute incubation at room temperature. Samples were centrifuged at 13,000rpm for 3 minutes, 4°C. The flowthrough containing isolated RNA was then treated with a second DNA removal kit by adding 5µL of 10x DNase I buffer and 1µL of rDNase I to each sample (Ambion DNA-free DNA Removal Kit, Life Technologies, Catalog No. AM1906). Samples were incubated at 37°C for 30 minutes. 5µL of resuspended DNase inactivation reagent was added to each sample and were incubated for 2 minutes, mixing occasionally. Samples were centrifuged at 10,000rpm for 1.5 minutes and the supernatant RNA was removed and collected in fresh 1.5mL eppendorf tubes. The concentration of RNA was measured using a NanoDrop spectrophotometer. Approximately 15µL was removed from each sample to run a denaturing RNA gel and the remaining sample was frozen at -20°C until ready for further use.

### **3.4.3 Denaturing RNA Gel**

For the denaturing RNA gel the work area was sterilized with 70% ethanol and RNaseZap RNase decontamination solution as mentioned previously. The horizontal gel apparatus, gel tray, and well-comb were treated with RNaseZap RNase decontamination solution and washed with nuclease-free water. 1g of agarose powder (Sigma, Catalog No. A9539) was melted into 72mL of nuclease-free water for approximately 2 minutes. After allowing to cool, 10mL of 10X nuclease-free MOPS buffer was added along with 1µL GelStar nucleic acid gel stain (Lonza, Catalog No. 50535). In a laminar flow hood 18mL of formamide (Sigma, Catalog No. F9037) was added, mixed, and the solution was poured into the gel apparatus. Once the combs were placed, the gel was allowed 30



minutes to solidify. While the gel was forming, RNA samples were prepared using 3 $\mu$ g of sample and 2 $\mu$ L of formaldehyde RNA loading dye (New England Biolabs, Catalog No. B0363S). Samples were brought to a volume of 12-13 $\mu$ L with nuclease-free water and were heated in a 55°C water bath for 15 minutes. Following heating, approximately 12 $\mu$ L of each sample was loaded into the wells of the gel followed by 1X nuclease-free MOPS running buffer filling the gel apparatus. Samples were run at 35V for one hour followed by visualization and photo capture using a UV transilluminator photo box. Clear bands should be observed at 28S rRNA and 18S rRNA for a properly intact isolated RNA gel sample.

#### **3.4.4 Library Generation**

RNA isolate concentrations were checked via nanodrop spectrophotometer and visually via Denaturing RNA gel and if determined to be sufficient, library generation preparation began. Prior to performing the library generation protocol the work area was sterilized with 70% ethanol and RNaseZap RNase decontamination solution as mentioned previously.

cDNA library generation was performed using NuGEN Technologies Ovation Complete Prokaryotic RNA-Seq DR Multiplex Systems Kit (NuGEN Technologies, Catalog Nos. 0326 and 0327). This kit creates double stranded cDNA aligned to the strand from which the RNA originated enabling detection of both sense and antisense expression. It can be performed with as little as 100-400ng of total RNA and does not require dedicated steps for reducing rRNA levels.

The kit is designed for strand-specific expression analysis by incorporation of a nucleotide analog during the second strand cDNA synthesis and subsequent ligation to a pair of double-stranded adaptors also containing the same analog in one strand. After ligation the cDNA strand and adaptor containing the analog were selectively removed (Strand Selection), leaving only one cDNA strand, with both adaptor sequences attached. This product was then converted into a sequence-ready library by PCR amplification (NuGEN Technologies, Catalog Nos. 0326 and 0327).

The kit provides 16 unique dedicated read barcoded adaptors to prepare libraries for multiplex sequencing using a dedicated read design strategy with a second sequencing primer enabling up to 16-plex sequencing. Once libraries were prepared, they were submitted to the VCU Nucleic Acids Research Facility for sample quality check and Illumina Sequencing.

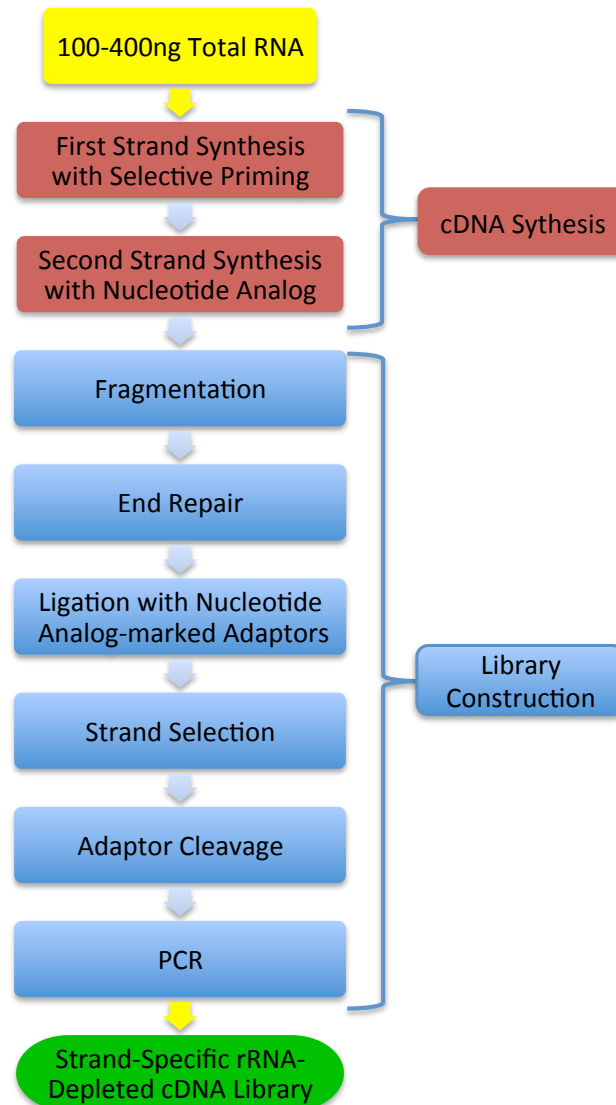


**Figure 5: Ovation Complete cDNA Library Generation Workflow.** This streamlined workflow consists of a double-stranded cDNA, end repair to generate blunt ends, adaptor ligation, strand selection via nucleotide analog-targeted degradation and PCR amplification to produce the final library. The entire workflow takes approximately 10 hours and yields DNA libraries ready for cluster formation for single read or paired-end sequencing. This figure was adapted from NuGEN Ovation Complete Prokaryotic RNA-Seq DR Multiplex Systems Kit protocol.

### 3.5 Proteomics

#### 3.5.1 Proteome Preparation

For proteomic studies, wild-type and mutant cultures were grown, pelleted, and frozen for storage as mentioned previously. Pellets were thawed and washed with 1mL of a wash buffer consisting of 10mM Tris-HCl and 5mM Mg-acetate, pH 8.0. After a second wash pellets were suspended in 100 $\mu$ L of a lysis buffer consisting of 10:1 dilution of wash buffer mentioned above, 1x lysis buffer (New England Biolabs, Catalog No. 9803S), a protease tablet (10 $\mu$ g/mL: Sigma-Aldrich, Catalog No. S8820), 10mM TLCK (Sigma-Aldrich, Catalog No. T7254), 8M urea, and lysozyme (50 $\mu$ g/mL: Thermo Fisher Scientific, Catalog No. 90082). Samples were incubated at room temperature for 30 minutes on a test tube rocker. Following incubation, samples were sonicated for 4 cycles of 1 minute followed by a 30 second break at 40% power and 10% pulse rate. Samples were placed on ice immediately after sonication and were spun in a temperature-controlled centrifuge for 20 minutes at 13,000 RPM, at 4°C. Approximately 90 $\mu$ L of supernatant was collected from each sample and transferred to sterile 1.5mL eppendorf tubes. Next an acetone precipitation technique was performed to remove interferences using 4 volumes of cold acetone mixed with each sample. This mixture was incubated at -80°C for 10 minutes followed by an overnight incubation at -20°C. Samples were then centrifuged for 15 minutes at 15,000 RPM, at 4°C. The supernatant was removed and pellets were inverted and left to dry for 15 minutes. Samples were further dried in a speedvac to eliminate any acetone residue. Samples were resuspended in 50 $\mu$ L of 6M Urea. 8 $\mu$ L of each sample was diluted 1:1 with blue protein dye and boiled for 15 minutes in preparation for 1D SDS-PAGE gel. Samples were loaded into a NuPAGE 12% Bis-

Tris gel (Thermo Fisher Scientific, Catalog No. NW00120BOX), run at 150V for 1 hour, and analyzed to ensure sufficient levels of protein were present.

### **3.5.2 Tryptic Digestion**

A 30 $\mu$ L aliquot of each sample was transferred to a siliconized tube from the ProteoExtract Trypsin Digestion Kit (Calbiochem, Catalog No. 650212). Samples were centrifuged for 15 minutes at 10,000 RPM followed by 25 $\mu$ L of supernatant transferred to a sterile eppendorf tube containing 25 $\mu$ L of digest buffer (Calbiochem, Catalog No. 650212). 1 $\mu$ L of reducing agent (Calbiochem, Catalog No. 650212) was mixed into each sample followed by a 10 minute incubation at 37°C. Samples were allowed to cool and 1 $\mu$ L of blocking agent was added (Calbiochem, Catalog No. 650212) followed by a 10 minute incubation at room temperature. Following incubation 1 $\mu$ L of Trypsin was added to each sample and incubated for 4 hours at 37°C. Another 1 $\mu$ L of Trypsin was added to each sample and they were incubated overnight at 37°C. Samples were stored at -20°C until they could be submitted to the Chemical and Proteomic Mass Spectrometry Core Facility at Virginia Commonwealth University where they were analyzed for protein ID with spectral counting analysis using a Waters Synapt G2Si mass spectrometer. Data analysis was performed using Scaffold (TM) software, version: Scaffold\_4.4.4 (Proteome Software Incorporated, Portland, Oregon).

### **3.6 Antibiotic Resistance Assay**

#### **3.6.1 Endothelial Cell Preparation**

Endothelial cells were seeded and prepared in T-75 cell culture flasks as previously mentioned. On the day before an experiment, cell viability and confluence were checked and cells were washed once with pre-warmed PBS. Because cells adhere to the bottom of the flask they were freed from adherence by the addition of 2 mL trypsin-EDTA (0.25%) and were incubated for 5 minutes at room temperature. Following incubation a 2 mL aliquot of trypsin neutralizing solution was added to each T-75 flask and the newly suspended HUVEC cells were collected and transferred to 50 mL falcon conical tubes (Thermo Fisher Scientific, Waltham, MA). The T-75 flasks were then washed with PBS and transferred to the 50mL conical tubes to ensure optimal cell collection. The HUVECs were centrifuged to a pellet, supernatant was removed, and cells were resuspended in 10mL of pre-warmed VEGF media. A sample of cells was taken and counted using a hemocytometer. Using this cell count, aliquots of suspended cells were added to each well of two 6-well Corning Costar cell culture plates (Sigma, St. Louis, MO) so that there were approximately 400,000 cells per well. The 6-well plates were incubated overnight at 37°C in 5% CO<sub>2</sub>.

#### **3.6.2 Bacterial Culture Preparation**

Wild-type and mutant strains were cultured as mentioned previously. On the morning of experiment 500µL from an overnight culture was diluted into 4.5mLs of BHI broth. DP positive and negative samples were created by the addition of 20µl DP (10 mg/ml) to half of the cultures for each strain. Cultures were incubated anaerobically at

37°C for 2-3 hours until they reached mid-logarithmic growth (OD<sub>660</sub> 0.5-0.7). Cultures were then centrifuged to pellet, supernatant was discarded, and washed with PBS. This wash sequence was repeated for a total of three washes before resuspending cultures in 4-5mL of pre-warmed, anaerobic VEGF media. Optical density measurements were checked to ensure minimal cell loss during washes and so that samples were at OD<sub>660</sub> of 0.7, corresponding to mid-logarithmic phase of approximately  $7 \times 10^8$  cells/mL, and were ready for infection.

### **3.6.2 Infection**

Prior to infection, HUVEC cell number was determined by performing a trypan exclusion test on a single well to confirm they were ready for infection. Once the bacterial cultures were ready for infection, the 6-well plates containing HUVECs were transferred from the tissue culture incubator into the anaerobic chamber. The media was aspirated from the wells and each well was washed three times with anaerobic PBS. Following the wash, 2mLs of anaerobic VEGF media was added to each well and plates were incubated at 37°C for 20 minutes to equilibrate the temperature for infection. Each well of endothelial cells was then infected with bacteria at a multiplicity of infection (MOI bacteria:host) of 100:1 followed by a 30 minute anaerobic incubation at 37°C to allow the bacteria to interact with the host.

### **3.6.3 Interaction**

For the interaction portion of the assay, the 6-well plates containing endothelial cells were removed from the incubator following incubation. The media was aspirated

and each well was washed three times with 1mL anaerobic PBS followed by the addition of 2mL filter-sterilized 1.0% saponin in BHI (Sigma Aldrich, Catalog No. 47036). Plates were incubated anaerobically for 15 minutes at 37°C to allow host-cell lysis. Using a cell scraper or bent inoculating loop, the cell culture of each well was scraped to remove the cell mixture from its adherence to the bottom of the well. Cell mixture was then collected and diluted 1:1 into BHI. Serial dilutions were then performed in a set of 15mL conical tubes containing 900µL BHI at dilution factors of 1:10, 1:100, and 1:1000. Dilutions of 1:100 and 1:1000 were then plated on blood agar plates using 200µL aliquots dispensed and spread onto each plate. A control plate containing only bacterial culture for each sample was also plated to ensure samples were not contaminated prior to infection. Plates were then wrapped with a protective layer of parafilm and placed in the incubator at 37°C. Samples were grown for seven days before they were removed from the incubator and colony forming units (CFU) could be observed. Plates were placed on a light box, photographed, and CFUs were counted manually. Plates containing larger quantities of CFUs (100+) were confirmed using Promega colony counting software (Promega Colony Counter; Promega Life Sciences, Madison, WI).

#### **3.6.4 Invasion**

For the invasion portion of the assay, the 6-well plates containing endothelial cells were removed from the incubator following incubation. The media was aspirated and each well was washed three times with 1mL anaerobic PBS followed by the addition of 2mL VEGF media supplemented with the antibiotics; gentamicin (300µg/mL) and metronidazole (400µg/mL). Plates were incubated for 1 hour at 37°C. Following



incubation, media was aspirated from each well and 2mL filter-sterilized 1.0% saponin in BHI was added. Plates were incubated anaerobically for 15 minutes at 37°C to allow host-cell lysis. Using a cell scraper or bent inoculating loop, the cell culture of each well was scraped to remove the cell mixture from its adherence to the bottom of the well. Cell mixture was then collected and diluted 1:1 into BHI. Serial dilutions were then performed in a set of 15mL conical tubes containing 900µL BHI at dilution factors of 1:10, 1:100, and 1:1000. Dilutions of 1:100 and 1:1000 were then plated on blood agar plates using 200µL aliquots dispensed and spread onto each plate. Plates were then wrapped with a protective layer of parafilm and placed in the incubator at 37°C. Samples were grown for seven days before they were removed from the incubator and colony forming units (CFU) could be observed. Plates were placed on a light box, photographed, and CFUs were counted manually. Plates containing larger quantities of CFUs (100+) were confirmed using Promega colony counting software (Promega Colony Counter; Promega Life Sciences, Madison, WI).

### **3.7 Protease Activity Assay**

Wild-type and mutant bacterial cultures were grown, pelleted, and stored as previously described. Frozen pellets were thawed and suspended in 3mLs of PBS. A 25µL aliquot was taken from each sample and diluted into 200-400µL PBS so that when 5-10µL of the sample was combined with 600µL of 50 mM Tris-HCl + 4mM *tris*(2-carboxyethyl)phosphine (TCEP) pH 8.0 in VIS cuvettes, the OD<sub>405</sub> was approximately 0.05. The chromogenic substrates N-alpha-Benzoyl-D,L-arginine 4-nitroanilide hydrochloride (DL-BAPNA; Sigma, Catalog No. B4875) and D-Phe-Pro-Lys-pNA

(Sigma, Catalog No. SCP0126) were dissolved in Dimethyl sulfoxide (DMSO: Sigma, Catalog No. D4540) at concentrations of 4.3mg/mL and 4.9mg/mL respectively. The addition of these substrates to proteins results in a hydrolytic reaction cleaving the bond between p-nitroaniline and arginine (DL-BAPNA) or lysine (D-Phe-Pro-Lys-pNA). The p-nitroaniline chromophore is released resulting in a yellow hue that can be detected by colorimetric analysis using a spectrophotometer.

### **3.7.1 Arg-X Activity Assay**

For the Arg-X activity assay, 5-10 $\mu$ L of each sample was added into VIS cuvettes containing 600 $\mu$ L of 50 mM Tris-HCl + 4mM TCEP. Baseline absorbance values were taken with a spectrophotometer and sample volumes were adjusted to ensure OD<sub>405</sub> were approximately 0.05. 50 $\mu$ L of DL-BAPNA (4.3 mg/mL in DMSO) was added to each sample, including a control cuvette containing only the 600 $\mu$ L of 50 mM Tris-HCl + 4mM TCEP and samples were placed at 37°C. The optical density (OD<sub>405</sub>) was checked 5 minutes following the addition of DL-BAPNA and every 15-30 minutes following until a plateau in absorbance values could be seen.

### **3.7.2 Lys-X Activity Assay**

For the For the Lys-X activity assay, 5-10 $\mu$ L of each sample was added into VIS cuvettes containing 600 $\mu$ L of 50 mM Tris-HCl + 4mM TCEP. Baseline absorbance values were taken with a spectrophotometer and sample volumes were adjusted to ensure OD<sub>405</sub> were approximately 0.05. 50 $\mu$ L of D-Phe-Pro-Lys-pNA (4.9 mg/mL in DMSO) was added to each sample, including a control cuvette containing only the 600 $\mu$ L of 50

mM Tris-HCl + 4mM TCEP and samples were placed at 37°C. The optical density (OD<sub>405</sub>) was checked 5 minutes following the addition of D-Phe-Pro-Lys-pNA and every 15-30 minutes following until a plateau in absorbance values could be seen.

## CHAPTER 4: RESULTS

### Aim 1

The first aim of this project was to identify the changes in the transcriptome of *P. gingivalis* in response to environmental stress and compare between strains W83 and ATCC 33277. This involved techniques such as RNA isolation, cDNA library generation, high-throughput RNA sequencing, and bioinformatic data analysis.

#### 4.1 RNA Sequencing

##### 4.1.1 RNA Isolation

Following the transcriptome preparation mentioned previously, RNA isolation was performed on W83, ATCC 33277, and the PG0214-deficient strain (V0214) in multiple environmental stress conditions for further RNA library preparation. At this step a denaturing RNA gel was performed to confirm that the RNA had been isolated, did not degrade, and could be used for sequencing. The double bands seen in figure 6 correspond to 28S and 18S rRNA and are an indication of an intact, isolated RNA sample.

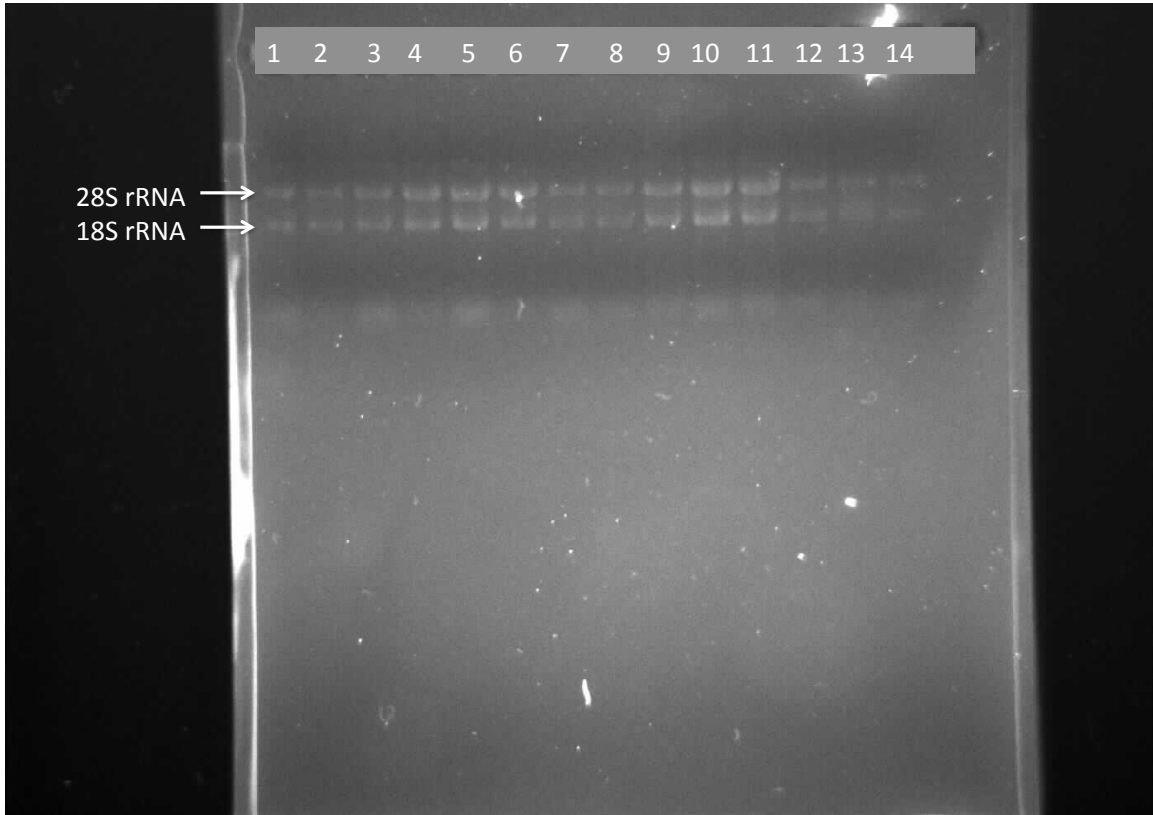


**Figure 6. Denaturing RNA gel for confirmation of RNA isolates.**

This figure depicts a denaturing RNA gel used for the confirmation of RNA isolates.

Lane 1: wild-type W83; Lane 2: W83+2,2-dipyridyl(DP); Lane 3: ATCC 33277(77);

Lane 4: 77+DP; Lane 5: V0214; Lane 6: V0214+DP; Lane 7: W83 6% O<sub>2</sub>; Lane 8:

W83+DP 6% O<sub>2</sub>; Lane 9: 77 6% O<sub>2</sub>; Lane 10: 77+DP 6% O<sub>2</sub>; Lane 11: V0214 6% O<sub>2</sub>;

Lane 12: V0214+DP 6% O<sub>2</sub>; Lane 13: 77; Lane 14: 77+DP. Clear double bands can be

seen at 28S and 18S indicating a properly denatured RNA sample.

### **4.1.2 RNA Library Generation**

RNA isolated from wild-type W83, wild-type ATCC 33277, and mutant V0214 strains was then used to generate cDNA libraries as described previously. Four biological replicates were generated for each strain and samples were submitted to the VCU Nucleic Acid Research Facility for validation and sequencing.

#### **4.1.2.1 Validation of cDNA Library**

Figure 7 depicts the bioanalyzer results of the cDNA/ RNA library samples. Once samples were validated with this quality check step, further high-throughput sequencing could be performed. These results indicate that the RNA libraries were ready to be sequenced as peaks were found between 60 and 100s indicating good fragment size and quality.

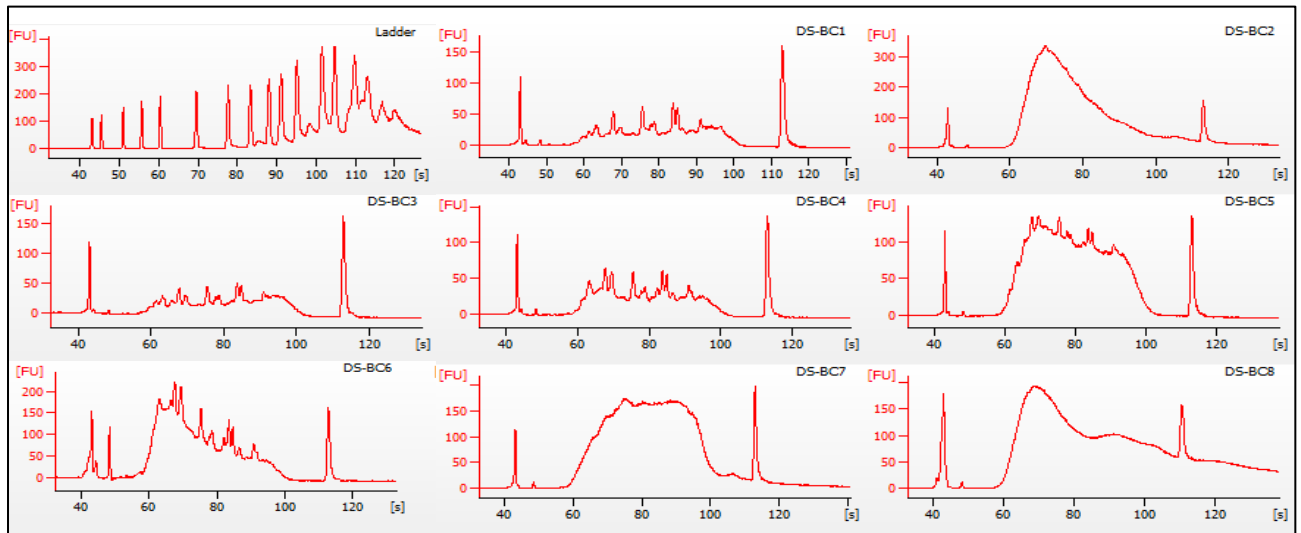


**Figure 7. Electropherogram results from bioanalyzer of cDNA from 5.26.15.**

BC1: W83- 6%O<sub>2</sub>, BC2: W83+DP 6%O<sub>2</sub>, BC3: ATCC 33277-DP 6%O<sub>2</sub>, BC4: ATCC 33277+DP 6%O<sub>2</sub>, BC5: V0214 -DP 6%O<sub>2</sub>, BC6: V0214+DP 6%O<sub>2</sub>, BC7: ATCC 33277-DP 6%O<sub>2</sub> BC8: ATCC 33277+DP.

### **4.1.3 RNA Sequencing of RNA Libraries**

Following successful validation of the cDNA libraries for each strain under each condition, next-generation high-throughput sequencing was performed to compare how the RNA levels change and how genes are regulated between the strains.

### **4.1.4 Statistical Analysis**

Statistical analysis of the transcriptomes was performed for each strain under each condition. Each of the three strains was grown under normal conditions as well as with the addition of 2,2,-dipyridyl and/or in microaerobic atmosphere. These conditions were used to examine the effect of iron and oxygen on differential gene expression. Each strain and condition was sequenced in biological triplicate to ensure significant interpretation. Statistical analysis of the transcriptomes was performed by comparing the reads per kilobase of transcript per million mapped reads (RPKM) values between strains and conditions. RPKM values and fold changes were calculated to illustrate the differences in RNA levels between strains. All data sets were trimmed at an RPKM value of 1 or greater and a fold change of +/-2 to ensure statistical relevance. Genes were ranked by the most differentially regulated as shown in tables 3, 5, 7, 9, 11, 13, 15, and 17.

Further analysis was conducted using the database for annotation, visualization and integrated discovery, or DAVID (<https://david.ncifcrf.gov/>). Using this software, the list of statistically relevant genes for each comparison was used to retrieve functional annotation clustering. This process groups similar and related genes into functional categories and determines which categories are most affected based on the number of gene hits. In order to determine the most relevant categories, an enrichment score was



given to each annotation cluster. This enrichment score is based off of a modified one-tail Fisher exact probability value used for gene enrichment analysis, or EASE score, given to each functional category. Enrichment scores range from values of 0-4. Clusters with an enrichment score above 0.5 were deemed statistically relevant and are shown in tables 4, 6, 8, 10, 12, 14, and 16.

Using the gene cluster data, pathways were created based on the number of gene hits and enrichment scores. These pathways were created using the Kyoto encyclopedia of genes and genomes pathway database, or KEGG (<http://www.genome.jp/kegg/pathway.html>). Each pathway illustrates the genes found in *Porphyromonas gingivalis* W83 as well as those that match the gene list data sets.

**Table 3. The Most Differentially Regulated Genes for W83 vs W83 + DP.**

This table depicts the most differentially regulated genes for the comparison of the wild-type W83 strain under normal and iron-stress conditions. For statistical relevance, this gene list was trimmed at an RPKM value of 1 or greater and a fold change of +/-2 resulting in 217 differentially regulated genes.

Gene ID <sup>1</sup>	Fold Change <sup>2</sup>	RPKM W83 <sup>3</sup>	RPKM W83 + DP <sup>4</sup>
hmuY	12.49341381	11.26543054	140.7436854
PG0049	7.207738735	1.952674626	14.07436854
PG1871	7.207738735	2.214373288	15.96062412
PG0940	7.207738735	1.073971044	7.740902698
PG1553	6.118569326	5.479444104	33.52635862
PG1858	6.05756766	60.81522782	368.3923573
PG0495	5.892457944	31.30511342	184.4640643
PG0858	5.285675073	4.794513591	25.34224097
rplP	4.905266639	17.77607246	87.19637521
PG0007	4.805159157	6.079081384	29.21095358
PG1462	4.805159157	1.413119795	6.790265524
PG0901	4.805159157	2.587882035	12.43518506
PG0691	4.805159157	11.30495836	54.32212419
PG1375	4.404729227	17.41574667	76.71164835
PG1975	4.324643241	1.529873283	6.616156152
PG2161	4.324643241	1.789951741	7.740902698
PG1787	4.204514262	2.753771909	11.57827327
PG1019	4.118707849	3.816140767	15.71756893
PG1237	4.004299297	9.6657394	38.70451349
PG1179	4.004299297	1.220421641	4.886933521
PG0041	4.004299297	2.058730437	8.243772841
PG1180	3.931493856	2.946055234	11.58239805
PG0426	3.904191815	2.744973916	10.71690469
PG0040	3.844127325	4.130657863	15.87877476
PG1791	3.844127325	7.458132253	28.67000999
PG1674	3.603869368	1.775158751	6.397440246
PG0843	3.603869368	2.065328932	7.443175671
PG1181	3.603869368	6.443826267	23.22270809
PG0219	3.603869368	3.521216539	12.69000442
PG1426	3.603869368	4.052720922	14.60547679
PG1063	3.494661205	8.03651802	28.08490775
PG1176	3.470392724	1.683926725	5.843887054
PG1644	3.414192032	6.519313049	22.25818667
radC	3.36361141	2.355199659	7.921976445
maf	3.36361141	5.163322329	17.3674099
PG1236	3.357450949	35.34588248	118.6720667
PG1891	3.30354692	5.053981386	16.69606464

PG1661	3.224514697	42.51135384	137.0784853
PG0009	3.203439438	2.478394718	7.939387382
PG0059	3.203439438	2.517119635	8.06344031
PG2115	3.203439438	3.820450356	12.23858134
PG0397	3.203439438	6.643119863	21.28083216
PG0822	3.203439438	9.476215098	30.35648117
PG1995	3.203439438	13.76885954	44.10770768
PG1001	3.109220631	10.199725	31.71319541
PG1784	3.07530186	10.13180231	31.15835048
rplA	3.043267466	82.96772017	252.4929635
PG0634	3.043267466	8.851409707	26.93720719
PG1486	3.003224473	1.591068214	4.778334999
PG1363	3.003224473	4.669439324	14.02337445
rpsJ	2.928143861	33.69320924	98.65856379
rpsS	2.908385805	45.3454441	131.882046
hmuR	2.895416415	6.473704905	18.74407145
PG0819	2.883095494	1.309720786	3.776050096
PG2133	2.883095494	1.766399744	5.092699143
PG1333	2.883095494	2.684927611	7.740902698
PG0984	2.883095494	7.782398873	22.43739912
PG0927	2.853063249	12.36225663	35.27030006
purN	2.803009508	3.321559931	9.310364069
PG0632	2.803009508	9.205466095	25.80300899
PG2000	2.772207206	6.680202669	18.51890598
PG0218	2.669532865	3.020543563	8.06344031
PG1381	2.642837536	4.295884178	11.35332396
PG0867	2.620995904	5.09210409	13.34638396
PG1857	2.597383328	33.67536326	87.46782709
PG1747	2.536056222	13.2407389	33.57925828
PG0544	2.530717156	12.41106754	31.40890155
PG0846	2.529031135	10.46433325	26.46462461
PG0652	2.522708557	21.26675336	53.64982068
PG1178	2.488385992	7.058964611	17.56542866
PG1374	2.488385992	7.009601223	17.44259349
PG1079	2.47766019	13.37240211	33.13226836
PG1033	2.425681305	44.85662194	108.8078692
PG1027	2.402579578	1.325890178	3.185556666
PG1512	2.402579578	1.564035502	3.757719756
PG1534	2.402579578	1.652263145	3.969693691
PG1504	2.402579578	1.958609808	4.705715926
PG0722	2.402579578	2.105825577	5.059413528
PG1555	2.402579578	2.225846724	5.347773884
PG1639	2.402579578	2.237439676	5.375626873
PG0662	2.402579578	3.068488698	7.372288283
PG0997	2.402579578	7.240254232	17.39528696
PG1050	2.402579578	11.49400449	27.61526046
PG1257	2.402579578	31.17980452	74.91196159
PG0080	2.402579578	1.220421641	2.932160113
PG0492	2.402579578	1.234449476	2.965863103
PG1022	2.402579578	1.521821318	3.656296821
PG1113	2.402579578	1.84259738	4.426986837

PG0772	2.402579578	2.147942089	5.160601798
PG2104	2.402579578	2.386602321	5.734001998
PG0283	2.402579578	2.833017144	6.806549135
PG1811	2.402579578	3.464422724	8.323551288
PG0681	2.402579578	5.213451672	12.52573252
PG1345	2.402579578	5.456002632	13.1084805
PG0617	2.402579578	8.591768356	20.64240719
rnpA	2.402579578	10.11711853	24.30718238
PG1470	2.402579578	12.55290831	30.15936116
rplT	2.402579578	15.73923082	37.81475456
PG1215	2.402579578	49.93370908	119.9697097
PG0686	2.368740429	14.72045254	34.86893107
rpsQ	2.356960979	199.6322647	470.5254581
PG1662	2.319732007	49.83225646	115.5974803
PG1471	2.311916198	36.48747779	84.35599094
PG1244	2.295798264	13.35046878	30.64998306
PG1673	2.293371416	6.121078492	14.03790645
PG0475	2.293371416	6.267205034	14.37302888
PG1863	2.276128022	40.01068597	91.0694435
PG2128	2.261251368	5.833069571	13.19003655
PG1691	2.261251368	7.769152236	17.56800612
PG2223	2.236884435	9.642464486	21.56907872
PG1713	2.217765765	10.34194339	22.93600799
pth	2.217765765	7.506249235	16.64710258
PG0311	2.207775829	12.49588951	27.58812282
etfA-1	2.196644186	11.05558428	24.28518493
rpsF	2.19070484	546.9971167	1198.309231
PG0654	2.188790718	64.82280473	141.8835533
PG1722	2.184163253	11.58204068	25.29706764
rplN	2.184163253	19.36669097	42.30001474
PG0178	2.162321621	2.32461265	5.026560193
PG1276	2.162321621	6.354858251	13.74124739
PG1974	2.154036863	17.11272543	36.86144142
PG0972	2.145160338	6.960923436	14.93229687
PG0285	2.135626292	1.925446096	4.112033306
PG1282	2.135626292	6.359039079	13.58053105
PG1160	2.135626292	2.876708155	6.14357357
mraY	2.135626292	18.41093219	39.31887085
kamE	2.12320986	17.49271019	37.14069476
PG0116	2.119923157	4.474879352	9.486400365
PG0702	2.119923157	5.276736346	11.18627557
PG1308	2.119923157	51.79434824	109.8000383
PG0515	2.117527764	23.82116226	50.44197247
PG2168	2.117527764	33.34962717	70.61876145
PG1601	2.114270029	10.40669617	22.00256581
PG1335	2.112906863	97.69672082	206.4240719
PG1535	2.102257131	7.536638908	15.84395289
PG0294	2.102257131	2.892851298	6.081517271
ispD	2.102257131	3.852810922	8.099599235
etfB-2	2.09367649	28.69388287	60.07570796
rpmH	2.09256931	65.2805929	136.6041653

aroK	2.082235635	8.614740998	17.93792069
PG0727	2.082235635	23.34719662	48.61436477
PG1201	2.07495509	4.932643628	10.23501401
PG0949	2.072813754	16.30134621	33.78965463
rpsD	2.070307935	49.97687039	103.4675113
rplF	2.065375427	33.26975518	68.71453482
PG0560	2.059353924	9.168045501	18.88025048
PG1870	2.059353924	3.417180596	7.037184271
PG1457	2.059353924	4.81910084	9.924234228
PG0434	2.05220339	14.31961393	29.38676024
PG1042	2.049259052	13.30237359	27.2600095
PG2009	2.042192642	17.46294381	35.66269535
PG2145	2.027176519	17.01340268	34.48917043
PG0847	2.023224908	3.872001868	7.833930624
PG0873	2.018166846	11.52329447	23.25593085
PG0384	2.018166846	12.770167	25.77232765
infA	2.016980387	119.1666501	240.3567961
trmB	2.016450718	24.54790959	49.4996499
hup-2	2.015723545	408.8018814	824.0315775
PG1248	2.01447057	57.21976876	115.2675402
PG0437	2.006860589	29.63881129	59.48096229
PG1572	2.002149649	2.395474449	4.796098326
PG0024	-2.000650772	280.5075057	140.2081311
PG1355	-2.011726636	35.19227151	17.49356542
radA	-2.015029964	70.90068584	35.18592135
PG1790	-2.034849931	57.2784557	28.14873708
PG1654	-2.037610921	169.3569724	83.11546166
PG0124	-2.03947459	25.42250298	12.46522174
pyrH	-2.044505812	200.027107	97.8364091
PG0062	-2.057447696	68.60167465	33.34309532
PG1112	-2.08109652	6.588779414	3.166013373
PG0031	-2.08109652	7.159806963	3.440401199
PG0333	-2.08109652	30.12790059	14.47693574
PG0313	-2.08109652	5.213451672	2.505146504
PG2208	-2.08109652	6.317476732	3.035648117
PG0068	-2.08109652	6.392684788	3.071786785
PG0143	-2.114394064	139.6528901	66.04865783
PG0290	-2.130851471	462.6177014	217.1046211
PG1007	-2.185151346	18.1882193	8.323551288
PG0025	-2.218660527	307.058085	138.3979573
PG1709	-2.219836288	13.21810516	5.954540537
PG1977	-2.219836288	35.9595686	16.19919847
PG1354	-2.229746272	29.39701764	13.18401919
PG2079	-2.289206172	7.429988358	3.245661508
PG0875	-2.330828103	9.99042832	4.286214118
PG1969	-2.358576056	18.19685158	7.715185413
PG1150	-2.358576056	20.7471679	8.796480338
PG0564	-2.393260998	38.00205234	15.87877476
fmt	-2.4261763	757.4147644	312.1845532
PG0222	-2.437855924	28.22616207	11.57827327
folB	-2.497315824	5.460869718	2.186695677

PG1695	-2.497315824	40.27391417	16.12688062
PG2064	-2.497315824	9.546409284	3.822667999
PG1207	-2.497315824	109.4234649	43.81643036
cas4	-2.566685708	46.47593994	18.10737473
PG1966	-2.569077773	71.46498772	27.81737029
PG1816	-2.622181615	38.88515851	14.82931551
PG2043	-2.643938534	164.4794011	62.20999428
thiC	-2.705425476	7.123277336	2.632960101
coaD	-2.705425476	9.065989336	3.351040129
aroA	-2.754392453	115.0683262	41.77630027
PG0246	-2.844165244	68.80127004	24.19032093
PG0612	-2.854075228	75.80972078	26.56192102
PG0261	-2.856125569	71.00340128	24.86004189
PG1527	-2.913535128	9.891838567	3.395132762
PG0221	-2.913535128	10.15918556	3.486893107
PG0814	-2.913535128	12.9617195	4.448794654
PG1659	-2.913535128	5.738776573	1.969695343
PG1421	-2.940387987	3301.047842	1122.657233
PG1494	-3.12164478	11.03394909	3.534658766
PG0508	-3.260384548	25.11275577	7.702390744
PG1477	-3.329754432	8.949758704	2.687813437
PG2212	-3.329754432	63.30776683	19.01274347
PG1997	-3.537864084	33.81019955	9.556669997
PG0831	-4.578412344	8.261315727	1.804406223
PG0195	-4.799334071	3856.27945	803.5030261
PG1602	-5.2027413	21.14116229	4.063465983
PG0507	-6.659508864	26.43621032	3.969693691

1. Gene ID according to JVICI (formerly TIGR)
2. Fold Change = ratio of transcript abundance in normal conditions compared to iron-deficient conditions
3. RPKM W83 = The reads per kilobase of transcript per million mapped reads for W83 in normal conditions
4. RPKM W83 + DP = The reads per kilobase of transcript per million mapped reads for W83 in iron-deficient conditions

In the transcriptome comparison of the wild-type W83 in normal and iron-deficient conditions several observations can be made. The most upregulated gene for this set is *hmuY*, PG1551, which is a tonB-dependent receptor gene that is essential for regulating the transport, binding and uptake of hemin. PG1552, or *hmuR*, is another component of this hemin uptake locus that is also shown to be highly upregulated for this comparison (Lewis, 2010). Ribosomal protein encoding genes such as *rplP*, *rplA*, *rpsJ*, and *rpsS* are also shown to be highly upregulated as seen in table 3.

**Table 4. DAVID Functional Annotation Clustering for W83 vs W83 + DP.**

This table depicts the results from DAVID functional clustering analysis for the wild-type W83 under normal and iron-stress conditions. Annotation clusters show functionally similar and related gene groups. The count displays the number of genes identified in the data set for each functional group.

<b>W83 vs W83 + DP</b>		
Annotation Cluster 1	Enrichment Score: 3.31	Count
	Ribosome	11
	rRNA binding	9
	structural constituent of ribosome	11
	structural molecule activity	11
	ribosome	11
	Ribosome	11
	ribonucleoprotein complex	11
	rrna-binding	9
	ribonucleoprotein	11
	translation	14
	ribosomal protein	11
	RNA binding	12
	rna-binding	10
	intracellular non-membrane-bounded organelle	11
	non-membrane-bounded organelle	11
	ribosomal subunit	5
Annotation Cluster 2	Enrichment Score: 0.51	Count
	response to DNA damage stimulus	5
	DNA repair	5
	cellular response to stress	5

The wild-type W83 iron comparison resulted in clusters mostly relating Ribosome, RNA binding, and translation at an enrichment score (ES) of 3.31 and DNA repair, cellular response to stress, and response to DNA damage at an ES of 0.51 (Table 4).





**Table 5. The Most Differentially Regulated Genes for W83 vs W83 6%O<sub>2</sub>.**

This table depicts the most differentially regulated genes for the comparison of the wild-type W83 strain under normal and oxygen-stress conditions. For statistical relevance, this gene list was trimmed at an RPKM value of 1 or greater and a fold change of +/-2 resulting in 251 differentially regulated genes.

Gene ID <sup>1</sup>	Fold Change <sup>2</sup>	RPKM W83 <sup>3</sup>	RPKM W83 6%O <sub>2</sub> <sup>4</sup>
PG1222	8.996886544	80.04123822	720.1219391
PG0618	6.421384378	34.66255752	222.5816054
PG1639	6.317813662	2.237439676	14.13572695
PG2161	6.001922979	1.789951741	10.74315248
PG0843	5.528086954	2.065328932	11.41731792
PG1426	5.528086954	4.052720922	22.40379366
PG0080	4.738360247	1.220421641	5.78279739
PG0492	4.738360247	1.234449476	5.849266325
PG0691	4.738360247	11.30495836	53.5669653
PG0619	4.554090681	12.4880354	56.87164565
PG0426	4.54092857	2.744973916	12.46473048
<i>cydA</i>	4.431899136	13.62804166	60.39810607
PG1735	4.343496893	4.644199111	20.17206441
PG0059	4.211875775	2.517119635	10.60179521
PG1975	4.10657888	1.529873283	6.282545312
PG1482	3.948633539	1.917805437	7.572710868
PG1871	3.948633539	2.214373288	8.743748631
<i>fetB</i>	3.849230873	577.5334086	2223.059427
<i>rplP</i>	3.817012421	17.77607246	67.85148937
<i>acpP</i>	3.626893028	36.70533949	133.1263399
PG1068	3.594062364	38.41210305	138.0554939
PG1572	3.422149067	2.395474449	8.197670649
PG1842	3.356338508	38.93550614	130.6807386
PG1237	3.334401655	9.6657394	32.22945745
PG0867	3.302493505	5.09210409	16.81664069
PG0847	3.242035958	3.872001868	12.55316929
<i>sodB</i>	3.223206083	1071.733605	3454.418274
PG0434	3.191812111	14.31961393	45.70551715
PG0132	3.158906831	3.356159514	10.60179521

PG1811	3.158906831	3.464422724	10.94378861
PG1179	3.158906831	1.220421641	3.85519826
PG0294	3.158906831	2.892851298	9.138247727
PG1381	3.158906831	4.295884178	13.57029787
PG2103	3.158906831	4.773204642	15.07810875
PG0493	3.158906831	6.079081384	19.20325171
PG2000	3.158906831	6.680202669	21.10213784
PG0979	3.158906831	8.105441845	25.60433561
PG0634	3.158906831	8.851409707	27.96077859
PG0799	3.158906831	5.196634086	16.41568291
PG2008	3.131674876	7.468863379	23.39005179
PG1244	3.088708902	13.35046878	41.23571177
prtQ	3.07993416	6.754534871	20.80352269
tlr	3.046423502	51.02371832	155.4398547
PG0218	2.983412007	3.020543563	9.011525932
PG1891	2.961475154	5.053981386	14.9672403
PG1827	2.933653712	295.592965	867.1673992
PG1385	2.922831943	150.5166401	439.9348438
PG1467	2.915913998	6.843933126	19.9563204
folB	2.895664595	5.460869718	15.8128471
PG0047	2.852106527	199.3379491	568.5330656
PG2208	2.843016148	6.317476732	17.96068836
PG1791	2.843016148	7.458132253	21.20359043
PG0819	2.843016148	1.309720786	3.723557344
PG0686	2.82521949	14.72045254	41.58850941
PG2145	2.813401396	17.01340268	47.86553087
PG1160	2.807917183	2.876708155	8.077558259
rplA	2.807917183	82.96772017	232.9664871
PG0707	2.794672291	60.33971593	168.6297321
rpsF	2.780468742	546.9971167	1520.908385
tuf	2.755306315	379.9579377	1046.900505
cydB	2.746095143	24.35810616	66.88967702
PG1359	2.743261195	18.89393504	51.83099883
PG1079	2.714685558	13.37240211	36.30186688
PG1044	2.710782839	74.24558667	201.2636622
PG1333	2.685070806	2.684927611	7.209220746
PG1767	2.662507186	10.83256097	28.84177142
PG0778	2.656353472	9.844734574	26.15109486
PG1784	2.653481738	10.13180231	26.88455239
topA	2.637389194	28.85701666	76.1071839
PG1282	2.632422359	6.359039079	16.73967665

PG1375	2.632422359	17.41574667	45.84560093
PG0460	2.610933197	14.53717712	37.95559834
trxB	2.587394082	51.98840725	134.5144972
PG0616	2.572056215	214.4829129	551.6621093
4hbD	2.561006485	91.51850029	234.3794727
PG0553	2.544833623	63.11434512	160.6155075
PG1042	2.531770916	13.30237359	33.67856258
PG0257	2.529063445	36.31893781	91.85289796
aroK	2.527125465	8.614740998	21.77053135
PG0789	2.513457118	93.46693609	234.9251358
PG1041	2.50854366	17.22406392	43.20731635
PG1235	2.502104421	34.00347194	85.08023746
hprA	2.488634583	80.37896496	200.033872
rpsT	2.485922332	145.3019648	361.2093993
PG1870	2.481998224	3.417180596	8.481436172
nqrD	2.463292633	98.70305313	243.1345036
PG1613	2.453793699	89.09981998	218.6325769
PG1100	2.45230925	14.3700351	35.23977001
pabB	2.44660431	10.14305986	24.81605398
PG1032	2.442180071	42.45932036	103.693306
PG2078	2.441667116	56.85729059	138.8265767
dtd	2.43364761	69.70143202	169.6287234
pruA	2.429928332	7.699424767	18.70905038
PG0654	2.429413516	64.82280473	157.481398
PG0727	2.42182857	23.34719662	56.54290781
PG0651	2.420461078	44.94335349	108.7836379
PG1248	2.41777869	57.21976876	138.3447376
tsf	2.413546792	34.75760835	83.88911414
PG1779	2.387545861	27.98833631	66.8234365
PG0450	2.382239138	520.672038	1240.365307
PG1486	2.369180123	1.591068214	3.769527187
PG1504	2.369180123	1.958609808	4.640299425
PG1742	2.369180123	3.640579812	8.625189327
PG1574	2.369180123	4.211651155	9.978160202
PG0901	2.369180123	2.587882035	6.131158678
PG1869	2.369180123	107.3971044	254.4430852
abfD	2.361063966	708.1151999	1671.905282
PG1841	2.349271047	41.49433581	97.48144171
PG0718	2.339930986	19.86110836	46.47362286
PG1691	2.322725611	7.769152236	18.04560888
PG0491	2.316702336	92.93690525	215.3071455

PG0723	2.301893991	219.7206816	505.7737167
PG0626	2.297386786	4.087779062	9.391209602
PG0310	2.281432711	16.10956567	36.75289008
feoB-1	2.268669451	32.5445771	73.83288789
rplJ	2.264271778	332.6241749	753.1515321
PG0668	2.263883229	42.50545031	96.22737609
PG0645	2.253610361	24.53081494	55.28289872
PG0360	2.250296533	101.4003118	228.1807701
ispF	2.247683707	17.13082648	38.50467955
PG1345	2.244486433	5.456002632	12.24592388
PG0846	2.244486433	10.46433325	23.48705401
PG0970	2.244486433	10.57277194	23.73044317
PG0006	2.228676599	39.51631608	88.06908892
PG1184	2.225593449	9.229438663	20.54097823
PG1829	2.222934437	5.196634086	11.55177686
PG0646	2.221942941	37.94268959	84.30649129
PG1050	2.221106366	11.49400449	25.52940654
rluB	2.220525684	144.9008552	321.7560706
PG0004	2.219772368	16.90933134	37.53486646
PG0275	2.212095519	231.8513961	512.8774344
PG1276	2.211234782	6.354858251	14.0520836
PG0984	2.211234782	7.782398873	17.20871107
PG0209	2.211234782	18.44606756	40.78858617
PG1424	2.210066979	104.3120889	230.5367031
rpsG	2.20913584	203.3114996	449.1427205
fhs	2.206066836	94.45536704	208.3748527
PG0199	2.20527458	23.91616191	52.74170393
PG0569	2.20527458	11.18280262	24.66115036
PG1271	2.205130614	108.4448811	239.1351272
rpmJ	2.197500404	253.3470156	556.7301692
efp-2	2.193685299	20.45659132	44.87532366
mnmA	2.190854738	9.196989607	20.14926825
PG2224	2.181787345	68.13364691	148.6531286
PG2101	2.175910617	352.9224125	767.9276245
PG1943	2.174985031	15.27091695	33.21401578
nqrC	2.174985031	26.73968723	58.15841946
ispD	2.171748446	3.852810922	8.367336134
abfT-1	2.171748446	55.68738749	120.9389973
gdh	2.170405374	141.5908014	307.3094362
PG2170	2.164436162	13.48707823	29.19191985
ftn	2.162346938	56.03327188	121.1633739

pgk	2.155016948	30.24548526	65.17953335
PG1281	2.153375927	187.3913395	403.5239993
PG0781	2.151602357	134.0753661	288.4768736
PG0771	2.147069487	78.10698505	167.7011243
tnaA	2.143668307	211.7590733	453.9412142
PG0259	2.142601151	86.06151896	184.3955096
PG0311	2.134396507	12.49588951	26.67118293
umuC	2.132262111	4.960605286	10.5773107
PG0147	2.132262111	11.93301161	25.44430852
PG0176	2.132083843	403.1942141	859.6438696
PG0838	2.129869	16.36999744	34.86595008
PG0708	2.119577381	74.82902945	158.6059183
PG0775	2.111310178	18.336091	38.71317556
PG1096	2.109866876	79.72970635	168.2190665
PG0041	2.105937887	2.058730437	4.335558426
PG2131	2.105937887	2.624776483	5.527616242
PG0869	2.105937887	2.730434859	5.750126218
purN	2.105937887	3.321559931	6.994998905
PG1181	2.105937887	6.443826267	13.57029787
PG1733	2.105937887	6.620369452	13.94208686
PG0415	2.102108909	64.06551784	134.6726958
serC	2.092500929	128.2220277	268.3047121
hutH	2.089738365	14.01769436	29.29331369
PG0929	2.082006775	14.67538073	30.55424211
purB	2.081335809	51.30129543	106.7752232
guaA	2.079424281	147.2208828	306.1346784
PG1102	2.076800388	60.77330748	126.2140286
PG0780	2.073354158	160.8337125	333.4652466
PG1010	2.067683474	315.9653942	653.316424
hemH	2.067501839	201.4550781	416.5087445
PG0472	2.065439082	4.205308307	8.685808128
PG1879	2.065439082	16.4254395	33.92574469
acdA	2.04937344	34.19749905	70.08344626
PG0804	2.045869189	79.4152286	162.4731693
PG0702	2.043998538	5.276736346	10.78564137
PG1553	2.042759751	5.479444104	11.19318787
PG1097	2.040127328	18.76842602	38.28997883
trx	2.037172569	250.5932437	510.501682
cdsA	2.035938538	2397.781669	4881.736104
PG0851	2.023674689	8.834723245	17.87860581
PG0079	2.023674689	39.59340256	80.1241666

fkpA	2.016840515	137.4175549	277.1492922
upp	2.015818924	164.8075382	332.2221542
PG0202	2.013447372	95.75163529	192.7908784
batC	2.010065715	420.927361	846.0916568
PG2185	2.006332717	9.051692174	18.16070615
PG0078	2.000640993	6.913976681	13.83238517
pyrB	2.000640993	73.94554732	147.9384932
PG5SB	-2.015719431	3153.298317	1564.353783
PG0682	-2.0400869	15.8903879	7.789074035
PG0841	-2.045498271	15.13650465	7.399910754
PG5SA	-2.048600331	3030.984948	1479.539421
PG0679	-2.053992865	134.6687287	65.56436052
trmD	-2.08560608	26.6116719	12.75968274
PG1250	-2.107543718	118.0882189	56.03120729
PG1521	-2.110434724	12.27395479	5.815841946
hup-1	-2.110434724	494.7507059	234.4307077
PG5SC	-2.121788329	3159.264822	1488.963239
PG0115	-2.136815158	19.86110836	9.294724572
PG1522	-2.142902951	26.47323583	12.35391263
pyrH	-2.144009822	200.027107	93.29579789
PG1966	-2.179429706	71.46498772	32.7906826
PG1866	-2.21595646	35.79903482	16.15511652
PG0814	-2.21595646	12.9617195	5.849266325
PG0834	-2.236055839	113.5195047	50.76774146
PG0425	-2.271820909	25.49114152	11.22057704
PG0831	-2.321478197	8.261315727	3.558644548
yadS	-2.321478197	11.19780236	4.823565595
PG1451	-2.321478197	26.05959152	11.22543023
PG1492	-2.32967406	170.3075422	73.10359211
cas4	-2.342582544	46.47593994	19.83961678
PG0965	-2.374239065	14.51312222	6.11274679
PG1645	-2.532521669	6.609052581	2.609672668
PG2129	-2.532521669	6.609052581	2.609672668
PG0039	-2.532521669	10.73971044	4.240718086
PG1695	-2.532521669	40.27391417	15.90269282
PG1421	-2.561765568	3301.047842	1288.58311
PG0119	-2.769945575	16.13261226	5.824162178
PG0770	-2.849086878	6.953769353	2.440701057
PG2043	-2.900982813	164.4794011	56.69781989
PG0564	-2.912399919	38.00205234	13.04836334
PG0313	-3.165652086	5.213451672	1.64688081

PG0681	-3.165652086	5.213451672	1.64688081
PG1898	-3.165652086	7.935746634	2.506828425
PG1203	-3.165652086	23.01366524	7.269802433
PG0200	-3.165652086	6.973837951	2.202970434
PG1508	-3.323934691	12.32425789	3.70773166
PG1085	-3.552565119	261.3760855	73.57390414
PG0606	-3.957065108	149.1626451	37.69527187
PG1710	-4.115347712	4.460582613	1.083889607
PG1450	-4.431912921	7.159806963	1.615511652
PG1457	-4.431912921	4.81910084	1.087363612
PG1532	-4.748478129	24.78394718	5.219345336
PG0161	-4.959521602	100.9532782	20.35544681
PG2058	-5.698173755	7.435184154	1.304836334
PG0197	-5.698173755	10.98379477	1.92759913
PG0823	-5.698173755	9.205466095	1.615511652
PG1419	-8.230695424	10.57698756	1.285066087
PG0507	-10.13008668	26.43621032	2.609672668

1. Gene ID according to JVICI (formerly TIGR)
2. Fold Change = ratio of transcript abundance in normal conditions compared to microaerobic conditions
3. RPKM W83 = The reads per kilobase of transcript per million mapped reads for W83 in normal conditions
4. RPKM W83 6% O<sub>2</sub> = The reads per kilobase of transcript per million mapped reads for W83 in microaerobic conditions

The transcriptome comparison of the wild-type W83 in anaerobic and microaerobic conditions resulted in the differential regulation of several noteworthy genes (Table 5). The *sodB* gene (superoxide dismutase Fe/Mn), a detoxification gene important for the aerotolerance of the bacterium, is highly up-regulated for this set. The highly up-regulated genes *cydA* and *cydB* are cytochrome d oxidase subunits. The *feoB1* gene, a ferrous iron transporter in *P. gingivalis* is also up-regulated. Additionally, PG0618, an ABC transport component is the second most highly regulated gene for this comparison.

**Table 6. DAVID Functional Annotation Clustering for W83 vs W83 6%O<sub>2</sub>.**

This table depicts the results from DAVID functional clustering analysis for the wild-type W83 under normal and oxygen-stress conditions. Annotation clusters show functionally similar and related gene groups. The count displays the number of genes identified in the data set for each functional group.

<b>W83 vs W83 6%O2</b>		
Annotation Cluster 1	Enrichment Score: 1.29	Count
	acyl-CoA dehydrogenase activity	3
	Acyl-CoA oxidase/dehydrogenase, central region	3
	Acyl-CoA oxidase/dehydrogenase, type1/2, C-terminal	3
Annotation Cluster 2	Enrichment Score: 1.1	Count
	cellular homeostasis	6
	homeostatic process	6
	cell redox homeostasis	5
	Thioredoxin fold	5
	Thioredoxin-like	4
Annotation Cluster 3	Enrichment Score: 1.05	Count
	FAD	5
	oxidoreductase	9
	electron carrier activity	10
	Flavoprotein	4
	FAD binding	4
	coenzyme binding	10
Annotation Cluster 4	Enrichment Score: 0.9	Count
	Ribosome	10
	trna-binding	4
	tRNA binding	4
	Ribosome	7
	ribonucleoprotein	7
	ribosomal protein	7
	rRNA binding	5
	ribosome	7
	rrna-binding	5
	ribonucleoprotein complex	7
	non-membrane-bounded organelle	8
	intracellular non-membrane-bounded organelle	8
	structural constituent of ribosome	6
	structural molecule activity	6
	rna-binding	6
	RNA binding	8



	translation	10
Annotation Cluster 5	Enrichment Score: 0.7	Count
	iron-sulfur cluster assembly	3
	metallo-sulfur cluster assembly	3
	cofactor metabolic process	8
	cofactor biosynthetic process	6
Annotation Cluster 6	Enrichment Score: 0.68	Count
	pyrimidine base biosynthetic process	3
	pyrimidine base metabolic process	3
	'de novo' pyrimidine base biosynthetic process	3
	nucleobase biosynthetic process	3
	pyrimidine biosynthesis	3
	nucleobase metabolic process	3
	nucleotide biosynthetic process	7
	pyrimidine nucleotide biosynthetic process	3
	pyrimidine nucleotide metabolic process	3
Annotation Cluster 7	Enrichment Score: 0.66	Count
	translational elongation	3
	translation elongation factor activity	3
	elongation factor	3
	translation factor activity, nucleic acid binding	3
Annotation Cluster 8	Enrichment Score: 0.63	Count
	organic acid catabolic process	3
	carboxylic acid catabolic process	3
	amine catabolic process	3
	cellular amino acid catabolic process	3
Annotation Cluster 9	Enrichment Score: 0.58	Count
	cis-trans isomerase activity	3
	peptidyl-prolyl cis-trans isomerase activity	3
	Rotamase	3
	protein folding	3
	Isomerase	5
Annotation Cluster 10	Enrichment Score: 0.56	Count
	nucleoside monophosphate biosynthetic process	4
	nucleoside monophosphate metabolic process	4
	purine nucleoside monophosphate metabolic process	3
	purine nucleoside monophosphate biosynthetic process	3
	purine ribonucleoside monophosphate metabolic process	3
	purine ribonucleoside monophosphate biosynthetic process	3
	nucleobase, nucleoside, nucleotide and nucleic acid biosynthetic process	9
	nucleobase, nucleoside and nucleotide biosynthetic process	9
	nucleotide biosynthetic process	7
	ribonucleoside monophosphate biosynthetic process	3

	ribonucleoside monophosphate metabolic process	3
	purine nucleotide biosynthetic process	4
	purine nucleotide metabolic process	4
	nitrogen compound biosynthetic process	14
	purine ribonucleotide biosynthetic process	3
	purine ribonucleotide metabolic process	3
	ribonucleotide biosynthetic process	3
	ribonucleotide metabolic process	3
	Purine metabolism	3
Annotation Cluster 11	Enrichment Score: 0.53	Count
	Inorganic ion transport and metabolism	5
	cell envelope	8
	envelope	8
	external encapsulating structure	8
	tonb box	3
	receptor	3
	external encapsulating structure part	5
	cell outer membrane	4
	TonB-dependent receptor, plug	3
	TonB-dependent receptor, beta-barrel	3
	outer membrane	4
	cell membrane	7
	membrane	7
	plasma membrane	7

The most highly effected gene clusters for the comparison of W83 in normal and oxidative-stress conditions are shown in table 6 and include Acyl-CoA dehydrogenase activity (ES1.29), cellular homeostasis processing (ES1.1), FAD and oxidoreductase (ES1.05), and ribosome (ES0.9).



**Table 7. The Most Differentially Regulated Genes for 77 vs 77 + DP.**

This table depicts the most differentially regulated genes for the comparison of the wild-type ATCC 33277 strain under normal and iron-stress conditions. For statistical relevance, this gene list was trimmed at an RPKM value of 1 or greater and a fold change of +/-2 resulting in 1053 differentially regulated genes. The top 100 most upregulated genes are shown.

Gene ID <sup>1</sup>	Fold Change <sup>2</sup>	RPKM 77 <sup>3</sup>	RPKM 77 + DP <sup>4</sup>
PG1233	33.97956024	3.451914072	117.2945222
PG1021	15.57196254	13.54614765	210.9401038
PG0337	15.3412668	6.260824543	96.04897972
PG1460	14.55376838	14.36859233	209.1171646
PG1181	11.78086253	55.87785905	658.2893758
PG0283	11.23740584	34.30391347	385.4869976
PG0371	11.10223255	3.756494726	41.70547804
PG1571	10.80245526	34.77145224	375.6170571
PG1674	10.72893208	38.527355	413.3573751
PG1486	10.51831158	41.15448666	432.8757137
PG2130	10.42027724	36.53868839	380.7432629
PG1198	10.33516921	19.95637823	206.2525459
PG1857	10.3242352	34.63615476	357.5918081
PG2134	10.03560959	31.09360591	312.0432896
PG1975	9.791778419	45.12074577	441.8123446
PG0285	9.737539461	42.87043483	417.4525508
PG1482	9.72170416	33.07056964	321.5022944
PG0008	9.705532959	13.46577343	130.6925078
PG1554	9.689221139	31.08250061	301.1652219
PG2038	9.646801541	44.17411843	426.1389538
PG0280	9.627910108	37.33599611	359.4676144
PG1680	9.613639315	39.95837104	384.1453668
PG1534	9.612322558	24.07046236	231.3730483
thiE	9.594712196	51.64020836	495.472937
PG2131	9.536571718	43.5707484	415.5155669
PG1040	9.520289683	38.72824885	368.704148
PG1556	9.493670452	37.49602075	355.9748642
PG1485	9.390821212	34.1578939	320.7706746
PG0282	9.377489868	45.04439658	422.4033725
PG1478	9.295855323	39.91275646	371.0232096
PG1483	9.254045081	48.68565937	450.5392866
hmuY	9.187849199	100.9262429	927.2951001
PG2133	9.164060101	43.06376355	394.6389174
PG1489	9.065015072	45.91369081	416.2082992

PG1020	9.020611416	30.19227511	272.3527815
PG1679	9.003673446	33.50954865	301.7090334
PG1179	8.993529294	27.0922953	243.6553514
topB-2	8.980407779	50.68576981	455.1788815
PG1490	8.972544252	40.98503947	367.7400803
PG1180	8.897633905	39.89284985	354.9519734
PG1488	8.879747066	31.45363494	279.3003226
PG0524	8.853886864	55.12161735	488.0405637
PG1178	8.777341703	30.13132037	264.4728949
PG1475	8.681246609	38.09217459	330.6875615
PG0877	8.678875922	34.63615476	300.6028896
PG0541	8.675632403	30.01439286	260.3938392
PG1480	8.675515057	37.09985743	321.8603718
PG2063	8.522926002	22.21231664	189.313931
PG1481	8.509090083	46.71973013	397.5423923
PG2065	8.454459283	53.21700862	449.9210325
PG0819	8.394761701	29.4380916	247.1257639
PG1553	8.37853734	51.21865564	429.1374188
thiC	8.342511904	59.4075586	495.6082648
PG0470	8.319028251	14.33601048	119.2616762
thiG	8.243270425	58.70245412	483.9002039
PG1555	8.182877171	51.28685804	419.6740599
thiS	8.162115633	43.84446083	357.8635592
PG1476	8.116032702	47.68431521	387.0074616
PG0770	8.09278554	33.53820111	271.417469
PG1477	8.049883219	36.58669342	294.5186094
PG1742	8.038937129	20.56521689	165.3224856
PG0281	8.013848319	51.06050238	409.1911212
PG1459	8.007064691	13.8826979	111.1596602
PG1655	7.96481518	39.22853778	312.4480532
PG1454	7.962806885	29.1265774	231.929311
PG1019	7.932014634	42.14138753	334.2661026
PG1022	7.878285032	39.04016988	307.569586
PG1496	7.829673648	38.17741922	298.9167332
PG1479	7.817600754	52.61128657	411.2940336
PG1733	7.737919659	44.61480722	345.2257939
PG2223	7.713970313	58.32452337	449.9136419
PG0847	7.703208495	30.5366668	235.2303111
PG1678	7.681847778	21.28680345	163.5219838
PG1458	7.641796434	35.06061744	267.9261013
PG1874	7.618766911	45.07793671	343.4382926
purN	7.599389128	39.17210737	297.6840869
thiH	7.584265966	57.66371284	437.3369348
PG1734	7.534165498	43.31932294	326.3749483
fimA	7.52784754	34.96726839	263.2282653
PG1462	7.509146383	21.00671393	157.7424899
PG0562	7.468455736	48.20946899	360.0502852
cas2-1	7.43690219	25.01748034	186.0525543
PG1024	7.40148837	1.93516395	14.32309347
PG1333	7.34972971	49.81112006	366.098269
PG1858	7.346982742	137.7230536	1011.848898

PG0870	7.302021728	20.80438297	151.9140565
PG0222	7.292548714	42.9829685	313.4553917
PG2077	7.266915854	44.55377466	323.7685314
PG2057	7.207201086	96.09665581	692.5879221
PG0219	7.206455738	48.15703075	347.0415106
PG1507	7.204682714	39.89304646	287.4167422
PG1630	7.197590619	21.72570661	156.3727421
PG1160	7.189862236	47.13506477	338.8946222
coaD	7.152698845	49.34668072	352.9619462
PG0871	7.058587248	28.93892233	204.2679081
PG0174	7.041839224	50.258619	353.9131146
PG0732	7.015419677	36.74985878	257.8156824
pruA	6.986218194	50.59528834	353.4697239
PG2004	6.970333708	59.61591177	415.5427993

1. Gene ID according to JVICI (formerly TIGR)
2. Fold Change = ratio of transcript abundance in normal conditions compared to iron-deficient conditions
3. RPKM 77 = The reads per kilobase of transcript per million mapped reads for ATCC 33277 in normal conditions
4. RPKM 77 + DP = The reads per kilobase of transcript per million mapped reads for ATCC 33277 in iron-deficient conditions

The transcriptome results for the comparison of the wild-type ATCC 33277 strain in normal and iron-stress conditions yielded several noteworthy genes (Table 7). The first is *hmuY*, PG1551, which is a tonB-dependent receptor gene that is essential for regulating the transport, binding, and uptake of hemin, is highly regulated in this comparison. Additionally, the genes *thi-E*, *-C*, *-G*, *-S*, and *-H* which play a role in the thiamine biosynthetic pathway, are also highly regulated for this comparison.

**Table 8. DAVID Functional Annotation Clustering for 77 vs 77 + DP.**

This table depicts the results from DAVID functional clustering analysis for the wild-type ATCC 33277 under normal and iron-stress conditions. Annotation clusters show functionally similar and related gene groups. The count displays the number of genes identified in the data set for each functional group.

<b>77 vs 77 + DP</b>		
Annotation Cluster 1	Enrichment Score: 2.33	Count
	DNA integration	18
	Integrase-like, catalytic core, phage	8
	Integrase, catalytic core, phage	7
Annotation Cluster 2	Enrichment Score: 2.1	Count
	cation binding	87
	ion binding	87
	metal-binding	48
	metal ion binding	79
	transition metal ion binding	49
Annotation Cluster 3	Enrichment Score: 1.91	Count
	magnesium	20
	magnesium ion binding	21
	metal ion-binding site:Magnesium	8
Annotation Cluster 4	Enrichment Score: 1.07	Count
	nucleotide-binding	77
	atp-binding	68
	ATP binding	90
	adenyl ribonucleotide binding	90
	nucleoside binding	100
	adenyl nucleotide binding	97
	purine nucleoside binding	97
	ribonucleotide binding	99
	purine ribonucleotide binding	99
	purine nucleotide binding	106
	nucleotide binding	124
Annotation Cluster 5	Enrichment Score: 1.01	Count
	Biotin metabolism	5
	sulfur compound biosynthetic process	13
	cellular amide metabolic process	10
	amide biosynthetic process	5
	biotin biosynthetic process	5

	biotin metabolic process	5
Annotation Cluster 6	Enrichment Score: 1.01	Count
	Thiamine metabolism	7
	sulfur metabolic process	16
	sulfur compound biosynthetic process	13
	thiamin and derivative metabolic process	7
	thiamin and derivative biosynthetic process	7
	thiamin metabolic process	7
	thiamin biosynthetic process	6
	aromatic compound biosynthetic process	10
	thiamine biosynthesis	3
Annotation Cluster 7	Enrichment Score: 0.98	Count
	Porphyrin and chlorophyll metabolism	12
	cofactor metabolic process	42
	cofactor biosynthetic process	34
	vitamin metabolic process	31
	vitamin biosynthetic process	31
	heterocycle biosynthetic process	27
	coenzyme biosynthetic process	20
	water-soluble vitamin metabolic process	27
	water-soluble vitamin biosynthetic process	27
	coenzyme metabolic process	23
	porphyrin metabolic process	13
	porphyrin biosynthetic process	13
	tetrapyrrole metabolic process	13
	tetrapyrrole biosynthetic process	13
	cobalamin metabolic process	10
	cobalamin biosynthetic process	10
	nitrogen compound biosynthetic process	54
Annotation Cluster 8	Enrichment Score: 0.97	Count
	DNA replication	10
	Mismatch repair	10
	Homologous recombination	10
	DNA polymerase activity	6
	DNA-directed DNA polymerase activity	5
	nucleotidyltransferase activity	13
Annotation Cluster 9	Enrichment Score: 0.89	Count
	cellular response to stress	25
	DNA repair	24
	response to DNA damage stimulus	24
	dna repair	11
	DNA damage	11
Annotation Cluster 10	Enrichment Score: 0.87	Count



	Nucleotide excision repair	6
	Base excision repair	5
	HhH1	6
	Helix-hairpin-helix DNA-binding, class 1	6
Annotation Cluster 11	Enrichment Score: 0.86	Count
	Ubiquinone and other terpenoid-quinone biosynthesis	6
	vitamin K metabolic process	4
	vitamin K biosynthetic process	4
	quinone cofactor metabolic process	4
	quinone cofactor biosynthetic process	4
	fat-soluble vitamin biosynthetic process	4
	menaquinone metabolic process	4
	menaquinone biosynthetic process	4
	fat-soluble vitamin metabolic process	4
Annotation Cluster 12	Enrichment Score: 0.84	Count
	ncRNA metabolic process	27
	tRNA metabolic process	23
	ncRNA processing	17
	tRNA modification	9
	RNA processing	22
	tRNA processing	13
	trna processing	8
	RNA modification	10
Annotation Cluster 13	Enrichment Score: 0.82	Count
	Other glycan degradation	5
	glycosidase	7
	Glycoside hydrolase, subgroup, catalytic core	8
	Glycoside hydrolase family 2, immunoglobulin-like beta-sandwich	3
	Glycoside hydrolase family 2, carbohydrate-binding	3
Annotation Cluster 14	Enrichment Score: 0.8	Count
	metal ion-binding site:Magnesium	8
	phenylalanyl-tRNA aminoacylation	3
	phenylalanine-tRNA ligase activity	3
Annotation Cluster 15	Enrichment Score: 0.8	Count
	membrane	40
	cell membrane	35
	intrinsic to membrane	67
	transmembrane	39
	integral to membrane	65
	plasma membrane	39
Annotation Cluster 16	Enrichment Score: 0.73	Count
	iron ion binding	20
	iron-sulfur	12

	s-adenosyl-l-methionine	10
	iron	16
	4 iron, 4 sulfur cluster binding	14
	4fe-4s	10
	metal cluster binding	22
	iron-sulfur cluster binding	22
Annotation Cluster 17	Enrichment Score: 0.59	Count
	transport	26
	metal ion transport	17
	cation transport	24
	ion transport	27
	monovalent inorganic cation transport	11
Annotation Cluster 18	Enrichment Score: 0.59	Count
	Elp3	9
	Elongator protein 3/MiaB/NifB	9
	metal cluster binding	22
	iron-sulfur cluster binding	22
	Radical SAM	9
	radical SAM enzyme activity	3
	Uncharacterised protein family UPF0004	3
Annotation Cluster 19	Enrichment Score: 0.58	Count
	ligase	25
	ncRNA metabolic process	27
	tRNA metabolic process	23
	Aminoacyl-tRNA biosynthesis	10
	Aminoacyl-tRNA synthetase	11
	tRNA aminoacylation	11
	tRNA aminoacylation for protein translation	11
	amino acid activation	11
	aminoacyl-tRNA ligase activity	11
	ligase activity, forming carbon-oxygen bonds	11
	ligase activity, forming aminoacyl-tRNA and related compounds	11
	protein biosynthesis	13
	translation	32
	Aminoacyl-tRNA synthetase, class II, conserved region	5
	Aminoacyl-tRNA biosynthesis	7
	Aminoacyl-tRNA synthetase, class I, conserved site	4
Annotation Cluster 20	Enrichment Score: 0.5	Count
	Nicotinate and nicotinamide metabolism	7
	cellular amide metabolic process	10
	secondary metabolic process	10
	nicotinamide nucleotide biosynthetic process	4
	NAD biosynthetic process	4

	NAD metabolic process	4
	alkaloid metabolic process	5
	nicotinamide metabolic process	5
	nicotinamide nucleotide metabolic process	5
	pyridine nucleotide biosynthetic process	4
	oxidoreduction coenzyme metabolic process	5
	pyridine nucleotide metabolic process	5

Clustering for the comparison of the wild-type ATCC 33277 strain in normal and iron-stress conditions exhibited the most effected groups to be DNA integration, metal-binding, and ATP/nucleotide-binding at enrichment scores of 2.33, 2.1, and 1.07 respectively. Similar to the W83 iron-stress comparison, the ATCC 33277 comparison exhibited functional clusters such as DNA damage and repair at enrichment score of 0.97 (Table 8).

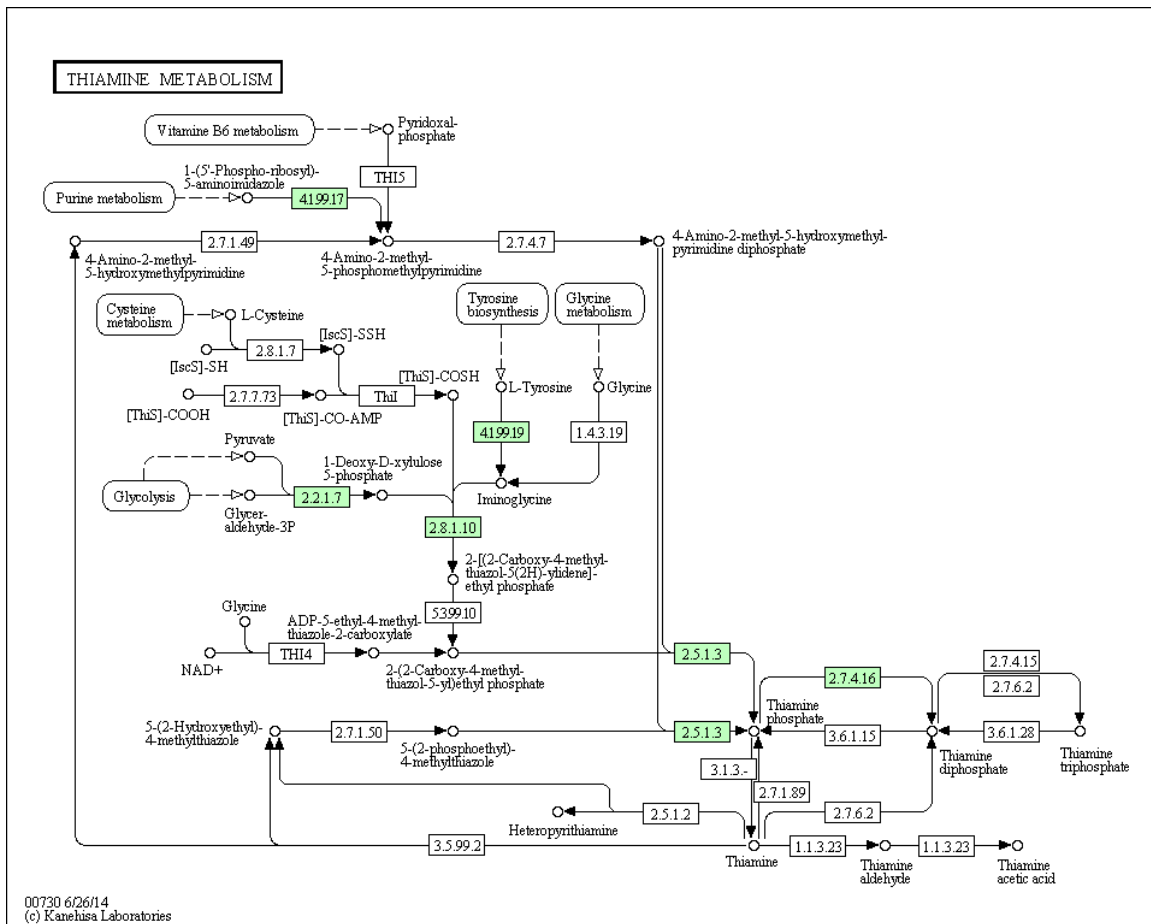


**Figure 10. KEGG Thiamine Metabolism Pathway for 77 vs 77 + DP.**

This figure depicts the KEGG thiamine metabolism pathway for the comparison of the wild-type ATCC 33277 strain under normal and iron-stress conditions. Green boxes depict genes that are found in *Porphyromonas gingivalis* W83 as well as those identified as differentially regulated in the data set for this particular condition.

The thiamine metabolism pathway in figure 10 is highlighted for the comparison of ATCC 33277 in normal and iron-deficient conditions as all 7 *P.g* genes found in the pathway were shown to be affected by the presence of iron-stress. These results show that

thiamine metabolism is affected in iron-stress conditions, which impacts the synthesis of important nutrients in the bacteria.

**Table 9. The Most Differentially Regulated Genes for 77 vs 77 6%O<sub>2</sub>.**

This table depicts the most differentially regulated genes for the comparison of the wild-type ATCC 33277 strain under normal and oxygen-stress conditions. For statistical relevance, this gene list was trimmed at an RPKM value of 1 or greater and a fold change of +/-2 resulting in 1312 differentially regulated genes. The top 100 most upregulated genes are shown.

Gene ID <sup>1</sup>	Fold Change <sup>2</sup>	RPKM 77 <sup>3</sup>	RPKM 77 6%O <sub>2</sub> <sup>4</sup>
PG2105	28.31027557	625.7550893	17715.29902
PG1446	27.52772462	1.414005952	38.92436647
PG0195	26.80606154	714.4968937	19152.8477
PG1219	26.12288033	410.6444209	10727.21507
PG1067	22.73928934	610.7107247	13887.12787
PG1671	20.66863044	546.3707931	11292.73601
PG0457	20.61916655	300.6514697	6199.182726
PG0101	20.51316238	544.5444841	11170.32943
PG1266	19.41811185	534.8041691	10384.88718
PG2075	19.30009765	532.9778601	10286.52474
rplS	18.57482498	430.7419772	8000.956836
PG1828	18.32915084	650.0159757	11914.24087
rpmJ	18.26938821	137.8785291	2518.956374
PG1207	16.70979558	217.1699708	3628.865817
PG2123	16.25835241	704.694395	11457.16981
PG5SB	15.53658831	5108.152614	79363.2642
PG5SD	15.47126351	5110.621514	79067.77211
PG1222	15.40467057	360.5524612	5554.191887
PG5SC	15.287259	5170.492321	79042.65529
PG5SA	15.15592168	5184.688492	78578.73271
PG1795	13.27297021	639.9224748	8493.671944
PG1430	13.16390301	455.2693401	5993.121435
PG1107	12.88789389	110.2967622	1421.492967
panD	12.84437172	470.5431573	6043.831221
ragB	12.60137582	570.2862254	7186.391053
tuf	12.24147978	555.1656703	6796.049327
PG0695	11.95888246	475.9181259	5691.448928
rpsF	11.68166764	480.7449051	5615.902201
proS	11.12948077	528.0195912	5876.583887
hup-1	10.75519959	397.9643719	4280.186251
PG0090	10.19650767	443.8463684	4525.682901
PG2083	10.17404257	627.201602	6381.175797
PG0386	9.81353181	511.2837982	5017.499817
PG1156	9.733332739	402.3161307	3915.876766

fmt	9.721802186	631.2152497	6136.549795
rpsR	9.637377012	355.2773197	3423.941474
PG1516	9.425441567	115.5541684	1089.149062
rpmB	9.382114442	617.4408492	5792.900708
PG0145	8.84276696	607.1957167	5369.290221
PG0785	8.842749948	449.1152239	3971.413623
PG0340	8.492985099	734.4084524	6237.320042
PG0087	8.342870341	603.3775158	5033.900381
fetB	7.938129452	523.1547193	4152.869885
PG0429	7.592631239	488.2686361	3707.243699
PG23SC	7.56907141	405.0893976	3066.150577
PG23SD	7.536378521	407.8179059	3073.470106
PG23SA	7.490056476	408.6411627	3060.745387
PG23SB	7.463235978	409.7702006	3058.211704
PG0771	7.27622858	254.2685704	1850.116239
efp-1	7.025868112	483.9042593	3399.847504
rplE	6.966163229	541.1246308	3769.562506
murl	6.95786831	549.1999119	3821.260663
PG1827	6.879280682	644.6942092	4435.03242
sodB	6.8155079	503.0768052	3428.72394
PG1085	6.7321739	533.8176688	3593.753377
rplJ	6.649665445	443.7670109	2950.902158
groES	6.644118543	464.3999549	3085.528352
PG1469	6.593950388	278.5154695	1836.517188
PG0618	6.437596493	548.8010404	3532.959653
PG0624	6.426838081	454.7887784	2922.853839
PG1317	6.420598238	550.798815	3536.457901
bcp	6.259135381	522.9657729	3273.313572
PG2100	6.209366398	636.9760147	3955.217462
PG0817	6.19396999	255.9278631	1585.209503
PG1152	6.097956001	349.6612521	2132.218931
clpC	6.01136567	540.1808088	3247.22437
cdsA	5.987597567	535.6991673	3207.551031
PG2213	5.959353429	349.6932753	2083.945819
PG2074	5.940531878	194.9498773	1158.10596
PG0607	5.847711292	394.2689324	2305.570888
PG1670	5.802324602	195.7883714	1136.027684
PG16SB	5.783388192	436.9750869	2527.196558
PG16SA	5.721851615	439.0087904	2511.943157
PG16SD	5.700626787	438.195309	2497.987917
PG16SC	5.675915502	441.494428	2505.885068
rpsN	5.674048857	381.9387189	2167.138952
PG0102	5.452351254	203.7540653	1110.938733
abfD	5.375693607	448.55388	2411.288225
PG1265	5.367158266	214.6544885	1152.084612
PG0469	5.322671032	468.4736387	2493.531066
PG2050	4.975403096	590.523138	2938.090649
PG2026	4.875082672	518.1775746	2526.158515
groEL	4.737899952	509.3936095	2413.455958
PG0853	4.719506351	541.3747481	2555.021562
rpsL	4.708627703	584.9645365	2754.380222

PG0616	4.695228007	391.2668645	1837.08714
PG0854	4.664254631	379.6136127	1770.614551
PG2152	4.65085384	543.2950031	2526.785652
PG0076	4.639715955	548.142817	2543.226973
PG1591	4.600548569	410.5860453	1888.921043
PG1672	4.519758083	681.2839393	3079.238592
PG1715	4.508246267	591.7100809	2667.574763
tnaA	4.502484945	532.7991994	2398.920374
spo0J	4.408401169	503.2468081	2218.513817
nusG	4.253307621	405.5167071	1724.7873
PG1267	4.238187502	695.1714978	2946.267154
PG0100	4.235138177	705.0911824	2986.158585
rplY	4.184154842	483.3158169	2022.268216
rpsP	4.156964476	455.9148726	1895.221929

1. Gene ID according to JVC1 (formerly TIGR)
2. Fold Change = ratio of transcript abundance in normal conditions compared to microaerobic conditions
3. RPKM 77 = The reads per kilobase of transcript per million mapped reads for ATCC 33277 in normal conditions
4. RPKM 77 6% O<sub>2</sub> = The reads per kilobase of transcript per million mapped reads for ATCC 33277 in microaerobic conditions

The results from the transcriptome comparison of the wild-type ATCC 33277 in normal and microaerobic conditions yielded regulation of several noteworthy genes (Table 9). The *sodB* gene (superoxide dismutase Fe/Mn), a detoxification gene important for the aerotolerance of the bacterium, is highly upregulated for this set. Additionally, many genes encoding for ribosomal proteins including *rplS*, *rpmJ*, *rpsF*, *rpsR*, and *rpmB* are highly regulated for this comparison.



**Table 10. DAVID Functional Annotation Clustering for 77 vs 77 6%O2.**

This table depicts the results from DAVID functional clustering analysis for the wild-type ATCC 33277 under normal and oxygen-stress conditions. Annotation clusters show similar and related gene groups. The count displays the number of genes identified in the data set for each functional group.

<b>77 vs 77 6%O2</b>		
Annotation Cluster 1	Enrichment Score: 2.43	Count
	Ribosome	42
	ribosomal protein	31
	ribonucleoprotein	30
	structural molecule activity	30
	Ribosome	30
	structural constituent of ribosome	29
	ribosome	32
	ribonucleoprotein complex	32
	translation	51
	rRNA binding	18
	rna-binding	18
	rna-binding	26
	RNA binding	38
	non-membrane-bounded organelle	37
	intracellular non-membrane-bounded organelle	37
Annotation Cluster 2	Enrichment Score: 2.25	Count
	DNA integration	18
	Integrase-like, catalytic core, phage	10
	Integrase, catalytic core, phage	9
Annotation Cluster 3	Enrichment Score: 0.92	Count
	signal	7
	signal peptide	7
	cell outer membrane	3
Annotation Cluster 4	Enrichment Score: 0.85	Count
	response to DNA damage stimulus	29
	DNA repair	29
	cellular response to stress	29
	dna repair	13
	DNA damage	13
Annotation Cluster 5	Enrichment Score: 0.7	Count
	DNA replication	10

	DNA polymerase activity	6
	DNA-directed DNA polymerase activity	5
Annotation Cluster 6	Enrichment Score: 0.66	Count
	Terpenoid backbone biosynthesis	8
	Isoprene biosynthesis	8
	isoprenoid biosynthetic process	8
	isoprenoid metabolic process	8
	terpenoid biosynthetic process	6
	terpenoid metabolic process	6
	secondary metabolic process	10
	Terpenoid backbone biosynthesis	3
Annotation Cluster 7	Enrichment Score: 0.65	Count
	Other glycan degradation	5
	glycosidase	7
	Glycoside hydrolase, subgroup, catalytic core	9
	Glycoside hydrolase family 2, immunoglobulin-like beta-sandwich	3
	Glycoside hydrolase family 2, carbohydrate-binding	3
Annotation Cluster 8	Enrichment Score: 0.64	Count
	Nucleotide excision repair	8
	nucleotide-excision repair	5
	deoxyribonuclease activity	8
	dna repair	13
	DNA damage	13
	excinuclease ABC activity	4
	excision nuclease	4
	dna excision	4
	response to extracellular stimulus	7
	cellular response to extracellular stimulus	7
	SOS response	7
	excinuclease repair complex	4
	endodeoxyribonuclease activity	6
	sos response	6
Annotation Cluster 9	Enrichment Score: 0.63	Count
	Chaperone	7
	unfolded protein binding	4
	protein folding	7
Annotation Cluster 10	Enrichment Score: 0.63	Count
	Ubiquinone and other terpenoid-quinone biosynthesis	6
	quinone cofactor metabolic process	4
	fat-soluble vitamin biosynthetic process	4
	quinone cofactor biosynthetic process	4
	vitamin K biosynthetic process	4
	menaquinone metabolic process	4

	fat-soluble vitamin metabolic process	4
	vitamin K metabolic process	4
	menaquinone biosynthetic process	4
Annotation Cluster 11	Enrichment Score: 0.6	Count
	Porphyrin and chlorophyll metabolism	13
	vitamin metabolic process	35
	vitamin biosynthetic process	35
	cobalamin metabolic process	13
	cobalamin biosynthetic process	13
	water-soluble vitamin metabolic process	31
	water-soluble vitamin biosynthetic process	31
	heterocycle biosynthetic process	28
	tetrapyrrole metabolic process	15
	tetrapyrrole biosynthetic process	15
	porphyrin biosynthetic process	14
	porphyrin metabolic process	14
	cofactor biosynthetic process	33
	nitrogen compound biosynthetic process	63
	cofactor metabolic process	40
	coenzyme biosynthetic process	17
	coenzyme metabolic process	20
Annotation Cluster 12	Enrichment Score: 0.52	Count
	transition metal ion binding	55
	metal-binding	46
	ion binding	86
	cation binding	86
	metal ion binding	77

Functional gene clustering for the oxidative-stress comparison of ATCC 33277 shows the most affected functional clusters are related to the ribosome and RNA binding (ES2.43), DNA integration (ES2.25), signal peptides (ES2.25), and DNA damage/ repair (ES0.92) (Table 10).

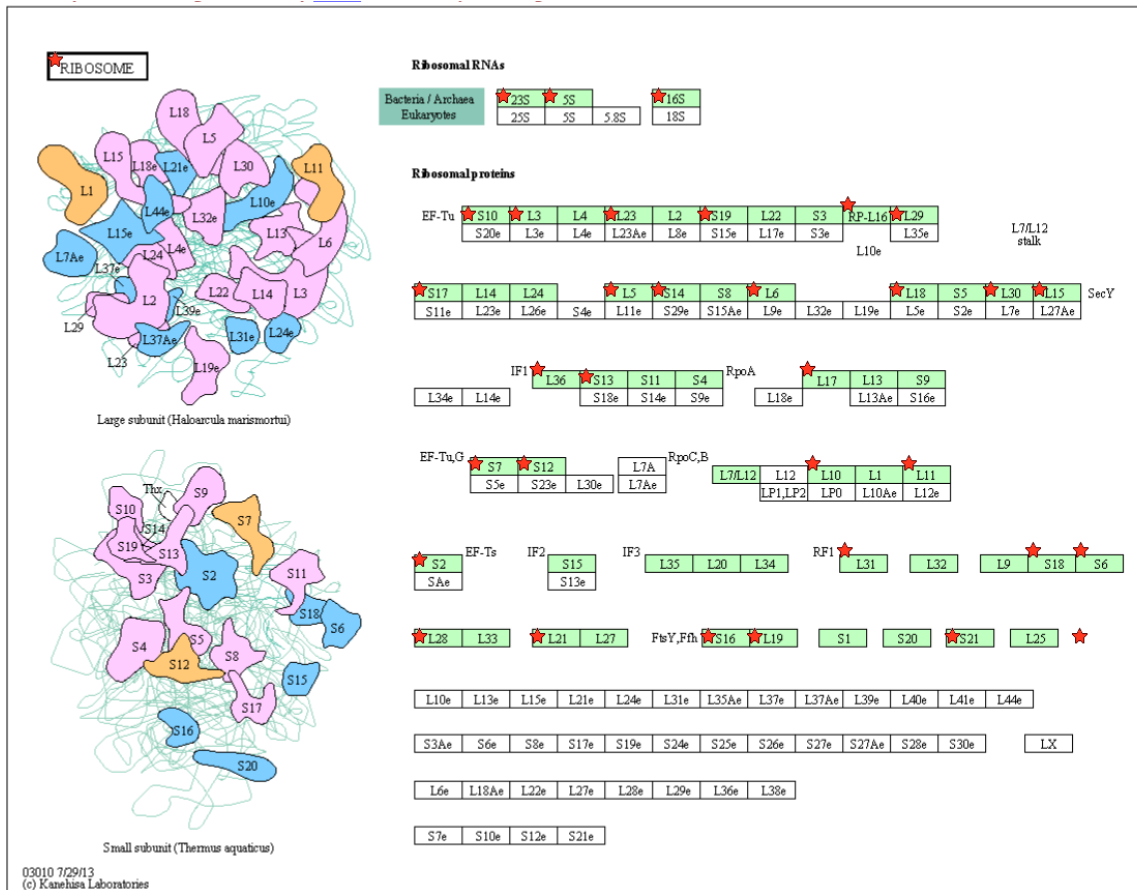


**Figure 11. KEGG Ribosomal Pathway for 77 vs 77 6%O<sub>2</sub>.**

This figure depicts the KEGG ribosomal pathway for the comparison of the wild-type ATCC 33277 strain under normal and oxygen-stress conditions. Green boxes depict genes that are found in *Porphyromonas gingivalis* W83. Genes that are starred are those that were identified as differentially regulated in the data set for this particular condition.

The ribosomal pathway in figure 11 is highlighted for the oxidative-stress comparison for the ATCC 33277 strain as 33 of the 57 genes found in *P.g.* matched the data set at an enrichment score of 2.43. These results suggest oxidative stress affects the ribosomal pathway, which can impact the translation of the bacteria.

## Aim 2

The second aim of this project was to determine the role of PG0214 in response to environmental stress. This aim involved the bioinformatics characterization of the gene, RNA isolation, cDNA library construction, high-throughput RNA sequencing, RNA library generation, bioinformatics data analysis, and proteomic studies. The following RNA tables, clusters, and pathway figures were created in the same manner as those mentioned above.

### 4.2 Bioinformatic Characterization of *Porphyromonas gingivalis* V0214.

The gene PG0214 of *P. gingivalis* is designated as PG0914 on the Oralgen database (<http://www.oralgen.lanl.gov>), as PG0214 on the BROP database (<http://genome.brop.org>), and as strain V0214 and S1 in our lab. This gene is 498 base pairs in length and is defined as a conserved hypothetical protein. Based on sequence similarity determined using BLAST, PG0214 belongs to the RNA polymerase sigma ( $\sigma$ ) factor 70 family. Residues 14-161 share a 32% and 31% sequence similarity to an extracytoplasmic function alternative sigma factor of *Mycobacterium smegmatis* and *Mycobacterium avium* respectively. Blast analysis also showed residues 14-160 had a 30% similarity to an ECF subfamily sigma subunit of *Mycobacterium leprae*. A paralog was found in residues 19-145 being 27% similar to PG1449 (designated SigG/SigW), a predicted RNA polymerase sigma factor subfamily gene.

Further blast search revealed that residues 9-77 place PG0214 in the Sigma70 family in region 2 and residues 109-158 place it in region 4. PG0214 (PG0194 on Oralgen) is located downstream of PG0193, designated *cbiH*, a probable cobalamin

biosynthesis precorrin-3 methylase and upstream of PG0195, a conserved hypothetical protein (Figure 12).

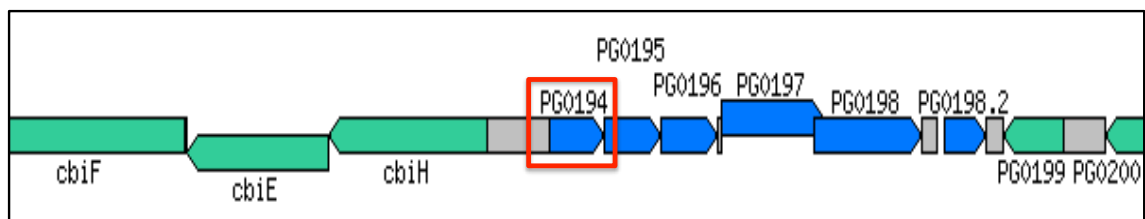


**Figure 12. Characteristics of *Porphyromonas gingivalis* PG0214.** Adapted from [http://www.oralgen.org/cgi-bin/gene\\_id\\_search.cgi?dbname=pgin&gene\\_id=PG0195](http://www.oralgen.org/cgi-bin/gene_id_search.cgi?dbname=pgin&gene_id=PG0195)

#### **4.2.1 Statistical Analysis of the Transcriptome of V0214.**

The following tables and figures depict the results for the RNA transcriptome studies (described in section 4.1.4) for the comparison of the wild-type W83 and mutant V0214 strains.

**Table 11. The Most Differentially Regulated Genes for W83 vs V0214.**

This table depicts the most differentially regulated genes for the comparison of the wild-type W83 and mutant V0214 strains under normal conditions. For statistical relevance, this gene list was trimmed at an RPKM value of 1 or greater and a fold change of +/-2 resulting in 1341 differentially regulated genes. Gene IDs are according to JVC1, which depict the name or identifier of each gene; RPKM values, reflect the reads per kilobase of transcript per million mapped reads, which is used as a normalization statistic to account for differing gene lengths; and fold changes in expression between the two conditions are provided. The top 100 most upregulated genes are shown.

Gene ID <sup>1</sup>	Fold Change <sup>2</sup>	RPKM W83 <sup>3</sup>	RPKM V0214 <sup>4</sup>
PG5SB	340.3485022	617.1575551	210048.6495
PG5SD	335.7270683	626.2001567	210232.3428
PG5SA	333.6675194	627.7072569	209445.5233
PG5SC	323.0428248	651.820861	210566.0522
PG0101	102.8791066	397.6267253	40907.48227
PG1671	95.05622874	434.4164877	41293.99302
PG2075	83.32951391	420.6667785	35053.95817
PG1266	78.40166682	446.3081281	34991.30116
PG1828	77.15568738	385.1384093	29715.6187
PG1085	47.21603827	423.9128023	20015.4831
rplS	38.46392654	458.2820109	17627.3256
panD	36.81442804	331.2327741	12194.14513
PG0195	31.31691339	610.1647661	19108.47713
hup-1	30.70270071	460.2582582	14131.17155
PG2050	26.67281409	546.0945017	14565.87712
PG1421	24.64766746	275.0854574	6780.214876
PG1446	24.03847562	1.849623042	44.46211841
PG2123	22.83909558	620.9584289	14182.12891
PG0246	20.9130976	286.1135644	5983.520896
PG1491	18.76123725	290.382134	5447.92811
PG1067	18.52120378	392.9358162	7277.644323
ragB	17.93044926	619.4001924	11106.12372
ompH-2	17.56840631	571.5034449	10040.40473
PG1669	15.81304901	502.9077626	7952.505096
PG0103	15.78570285	521.1668619	8226.985216
PG2105	15.7078011	653.828824	10270.21312
PG1207	15.30499924	254.8989944	3901.228915
PG2213	15.21117862	442.9392361	6737.627836



PG2073	14.94231485	531.0789443	7935.548795
PG1264	14.79280781	542.0344039	8018.210762
PG1795	13.43689867	599.4848795	8055.217579
PG16SA	12.76027208	271.9033651	3469.560917
PG16SB	12.71135158	269.4756565	3425.399813
PG16SC	12.64581762	273.7793218	3462.163372
PG2031	12.61652855	567.8873537	7164.767014
PG16SD	12.58868206	274.4965993	3455.550415
fmt	12.29450185	544.0631927	6688.985928
PG2074	12.20013097	358.2917592	4371.206386
PG1670	11.88644259	375.1826564	4459.587105
PG1265	11.88115524	372.1115841	4421.115498
PG1152	11.30105149	415.5621939	4696.289752
PG0695	11.27903324	536.6737879	6053.161494
PG0102	11.22005495	396.1683166	4445.03028
cdsA	11.19968987	464.0282369	5196.972343
PG1219	10.973509	358.9217227	3938.630756
proS	10.87684561	478.3060289	5202.46083
PG0340	10.54103112	467.6050446	4929.039329
PG0243	9.65718513	513.0396761	4954.519131
rpsQ	9.22000748	412.3426302	3801.802135
rpmB	9.061785795	826.3807483	7488.485326
PG0457	9.05900246	436.8130173	3957.090198
rpmJ	8.762652726	164.1579972	1438.459522
PG1257	8.619026872	61.25633302	527.9699803
PG0176	8.435640422	489.6798631	4130.763247
PG0607	8.21426128	308.4947038	2534.056101
yajC	7.909210321	457.3315735	3617.131601
PG1707	7.887645945	500.9749493	3951.513027
PG1108	7.832057822	394.9727374	3093.449318
PG1317	7.775165716	460.1826127	3577.996073
hup-2	7.707527618	439.2954168	3385.881557
PG0423	7.583093621	362.373884	2747.915088
PG0090	7.560083511	422.0069106	3190.407487
rpsP	7.40867479	477.4774731	3537.475318
PG1625	7.388396812	539.2412235	3984.128137
PG2198	7.319321785	543.4788069	3977.896271
PG1430	7.280846031	466.858856	3399.127448
PG23SD	7.088740093	291.2457951	2064.565745
PG23SB	7.082802053	296.2999521	2098.633909
PG23SA	7.039195269	295.8979169	2082.883217
PG1827	7.011724075	530.7669063	3721.591095
PG23SC	7.009086267	297.7932258	2087.258409
trx	6.865395542	456.0054777	3130.657974
PG0087	6.794645162	519.2288015	3527.975464
PG1267	6.593146856	575.9814231	3797.530109
rpmG	6.35388687	441.3650752	2804.383756
rpIL	6.32375244	411.6536701	2603.195901
PG1672	6.262611188	613.7665796	3843.781448
PG1223	6.193963043	260.1077737	1611.097938
PG0100	6.06736567	622.001806	3773.912404

PG0822	5.987344557	3.789913881	22.69152025
ragA	5.84023643	625.03208	3650.335123
PG0785	5.81166989	456.710096	2654.248313
rpmE2	5.727177267	385.7826169	2209.445433
rprY	5.478820748	480.4709136	2632.41401
PG0731	5.468583918	464.5172024	2540.251303
PG2083	5.405351947	558.640064	3019.646158
PG0817	5.373697448	241.7281162	1298.973761
groES	5.362576029	523.8680492	2809.282243
murl	5.247328473	493.3314579	2588.672205
PG0627	5.182080881	401.9344113	2082.856628
PG1492	5.160035062	629.6147792	3248.834337
PG0253	5.159602413	455.4988894	2350.193169
rpmH	4.911237853	319.6825603	1570.037091
PG0706	4.791057956	490.6359895	2350.665461
PG0779	4.763278376	459.112339	2186.879876
acpP	4.75384382	436.1052135	2073.176074
PG1801	4.739825157	597.9133384	2834.004683
PG1156	4.68072811	470.1553953	2200.669575
PG0694	4.629500345	541.1320607	2505.171062

1. Gene ID according to JVC1 (formerly TIGR)
2. Fold Change = ratio of transcript abundance in W83 in normal conditions compared to V0214 in normal conditions
3. RPKM W83 = The reads per kilobase of transcript per million mapped reads for W83 in normal conditions
4. RPKM V0214 = The reads per kilobase of transcript per million mapped reads for V0214 in normal conditions

The results from the transcriptome comparison of the wild-type W83 and mutant V0214 in normal conditions yielded regulation of several noteworthy genes (Table 11). The four most highly regulated genes for this comparison are PG5S(A-D), which are all 5S ribosomal RNA (rRNA) genes important in genetic information processing and translation at the ribosomal level. Additionally, genes PG16S(A-D), 16S ribosomal RNA genes, are shown to be highly regulated for this comparison as are the ribosomal genes *rplS*, *rpsQ*, *rpmB*, and *rpmJ*.

**Table 12. DAVID Functional Annotation Clustering for W83 vs V0214.**

This table depicts the results from DAVID functional clustering analysis for the comparison of the wild-type W83 and mutant V0214 strains under normal conditions.

Annotation clusters show similar and related gene groups. The count displays the number of genes identified in the data set for each functional group.

<b>W83 vs V0214</b>		
Annotation Cluster 1	Enrichment Score: 2.57	Count
	DNA integration	20
	Integrase-like, catalytic core, phage	10
	Integrase, catalytic core, phage	9
Annotation Cluster 2	Enrichment Score: 2.38	Count
	Ribosome	44
	ribosomal protein	33
	ribonucleoprotein	32
	structural molecule activity	32
	structural constituent of ribosome	31
	Ribosome	32
	ribosome	34
	translation	53
	ribonucleoprotein complex	34
	non-membrane-bounded organelle	41
	intracellular non-membrane-bounded organelle	41
	rna-binding	24
	RNA binding	36
	rrna-binding	15
	rRNA binding	15
Annotation Cluster 3	Enrichment Score: 0.83	Count
	Biotin metabolism	6
	sulfur compound biosynthetic process	15
	cellular amide metabolic process	11
	biotin metabolic process	5
	amide biosynthetic process	5
	biotin biosynthetic process	5

Annotation Cluster 4	Enrichment Score: 0.76	Count
	Terpenoid backbone biosynthesis	9
	secondary metabolic process	13
	Isoprene biosynthesis	8
	isoprenoid biosynthetic process	8
	isoprenoid metabolic process	8
	terpenoid metabolic process	6
	terpenoid biosynthetic process	6
	Terpenoid backbone biosynthesis	3
Annotation Cluster 5	Enrichment Score: 0.66	Count
	homeostatic process	17
	cellular homeostasis	15
	cell redox homeostasis	12
	Alkyl hydroperoxide reductase/ Thiol specific antioxidant/ Mal allergen	7
	Thioredoxin fold	12
	antioxidant activity	9
	Thioredoxin-like	9
Annotation Cluster 6	Enrichment Score: 0.63	Count
	ncRNA metabolic process	32
	tRNA metabolic process	27
	ncRNA processing	20
	tRNA modification	10
	tRNA processing	15
	RNA processing	25
	trna processing	9
	RNA modification	11
Annotation Cluster 7	Enrichment Score: 0.62	Count
	metal-binding	53
	cation binding	91
	ion binding	91
	metal ion binding	82
	transition metal ion binding	54
Annotation Cluster 8	Enrichment Score: 0.61	Count
	Base excision repair	5
	HhH1	7
	Helix-hairpin-helix DNA-binding, class 1	7
Annotation Cluster 9	Enrichment Score: 0.6	Count
	phenylalanine-tRNA ligase activity	4
	metal ion-binding site:Magnesium	8
	phenylalanyl-tRNA aminoacylation	3
Annotation Cluster 10	Enrichment Score: 0.59	Count
	Thiamine metabolism	6
	sulfur compound biosynthetic process	15

	sulfur metabolic process	17
	thiamin metabolic process	7
	thiamin and derivative metabolic process	7
	thiamin and derivative biosynthetic process	7
	thiamin biosynthetic process	6
	aromatic compound biosynthetic process	12
	thiamine biosynthesis	3
Annotation Cluster 11	Enrichment Score: 0.59	Count
	Ubiquinone and other terpenoid-quinone biosynthesis	6
	fat-soluble vitamin metabolic process	4
	quinone cofactor metabolic process	4
	vitamin K metabolic process	4
	vitamin K biosynthetic process	4
	menaquinone metabolic process	4
	fat-soluble vitamin biosynthetic process	4
	menaquinone biosynthetic process	4
	quinone cofactor biosynthetic process	4
Annotation Cluster 12	Enrichment Score: 0.57	Count
	Aminoacyl-tRNA biosynthesis	13
	ncRNA metabolic process	32
	tRNA metabolic process	27
	Aminoacyl-tRNA synthetase	13
	aminoacyl-tRNA ligase activity	14
	ligase activity, forming carbon-oxygen bonds	14
	ligase activity, forming aminoacyl-tRNA and related compounds	14
	amino acid activation	13
	tRNA aminoacylation	13
	tRNA aminoacylation for protein translation	13
	Aminoacyl-tRNA synthetase, class II, conserved region	7
	ligase	25
	protein biosynthesis	16
	Aminoacyl-tRNA biosynthesis	9
Annotation Cluster 13	Enrichment Score: 0.57	Count
	response to DNA damage stimulus	27
	DNA repair	27
	cellular response to stress	27
	DNA damage	13
	dna repair	13
Annotation Cluster 14	Enrichment Score: 0.54	Count
	metal ion-binding site:Magnesium	8
	magnesium	17
	magnesium ion binding	18
Annotation Cluster 15	Enrichment Score: 0.53	Count

	membrane	50
	cell membrane	43
	transmembrane	47
	plasma membrane	49
	intrinsic to membrane	77
	integral to membrane	75
Annotation Cluster 16	Enrichment Score: 0.52	Count
	Other glycan degradation	5
	Glycoside hydrolase, subgroup, catalytic core	9
	glycosidase	6
	Glycoside hydrolase family 2, immunoglobulin-like beta-sandwich	3
	Glycoside hydrolase family 2, carbohydrate-binding	3
Annotation Cluster 17	Enrichment Score: 0.5	Count
	vitamin biosynthetic process	35
	vitamin metabolic process	35
	coenzyme metabolic process	28
	coenzyme biosynthetic process	22
	cofactor metabolic process	46
	water-soluble vitamin metabolic process	31
	water-soluble vitamin biosynthetic process	31
	heterocycle biosynthetic process	28
	cofactor biosynthetic process	35
	nitrogen compound biosynthetic process	58

Functional gene clustering for the comparison of the wild-type W83 and mutant V0214 strains in normal conditions shows the most affected functional clusters are related to DNA integration (ES2.57), ribosome and translation (ES2.38), and biotin metabolism (ES0.83) to be highly affected (Table 12).

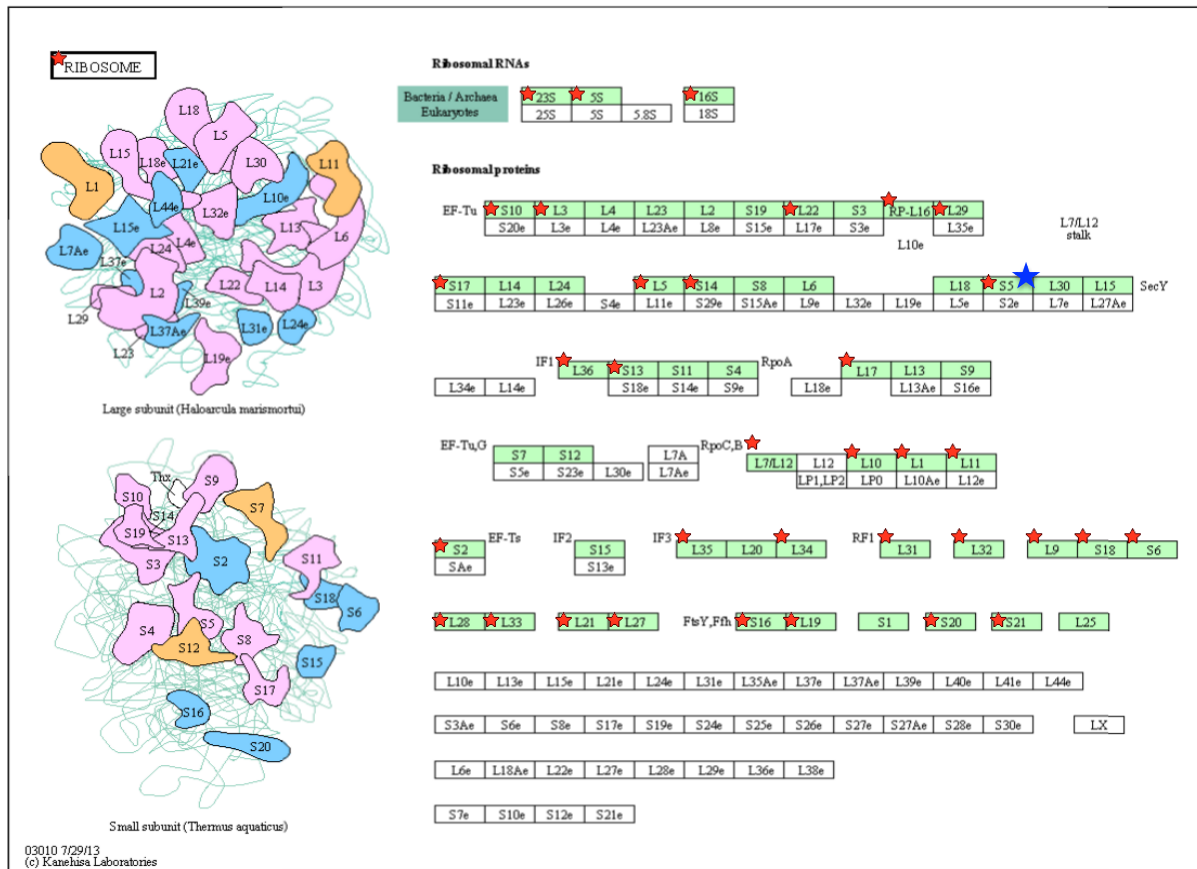


**Figure 13. KEGG Ribosomal Pathway for W83 vs V0214.**

This figure depicts the KEGG ribosomal pathway for the comparison of the wild-type W83 and mutant V0214 strains under normal conditions. Green boxes depict genes that are found in *Porphyromonas gingivalis* W83. Genes that are starred in red are those that were identified as differentially regulated in the data set for this particular condition. Genes that are starred in blue are those that were identified in the data set for the W83 + DP 6%O<sub>2</sub> vs V0214 + DP 6%O<sub>2</sub> comparison discussed below. Only one gene matched our data set for this comparison with no clustering.

The ribosomal pathway in figure 13 is highlighted for the comparison of the wild-type W83 and mutant V0214 strains in normal conditions as 35 of the *P.g* genes found in this pathway matched our data set at an enrichment score of 2.38. These results suggest

oxidative stress affects the ribosomal pathway, which can impact the translation of the bacteria.



**Table 13. The Most Differentially Regulated Genes for W83 + DP vs V0214 + DP.**

This table depicts the most differentially regulated genes for the comparison of the wild-type W83 and mutant V0214 strains under iron-stress conditions. For statistical relevance, this gene list was trimmed at an RPKM value of 1 or greater and a fold change of +/-2 resulting in 242 differentially regulated genes.

Gene ID <sup>1</sup>	Fold Change <sup>2</sup>	RPKM W83 + DP <sup>3</sup>	RPKM V0214 + DP <sup>4</sup>
PG0815	13.56900846	3.713977515	50.39499232
PG0554	11.36010011	3.65049072	41.46994001
PG1710	8.362295911	1.091648343	9.128686475
PG1456	7.7455228	4.674807518	36.20882822
PG0711	7.573400071	1.941397337	14.70297873
PG1015	6.78450423	28.47382761	193.1808039
PG1573	5.850214617	88.12850166	515.5706485
PG0039	5.806273388	10.67768535	61.99756032
PG0608	5.619623989	59.47866212	334.2477165
PG0447	5.38333102	15.57344041	83.83698484
PG1980	4.991559138	54.94949188	274.2836383
PG0680	4.882364287	97.81917811	477.5888618
thiG	4.247244634	4.052044699	17.2100251
PG1398	4.023368788	7.854848996	31.60295428
panE	3.980799292	193.9836002	772.2097782
PG1229	3.955749144	16.27075864	64.36303955
PG1462	3.951339167	8.617079409	34.04900338
PG0684	3.893219727	45.37117481	176.6399528
PG0421	3.880016897	76.75986395	297.8295692
PG1787	3.826984078	8.578653191	32.83036917
PG0682	3.826332481	38.17090921	146.0545897
PG1574	3.786700035	15.07437932	57.08215272
PG0025	3.697640017	148.5816095	549.4013052
PG0936	3.628308529	152.1447148	552.0279664
PG0607	3.579580571	608.7751408	2179.159666
PG0248	3.405972043	47.19985838	160.7613981
PG2209	3.401327908	37.85344141	128.7519667
pepT	3.217988556	112.7731892	362.9028322
PG2213	3.217242723	1156.224115	3719.853619
PG1088	3.213921879	34.75267165	111.6923718
PG0817	3.210858128	847.6048327	2721.538867
dinF	3.199221508	75.3872278	241.1804406
thiF	3.179857081	28.23252399	89.77539132
PG0683	3.11916005	34.39234184	107.2752187
PG0686	3.091645533	96.58014501	298.5915739

PG1869	3.075695176	120.5053061	370.6375888
cdsA	3.074915175	4958.742056	15247.7112
PG0282	3.02130322	5.974419186	18.05053192
PG0444	3.004740616	69.67459332	209.3540805
PG0505	2.962384381	102.0890892	302.4271235
PG1207	2.937138908	2744.232291	8060.191435
PG2104	2.926086391	6.960268972	20.36634832
PG0442	2.912846181	6.018857869	17.53200716
PG0265	2.902541301	113.8953104	330.5858425
PG0618	2.874871959	343.7951038	988.3669036
PG1373	2.864643053	261.8354148	750.0650019
PG2114	2.840025027	14.47821743	41.11849984
PG1630	2.840025027	2.348356916	6.669392414
PG0821	2.808469193	14.11925336	39.65348809
PG1709	2.788532244	52.34803692	145.9741888
PG1673	2.780108887	11.65509006	32.40241945
PG0313	2.763267593	10.22846235	28.26397853
PG1842	2.716233664	136.1754354	369.8843018
PG2123	2.676741253	21085.3387	56439.99593
slyD	2.613318944	318.7279761	832.9378579
PG0930	2.611670165	93.52557223	244.2579467
PG1441	2.603356274	16.27075864	42.35858158
PG0662	2.594590765	32.94828624	85.48731919
PG1389	2.543491177	141.9969312	361.1679416
PG2008	2.520522211	21.85041927	55.07446709
PG0140	2.500033013	146.4712997	366.1830847
sodB	2.496525334	941.2676242	2349.89847
PG0019	2.484337884	12.76158595	31.70409144
PG1124	2.483986904	159.2367859	395.5420909
PG0731	2.48312717	1697.118136	4214.160155
PG1770	2.472469027	1201.948298	2971.77994
PG0470	2.461355023	5.810985227	14.30289768
htrA	2.446083892	1039.266177	2542.132254
PG0560	2.419637141	102.436331	247.8587512
PG0516	2.405730636	268.8586415	646.8014706
PG0209	2.391196907	134.3269119	321.2020964
rplV	2.387913419	217.0825148	518.3742501
PG1391	2.377535307	445.9255131	1060.203652
PG2208	2.377206133	30.14875865	71.66981397
PG0841	2.349475249	42.04189312	98.77638731
PG0040	2.349299614	53.66221358	126.0686176
PG2194	2.344671824	12.68781956	29.74877303
uppS	2.34111356	361.6734417	846.7185987
PG0888	2.338844139	11.00125158	25.73021278
PG1769	2.33329857	127.077638	296.5100711
PG0889	2.330924244	64.22667882	149.7075228
tuf	2.330370795	1673.772119	3900.509663
PG1642	2.325978088	273.7109071	636.6455723
PG0685	2.324580812	168.7721418	392.3244825
foiK	2.311267968	98.89909457	228.5823093
PG1176	2.294017449	11.95503912	27.42506834

PG0199	2.279185538	328.7650348	749.3165127
PG1320	2.244807906	1990.481723	4468.249107
PG1313	2.222590311	334.8892853	744.321681
PG0825	2.210036154	220.0822366	486.3896997
PG0681	2.203977755	35.38495082	77.98764447
PG0333	2.19858099	77.52774845	170.451034
galM	2.197819383	343.6854979	755.3586489
PG0399	2.19249932	80.43454128	176.3526771
PG1509	2.18277932	20.04659612	43.75729545
PG0250	2.180221232	15.92603917	34.72228875
PG1761	2.178540815	35.44398333	77.21616434
PG2058	2.17735252	4.380588863	9.538086202
PG0915	2.17042563	8.91165597	19.34208652
PG2077	2.17042563	18.09964236	39.28392767
cls	2.169273731	886.2328666	1922.481677
PG2103	2.163828592	22.14631037	47.92081957
ompH-2	2.160913436	2158.628651	4664.609655
PG0184	2.156708202	221.1047774	476.858487
PG1639	2.14247502	22.54178019	48.29520097
PG0363	2.125878082	300.7290126	639.3132165
PG1270	2.120157572	17.63540291	37.38983301
PG1197	2.11917411	233.4539236	494.7295109
PG0326	2.117619268	60.67966176	128.4964209
PG1031	2.117377234	232.6673538	492.6445581
PG1624	2.11716249	230.2289874	487.4321761
PG0246	2.1112448	1082.450353	2285.317678
PG1729	2.096808236	428.3729176	898.2158618
PG2046	2.091765028	35.23245043	73.69800768
PG1177	2.087956981	228.8131617	477.7520382
PG2037	2.084895156	98.88883373	206.1728504
PG0327	2.076615093	119.9598659	249.1104682
pfk	2.073139496	105.7673269	219.2704228
PG2049	2.072538218	198.1868795	410.749882
PG1280	2.069057013	453.5962875	938.5165799
PG1448	2.067171885	239.0385694	494.1338101
luxS	2.066907103	21.35537071	44.1395674
PG0828	2.065472747	34.48206647	71.22176853
PG2031	2.065119457	918.7052194	1897.236024
PG0214	2.063005037	95.14009466	196.2744945
PG0225	2.061826079	17.4088687	35.89405948
PG1906	2.061562193	231.959441	478.1988138
PG0661	2.053351428	37.43781038	76.87298139
PG0487	2.044818019	18.44159819	37.70971229
PG0050	2.036921583	15.56470888	31.70409144
PG0722	2.028589305	15.63268967	31.71230707
PG0443	2.023686536	400.5916721	810.6719734
PG0847	2.020991592	14.42601892	29.15486295
PG1102	2.01114794	196.703105	395.5990444
PG1133	2.010354794	33.56517427	67.47790901
PG1325	2.007006461	311.1619881	624.5041206
feoB-1	2.003473437	76.87149052	154.0099893

PG2168	-2.000143553	322.353701	161.1652826
hup-1	-2.004961303	4103.750413	2046.797814
hup-2	-2.006759823	3713.232057	1850.361968
PG2020	-2.008278084	1068.538098	532.0668024
PG1056	-2.010034361	2254.720378	1121.732256
PG1199	-2.024630046	207.5381097	102.5066827
PG0564	-2.031401384	284.7382761	140.1683972
PG0987	-2.044122043	6154.634329	3010.893772
PG0475	-2.046636894	46.8269844	22.8799669
PG0563	-2.051372545	312.0256943	152.1058157
PG1546	-2.059841003	17.62665519	8.557289208
PG1096	-2.061686503	370.0808841	179.5039564
panC	-2.06696703	497.8880991	240.8785877
PG1174	-2.073457741	172.3867274	83.13973515
PG1514	-2.079775611	174.639476	83.9703452
PG1341	-2.083314975	2436.897906	1169.721302
PG1696	-2.085428462	2205.980991	1057.80708
kdsB	-2.091624345	199.8751036	95.55975196
PG0920	-2.095319521	818.591185	390.6760648
PG1367	-2.106638472	793.3006698	376.5718135
PG1277	-2.107194472	1223.227537	580.5005441
PG1526	-2.108140244	719.7946338	341.4358394
PG1846	-2.112657439	2.47598501	1.171976566
PG1463	-2.112657439	13.32817463	6.308724916
PG1021	-2.112657439	5.177059566	2.450496455
mpi	-2.119794795	40.85375266	19.27250352
PG1033	-2.126117939	379.3079767	178.404015
PG2167	-2.127821548	1614.821948	758.9085418
PG1997	-2.132219082	57.47494833	26.95546101
PG1989	-2.13492943	261.7251826	122.5919596
gmk	-2.136100766	233.3648623	109.2480589
PG1485	-2.159260177	30.68110107	14.20908022
PG0972	-2.165917711	128.6595174	59.40184926
PG1617	-2.17301908	26.79889658	12.33256386
pheS	-2.19299013	198.3147818	90.43122402
PG0627	-2.195425605	1233.091065	561.6637895
PG1513	-2.201508839	1010.853311	459.1638665
PG1034	-2.212435095	1721.446264	778.0776336
PG0112	-2.254306509	185.3808713	82.23410197
PG0710	-2.274702113	652.573641	286.8831207
hslR	-2.28653871	205.1675798	89.72845239
PG0323	-2.287002956	115.4484283	50.48022698
PG0910	-2.32163304	241.8039183	104.1525143
PG0937	-2.353361852	160.5640321	68.22751541
PG1466	-2.362541653	62.01629469	26.24982067
PG0221	-2.384742109	57.33243668	24.04135711
trkA	-2.387815914	391.371805	163.9036757
PG1742	-2.442760164	35.71293633	14.61991105
hpt	-2.442799023	1249.985125	511.7019916
PG0204	-2.44799989	304.1838169	124.2581007
PG1519	-2.45228718	95.46800702	38.93019048

PG1571	-2.4592653	8.988559988	3.654977764
PG0160	-2.469863335	168.0996401	68.06030022
PG1430	-2.47310369	9578.023645	3872.875887
PG0397	-2.489917696	29.06091684	11.67143672
PG0289	-2.501908682	418.2452431	167.1704671
PG0283	-2.508780709	7.784211865	3.102786878
PG1394	-2.558993518	56.61847803	22.12529169
PG0219	-2.562575227	20.38290392	7.954070461
PG1139	-2.581742018	873.2975519	338.2590305
PG0799	-2.603095773	31.6886146	12.173434
PG2105	-2.60971729	36335.67307	13923.22195
PG1895	-2.614739608	245.0215638	93.70782582
PG1795	-2.62944801	14294.58889	5436.345895
PG1460	-2.640821799	3.559228452	1.34777305
PG2166	-2.640821799	7.695629084	2.914103893
PG1281	-2.651619552	1261.507981	475.7499922
PG1130	-2.692273198	328.8598829	122.1495215
topA	-2.763329969	491.6697432	177.9265411
rpoD	-2.805356838	2014.424436	718.0635307
PG0917	-2.869721281	1460.362219	508.8864305
PG1335	-3.003287536	426.1889036	141.9074592
PG1591	-3.06943119	5296.131936	1725.4441
PG0940	-3.072956275	18.22324967	5.930201421
bcp	-3.199482578	4516.491418	1411.631821
PG1140	-3.303327616	178.0854375	53.91092201
PG0771	-3.387099976	4064.962458	1200.130639
PG1142	-3.504668713	922.2513009	263.149352
PG1027	-3.521095732	7.030574719	1.996700815
rpsU	-3.529182617	12685.0902	3594.342254
PG0726	-3.654543653	995.7078487	272.4575059
PG1166	-3.697150519	8.304866387	2.246288417
PG1534	-3.755835448	14.01788436	3.732294601
PG0456	-3.808343016	544.9806858	143.1017856
PG0850	-3.848582258	576.1112305	149.6944048
PG1429	-3.873205305	33.86076797	8.742311678
PG1486	-4.304539533	17.18975519	3.993401631
PG1649	-4.753479238	6.250352403	1.314900537
PG0080	-4.753479238	8.736288017	1.837872341
PG2063	-4.753479238	14.85591006	3.125270841
PG0164	-5.212752595	61.5577035	11.80905911
PG0161	-5.396185267	482.9161163	89.49213054
PG1970	-5.621177829	84.85200628	15.09505816
PG1442	-6.818121736	28.27470994	4.146994001
PG0609	-6.866136678	11.94063739	1.739062
PG1535	-7.54101336	64.19099734	8.512250844
PG1974	-8.256630925	635.8894084	77.01560288
PG1273	-8.450629757	8.761177727	1.0367485
PG0655	-8.450629757	28.47382761	3.369432626
PG0723	-9.010180933	2174.721237	241.36266
PG0732	-9.506958477	14.50553482	1.525780812
PG0786	-10.03512284	13.19518841	1.314900537

thiS	-11.26750634	27.19888011	2.413921881
PG1167	-11.61961592	40.85375266	3.515929697

1. Gene ID according to JVICI (formerly TIGR)
2. Fold Change = ratio of transcript abundance in W83 in iron-deficient conditions compared to V0214 in iron-deficient conditions
3. RPKM W83 + DP = The reads per kilobase of transcript per million mapped reads for W83 in iron-deficient conditions
4. RPKM V0214 + DP = The reads per kilobase of transcript per million mapped reads for V0214 in iron-deficient conditions

The results from the transcriptome comparison of the wild-type W83 and mutant V0214 in iron-deficient conditions yielded regulation of several noteworthy genes (Table 13). The gene PG1710, codes for a 50S ribosomal protein L33, and is highly upregulated for this comparison. The gene *dinF*, DNA damage-inducible protein is found to be upregulated in this comparison. The *feoB1* gene is also upregulated which codes for a protein required for ferrous iron acquisition (Anaya-Bergman et al., 2002).

**Table 14. DAVID Functional Annotation Clustering for W83 + DP vs V0214 + DP.**

This table depicts the results from DAVID functional clustering analysis for the comparison of the wild-type W83 and mutant V0214 strains under iron-stress conditions. Annotation clusters show functionally similar and related gene groups. The count displays the number of genes identified in the data set for each functional group.

<b>W83 + DP vs V0214 + DP</b>		
Annotation Cluster 1	Enrichment Score: 2.96	Count
	PIRSF004563:transposase IS5	8
	transposition, DNA-mediated	14
	transposition	14
	transposase activity	14
	DNA recombination	15
	Transposase, IS4-like	14
	DNA replication, recombination, and repair	11
	DNA metabolic process	19
	DNA binding	26
Annotation Cluster 2	Enrichment Score: 0.95	Count
	pantothenate biosynthetic process	3
	pantothenate metabolic process	3
	cellular amino acid derivative biosynthetic process	3
	pantothenate biosynthesis	3
	cellular amino acid derivative metabolic process	3
	coenzyme biosynthetic process	5
	cofactor biosynthetic process	7
	coenzyme metabolic process	5
	cofactor metabolic process	7
Annotation Cluster 3	Enrichment Score: 0.92	Count
	GCN5-related N-acetyltransferase	3
	N-acetyltransferase activity	3
	N-acyltransferase activity	3
	acetyltransferase activity	3
Annotation Cluster 4	Enrichment Score: 0.72	Count
	antioxidant activity	4
	Thioredoxin fold	4
	homeostatic process	4
	Thioredoxin-like	3
	cell redox homeostasis	3
	cellular homeostasis	3

Functional gene clustering for the comparison of the wild-type W83 and mutant V0214 strains in iron-deficient conditions shows the most affected functional clusters are related to DNA binding, replication, repair and transposition (ES2.96), coenzyme biosynthetic and metabolic processes (ES0.95), and acetyltransferase activity (ES0.92) (Table 14).



**Table 15. The Most Differentially Regulated Genes for W83 6%O<sub>2</sub> vs V0214 6%O<sub>2</sub>.**

This table depicts the most differentially regulated genes for the comparison of the wild-type W83 and mutant V0214 strains under oxygen-stress conditions. For statistical relevance, this gene list was trimmed at an RPKM value of 1 or greater and a fold change of +/-2 resulting in 1061 differentially regulated genes. The top 100 most upregulated genes are shown.

Gene ID <sup>1</sup>	Fold Change <sup>2</sup>	RPKM W83 6%O <sub>2</sub> <sup>3</sup>	RPKM V0214 6%O <sub>2</sub> <sup>4</sup>
PG1273	59.92489832	3.066182607	183.740681
PG0655	45.49853391	1.660848912	75.56619056
PG0496	38.28535171	1.714424684	65.63735199
PG0374	23.8589873	6.813739127	162.5689153
PG1234	23.72027225	4.943922343	117.271184
PG0844	21.63954662	3.428849367	74.19874572
PG0997	21.41760255	14.92897899	319.7429384
PG1233	20.75177035	7.18204935	149.0402387
PG1534	19.92083341	16.76179825	333.9089906
PG1840	15.81351484	8.391657662	132.7016029
PG0835	13.62489972	10.39835841	141.6765906
PG0049	13.5593954	15.46099351	209.6417242
PG0354	13.3782952	18.75782301	250.9476936
PG1496	13.26115806	23.10746313	306.4317208
PG1799	13.05655337	24.29584694	317.2200222
PG1462	12.34563878	19.58053454	241.7342065
PG1630	12.12369471	21.91635678	265.7072187
PG1556	11.31252227	32.66844099	369.5624661
PG0250	11.31198798	27.92478171	315.8847949
PG1733	11.0642414	36.76618962	406.7899974
PG1426	10.99112718	68.18881572	749.4719461
PG1456	10.94114897	25.38372069	277.7270695
PG1460	10.91225	30.55961999	333.4742133
PG0442	10.88913083	17.28363096	188.2037187
PG2103	10.59782924	23.62096231	250.330925
PG0519	10.44986653	8.61845922	90.06174853
PG0554	9.908217315	9.539234778	94.5168112
PG0870	9.89822294	34.62846457	342.7602624
PG0040	9.794369956	83.40016692	816.8520891
PG0786	9.6704201	9.073906252	87.74848541
PG0265	9.44387005	148.4109519	1401.573743
PG1363	9.348748673	49.68104572	464.4556103
PG1574	9.274091407	36.47354474	338.2589879
PG0219	9.241179902	49.66210518	458.9364483
PG0662	9.238945278	80.479993	743.5502513

PG1109	9.172141904	36.24729907	332.4653707
PG0470	9.071963774	21.69272049	196.7955744
PG1463	9.051836493	28.83516409	261.0111906
PG0283	8.86350229	54.54912878	483.4963279
PG1176	8.722488734	47.31393974	412.6953064
PG0872	8.695342933	32.33119216	281.1308032
PG0998	8.692809325	9.965093473	86.62465747
PG0828	8.596311904	33.64361833	289.2110368
PG2116	8.49728717	36.47354474	309.9261837
PG1445	8.40937426	37.5443277	315.724303
PG0868	8.376460476	44.69193437	374.3602218
PG2104	8.371151255	27.16410665	227.3948455
PG0871	8.347884401	48.86297105	407.9024338
PG1020	8.344906646	52.92028295	441.6148209
PG0039	8.322902545	19.93018695	165.8770037
PG0197	8.163866191	94.81937426	774.0926838
PG0116	8.055954705	51.71427593	416.6078645
PG1459	7.963875376	19.64134366	156.4212131
PG1570	7.941118025	45.25813286	359.4001746
PG1461	7.925252757	36.65321737	290.486012
PG0282	7.866824299	62.6377304	492.7600196
PG0178	7.843216979	53.49227665	419.5515325
PG0492	7.800053539	31.76612172	247.7774502
cas2-1	7.700226132	49.31180275	379.7120322
mpi	7.591248694	52.37691642	397.6061984
PG1503	7.571631696	18.945204	143.4461071
PG1200	7.567835098	30.14780716	228.1536331
PG1549	7.559969812	18.09265198	136.7799028
PG1442	7.543099063	27.50272884	207.4558082
PG0847	7.521796292	52.03783157	391.4179686
PG0546	7.465391374	41.17033923	307.3526954
PG1457	7.410068072	52.80647823	391.2995984
PG1454	7.383908412	53.92492858	398.1767338
PG0229	7.375452633	42.35789105	312.4086191
PG0711	7.364507706	26.5735826	195.7013538
PG0915	7.344746988	39.35324445	289.0396237
PG0428	7.238403122	31.17967025	225.6910225
PG1475	7.229453765	52.99176412	383.1015087
PG0280	7.216154671	67.18377541	484.8085147
PG0337	7.195842825	33.3472409	239.9615042
PG1975	7.162210799	57.68965794	413.1854911
PG1179	7.154299086	49.32217982	352.865626
PG0819	7.154099873	55.9989643	400.6221834
PG1571	7.152652005	55.7369635	398.6671037
PG1489	7.095958226	61.85981522	438.9546647
PG1485	7.09462234	48.20324285	341.9838036
PG1019	7.093045071	60.43129443	428.6418951
radC	7.078529947	55.71128281	394.3539838
PG0893	7.066307455	52.85568165	373.4944973
PG0427	7.023403945	141.0443999	990.6117949
PG0590	6.996063009	27.78147271	194.3609336

PG1465	6.988238894	54.87753801	383.4973455
thiE	6.968179014	75.78392074	528.0759261
PG1517	6.965028662	34.56302573	240.7324649
PG1490	6.964427958	63.6972741	443.6150766
PG0877	6.948963077	56.75036283	394.3561759
PG1478	6.86008937	56.2133478	385.6285897
PG1022	6.8543857	60.89331073	417.3862383
PG1059	6.80718696	43.58067546	296.6618057
PG1479	6.773813293	63.66137402	431.2302616
PG1154	6.759205703	27.19157289	183.7934345
PG1482	6.750798731	45.55471302	307.5306989
PG0524	6.729292523	48.11217059	323.7608698

1. Gene ID according to JVICI (formerly TIGR)
2. Fold Change = ratio of transcript abundance in W83 in microaerobic conditions compared to V0214 in microaerobic conditions
3. RPKM W83 6%O<sub>2</sub> = The reads per kilobase of transcript per million mapped reads for W83 in microaerobic conditions
4. RPKM V0214 6%O<sub>2</sub> = The reads per kilobase of transcript per million mapped reads for V0214 in microaerobic conditions

The results from the transcriptome comparison of the wild-type W83 and mutant V0214 in microaerobic conditions yielded regulation of several noteworthy genes (Table 15). The PG0496 and PG0844 genes are highly upregulated in this comparison and code for ABC transporters and ATP-binding proteins. What is particularly notable in this data set is the four most highly downregulated genes are PG5S(A-D), which are 5S ribosomal RNA (rRNA) genes important in genetic information processing and translation at the ribosomal level.

**Table 16. DAVID Functional Annotation Clustering for W83 6%O2 vs V0214****6%O2.**

This table depicts the results from DAVID functional clustering analysis for the comparison of the wild-type W83 and mutant V0214 strains under oxygen-stress conditions. Annotation clusters show functionally similar and related gene groups. The count displays the number of genes identified in the data set for each functional group.

<b>W83 6%O2 vs V0214 6%O2</b>		
Annotation Cluster 1	Enrichment Score: 3.96	Count
	DNA integration	20
	Integrase-like, catalytic core, phage	10
	Integrase, catalytic core, phage	9
Annotation Cluster 2	Enrichment Score: 2.44	Count
	DNA metabolic process	88
	DNA binding	108
	DNA recombination	47
Annotation Cluster 3	Enrichment Score: 0.96	Count
	Ubiquinone and other terpenoid-quinone biosynthesis	6
	quinone cofactor biosynthetic process	4
	menaquinone biosynthetic process	4
	fat-soluble vitamin biosynthetic process	4
	menaquinone metabolic process	4
	quinone cofactor metabolic process	4
	fat-soluble vitamin metabolic process	4
	vitamin K biosynthetic process	4
	vitamin K metabolic process	4
Annotation Cluster 4	Enrichment Score: 0.88	Count
	Thiamine metabolism	5
	aromatic compound biosynthetic process	12
	sulfur compound biosynthetic process	12
	thiamin and derivative metabolic process	7
	thiamin and derivative biosynthetic process	7
	thiamin metabolic process	7
	thiamin biosynthetic process	6
	sulfur metabolic process	13
	thiamine biosynthesis	3
Annotation Cluster 5	Enrichment Score: 0.86	Count
	iron ion binding	21

	iron	18
	4 iron, 4 sulfur cluster binding	14
	iron-sulfur	12
	4fe-4s	10
	iron-sulfur cluster binding	20
	metal cluster binding	20
	s-adenosyl-l-methionine	9
Annotation Cluster 6	Enrichment Score: 0.85	Count
	Other glycan degradation	5
	Glycoside hydrolase, subgroup, catalytic core	9
	Glycoside hydrolase family 2, immunoglobulin-like beta-sandwich	3
	glycosidase	5
	Glycoside hydrolase family 2, carbohydrate-binding	3
Annotation Cluster 7	Enrichment Score: 0.77	Count
	iron ion binding	21
	ion binding	69
	cation binding	69
	transition metal ion binding	42
	metal ion binding	60
	metal-binding	36
Annotation Cluster 8	Enrichment Score: 0.75	Count
	Ribosome	30
	Ribosome	18
	ribosome	20
	structural molecule activity	18
	ribonucleoprotein complex	20
	ribosomal protein	19
	structural constituent of ribosome	17
	ribonucleoprotein	18
	translation	33
	intracellular non-membrane-bounded organelle	24
	non-membrane-bounded organelle	24
	ribosomal subunit	6
	rRNA binding	10
	rrna-binding	10
	RNA binding	21
	rna-binding	13
Annotation Cluster 9	Enrichment Score: 0.71	Count
	Porphyrin and chlorophyll metabolism	11
	heterocycle biosynthetic process	26
	vitamin biosynthetic process	29
	vitamin metabolic process	29
	water-soluble vitamin metabolic process	25

	water-soluble vitamin biosynthetic process	25
	cobalamin biosynthetic process	10
	cobalamin metabolic process	10
	cofactor biosynthetic process	27
	coenzyme biosynthetic process	15
	porphyrin biosynthetic process	11
	porphyrin metabolic process	11
	cofactor metabolic process	32
	tetrapyrrole biosynthetic process	11
	tetrapyrrole metabolic process	11
	nitrogen compound biosynthetic process	48
	coenzyme metabolic process	16
Annotation Cluster 10	Enrichment Score: 0.67	Count
	Biotin metabolism	5
	sulfur compound biosynthetic process	12
	biotin biosynthetic process	4
	amide biosynthetic process	4
	biotin metabolic process	4
	cellular amide metabolic process	5
Annotation Cluster 11	Enrichment Score: 0.67	Count
	Terpenoid backbone biosynthesis	7
	Isoprene biosynthesis	7
	isoprenoid biosynthetic process	7
	isoprenoid metabolic process	7
	terpenoid metabolic process	5
	terpenoid biosynthetic process	5
	lipid biosynthetic process	16
	Terpenoid backbone biosynthesis	3
	secondary metabolic process	6
Annotation Cluster 12	Enrichment Score: 0.64	Count
	DNA recombination	47
	transposition	30
	transposase activity	28
	transposition, DNA-mediated	28
	Transposase, IS4-like	28
Annotation Cluster 13	Enrichment Score: 0.53	Count
	nucleoside bisphosphate metabolic process	6
	Pantothenate and CoA biosynthesis	4
	coenzyme A biosynthetic process	3
	coenzyme A metabolic process	3
Annotation Cluster 14	Enrichment Score: 0.52	Count
	Elp3	8
	Elongator protein 3/MiaB/NifB	8

	iron-sulfur cluster binding	20
	metal cluster binding	20
	Radical SAM	8
	transferase activity, transferring sulfur-containing groups	5
	sulfurtransferase activity	4
	radical SAM enzyme activity	3
Annotation Cluster 15	Enrichment Score: 0.51	Count
	nucleoside metabolic process	18
	ribonucleoside metabolic process	12
	purine ribonucleoside metabolic process	10
	purine nucleoside metabolic process	10
	nucleoside bisphosphate metabolic process	6
	guanosine metabolic process	6
	guanosine tetraphosphate metabolic process	3
	RelA/SpoT	3
	tRNA modification	7
	nucleoside biosynthetic process	5
	ribonucleoside biosynthetic process	4
	purine ribonucleoside biosynthetic process	4
	purine nucleoside biosynthetic process	4
	RNA modification	8
	7-methylguanosine metabolic process	3
	queuosine biosynthetic process	3
	7-methylguanosine biosynthetic process	3
	guanosine biosynthetic process	3
	queuosine metabolic process	3

Functional gene clustering for the comparison of the wild-type W83 and mutant V0214 strains in iron-deficient conditions shows the most affected functional clusters are related to DNA integration (ES3.96), DNA binding and recombination (ES2.44), and ubiquinone and other terpenoid-quinone biosynthesis (ES0.96) (Table 16).

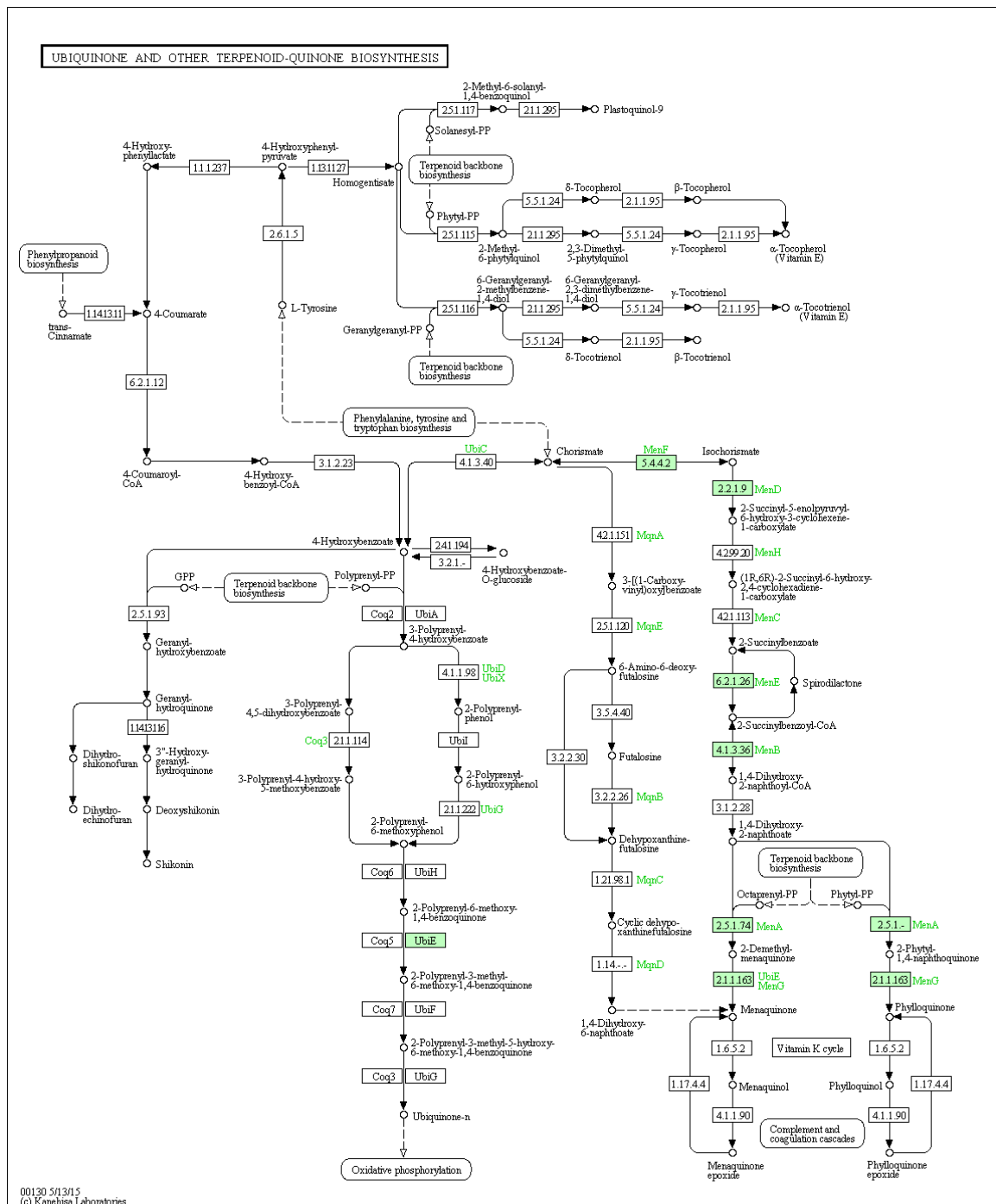


**Figure 14. KEGG Ubiquinone and Other Terpenoid-quinone Biosynthesis Pathway for W83 6%O<sub>2</sub> vs V0214 6%O<sub>2</sub>.**

This figure depicts the KEGG Ubiquinone and other terpenoid-quinone biosynthesis pathway for the comparison of the wild-type W83 and mutant V0214 strains under



oxygen-stress conditions. Green boxes depict genes that are found in *Porphyromonas gingivalis* W83 as well as those that were identified as differentially regulated in the data set for this particular condition.

The ubiquinone and other terpenoid-quinone biosynthesis pathway in figure 14 is highlighted for the comparison of the wild-type W83 and mutant V0214 strains in microaerobic conditions as 6 of the genes found in *P.g.* matched our data set. These results show that the PG0214 gene is important in the ubiquinone and other terpenoid-quinone biosynthesis pathway, especially in response to oxidative stress conditions. This pathway is vital to electron carriers like menaquinone for oxidative phosphorylation in the bacteria.

**Table 17. The Most Differentially Regulated Genes for W83 + DP 6%O<sub>2</sub> vs V0214 + DP 6%O<sub>2</sub>.**

This table depicts the most differentially regulated genes for the comparison of the wild-type W83 and mutant V0214 strains under both iron- and oxygen-stress conditions. For statistical relevance, this gene list was trimmed at an RPKM value of 1 or greater and a fold change of +/-2 resulting in 14 differentially regulated genes.

Gene ID <sup>1</sup>	Fold Change <sup>2</sup>	RPKM W83 + DP 6% O <sub>2</sub> <sup>3</sup>	RPKM V0214 + DP 6% O <sub>2</sub> <sup>4</sup>
PG1858	6.486311535	591.0638539	3833.824294
PG0822	4.391889995	1.565956967	6.877510738
PG1446	4.350939972	1.11040585	4.831309196
PG5SD	3.48290583	5708.087142	19880.72998
PG5SB	3.415693725	5700.431352	19470.9276
PG5SA	3.396419565	5715.04695	19410.69728
PG5SC	3.385196507	5810.39633	19669.33336
PG0495	2.371943389	470.7999645	1116.710864
PG2075	2.176881102	380.9780239	829.3438603
PG1266	2.119568177	384.4102583	814.7837504
PG1257	-2.413411945	139.0165669	57.60167352
PG0162	-2.584808952	537.0102326	207.7562569
PG1421	-2.618235658	460.8858612	176.0291744
PG0655	-4.832436476	64.20423567	13.28610029

1. Gene ID according to JVICI (formerly TIGR)
2. Fold Change = ratio of transcript abundance in W83 in both microaerobic and iron-deficient conditions compared to V0214 in both microaerobic and iron-deficient conditions
3. RPKM W83 + DP 6%O<sub>2</sub> = The reads per kilobase of transcript per million mapped reads for W83 in both microaerobic and iron-deficient conditions
4. RPKM V0214 + DP 6%O<sub>2</sub> = The reads per kilobase of transcript per million mapped reads for W83 in both microaerobic and iron-deficient conditions

The results from the transcriptome comparison of the wild-type W83 and mutant V0214 in both iron-deficient and microaerobic conditions yielded regulation of several noteworthy genes (Table 17). The most highly upregulated gene, PG1858, is a DNA-dependent transcription regulator. What is particularly notable in this data set is four of the most highly upregulated genes are PG5S(A-D), which are 5S ribosomal RNA (rRNA)

genes important in genetic information processing and translation at the ribosomal level, which follows the same trend as the normal conditions comparison.

### **4.3 Proteomics**

The purpose of proteomics was to determine what proteins were most differentially regulated when comparing the wild-type W83 to V0214 (designated as S1) under normal and iron-deficient conditions. Figure 17 shows there is no clear visual shift in protein band appearance between the two strains.

Proteomic studies were attempted on three separate occasions. Out of the three biological replicates, only one data set came back from the VCU Mass Spectrometry Core with usable results. Conclusions for full proteomic analysis are limited due to the lack of biological replicates.

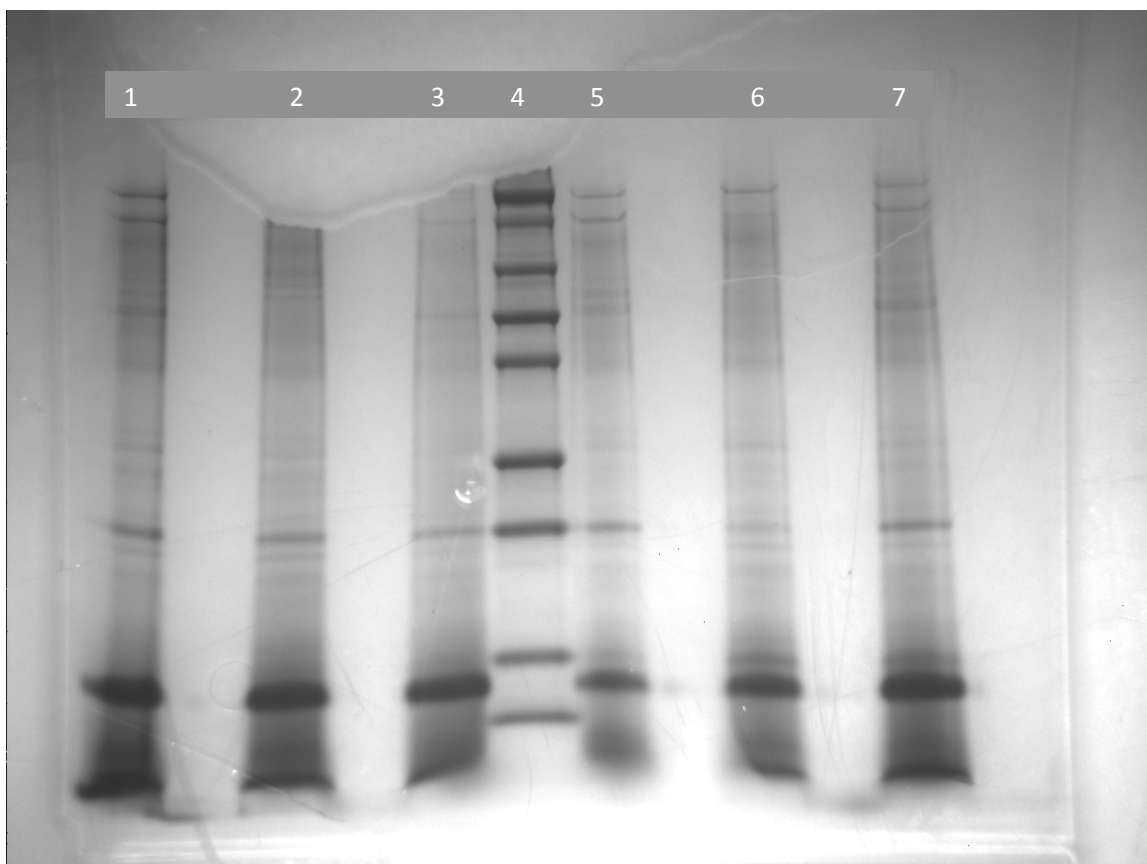


**Figure 15. Denaturing gel for protein band and sample quality confirmation.**

Following proteomics preparation, samples were run on a 12% Bis-Tris protein gel for visual confirmation. Denaturing gels were used to observe the fractionation of proteins following acetone precipitation and urea lysis steps. This gel was a test to observe any band variation between using the acetone precipitation technique mentioned previously or going straight to the resuspension in 6M Urea step. Lane 1: wild-type W83; Lane 2: W83 with acetone precipitation technique; Lane 3: W83 without acetone precipitation; Lane 4: 8 $\mu$ L Protein ladder; Lane 5: W83+DP; Lane 6: W83+DP with acetone precipitation technique; Lane 7: W83 without acetone precipitation.

The denaturing protein gel shown in figure 15 depicts sufficient levels of protein were present to move on with mass spec analysis and that there was little notable difference between techniques.

		Gene Name <sup>1</sup>	Gene ID <sup>2</sup>	Mol. Weight <sup>3</sup>	Sample ID <sup>4</sup>				
		Probability Legend:			S1+	S1-	W83+	W83-	
		<div style="background-color: #90EE90; width: 20px; height: 10px; margin-bottom: 2px;"></div> over 95% <div style="background-color: #FFD700; width: 20px; height: 10px; margin-bottom: 2px;"></div> 80% to 94% <div style="background-color: #FFA500; width: 20px; height: 10px; margin-bottom: 2px;"></div> 50% to 79% <div style="background-color: #FF6347; width: 20px; height: 10px; margin-bottom: 2px;"></div> 20% to 49% <div style="background-color: #FFFFFF; width: 20px; height: 10px; margin-bottom: 2px;"></div> 0% to 19%	Accession Number	Molecular Weight	Protein Grouping Ambiguity				
#	Visible? Starred?	Bio View: 100 Proteins in 98 Clusters				KD3-318-4	KD3-318-3	KD3-318-2	KD3-318-1
1	<input checked="" type="checkbox"/>	4-hydroxybutyryl-CoA dehydratase (abfD) {Porphyromonas gingivalis W83}	PG_0692	54 kDa		14	22	17	31
2	<input checked="" type="checkbox"/>	ribosomal protein L7-L12 (rplL) {Porphyromonas gingivalis W83}	PG_0393	13 kDa		6	5	2	7
3	<input checked="" type="checkbox"/>	glutamate dehydrogenase, NAD-specific (gdh) {Porphyromonas gingivalis W83}	PG_1232	49 kDa		4	21	9	23
4	<input checked="" type="checkbox"/>	translation elongation factor Tu (tuf) {Porphyromonas gingivalis W83}	PG_0387	?		4	8	3	13
5	<input checked="" type="checkbox"/>	ribosomal protein S16 (rpsP) {Porphyromonas gingivalis W83}	PG_2117	21 kDa		3	5		7
6	<input checked="" type="checkbox"/>	acyl carrier protein (acpP) {Porphyromonas gingivalis W83}	PG_1765	9 kDa		3	3	2	4
7	<input checked="" type="checkbox"/>	branched-chain amino acid aminotransferase (ilvE) {Porphyromonas gingivalis W83}	PG_1290	38 kDa		2	7	1	4
8	<input checked="" type="checkbox"/>	phosphoserine aminotransferase (serC) {Porphyromonas gingivalis W83}	PG_1278	40 kDa		2	10	1	8
9	<input checked="" type="checkbox"/>	translation elongation factor Ts (tsf) {Porphyromonas gingivalis W83}	PG_0378	30 kDa		2	4	0	0
10	<input checked="" type="checkbox"/>	DNA-binding protein HU (hup-1) {Porphyromonas gingivalis W83}	PG_0121	9 kDa		2	2	1	3
11	<input checked="" type="checkbox"/>	thioredoxin (trx) {Porphyromonas gingivalis W83}	PG_0034	11 kDa		2	3		1
12	<input checked="" type="checkbox"/>	glutamine-dependent NAD+ synthetase (nadE) {Porphyromonas gingivalis W83}	PG_0531	73 kDa		2	0		1
13	<input checked="" type="checkbox"/>	RNA polymerase sigma-70 factor, ECF subfamily {Porphyromonas gingivalis W83}	PG_1827	25 kDa		2			
14	<input checked="" type="checkbox"/>	ribosomal protein S13 (rpsM) {Porphyromonas gingivalis W83}	PG_1914	14 kDa		2			
15	<input checked="" type="checkbox"/>	translation initiation factor IF-2 (infB) {Porphyromonas gingivalis W83}	PG_0255	108 k...		1	0		2

1. Gene Name according to JVICI (Formerly TIGR)
2. GENE ID according to JVICI (Formerly TIGR)
3. Mol Weight = Molecular weight of the protein in kilodaltons
4. Sample ID = shows number of protein hits for each sample, S1 depicts mutant V0214 strain, W83 depicts the wild-type W83, +/- indicates the addition of iron chelator with + indicating iron-deficient environment and - indicating normal environment

**Figure 16. Protein ID results for W83 and V0214 under normal and iron-deficient conditions.**

This chart depicts the 15 most regulated proteins by W83 and V0214 strains in normal and iron-deficient conditions. The gene name and gene IDs are according to JVICI. The Mol. Weight indicates the molecular weight of the protein. The sample IDs indicate the strains used for this study and are designated as W83 for the wild-type, S1 for the V0214 mutant, and +/- indicating the addition or lack of of 2,2,-dipyridyl.

The comparison of the proteomic profiles in figure 16 between the wild-type W83 and the mutant V0214 strains in normal and iron-deficient conditions yielded limited results. Of these results, the most regulated proteins for this comparison were found to be: PG0692, AbfD, which is a 4-hydroxybutyryl-CoA dehydratase; PG0393, RpIL, a ribosomal protein L7-L12; PG1232, Gdh, a glutamate dehydrogenase NAD-specific protein; and PG2117, Tuf, a translation elongation factor Tu protein.

### **Aim 3**

#### **4.4 Interaction and Invasion of *P. gingivalis* with Eukaryotic Cells**

The third aim of this project was to observe the interaction and invasion of wild-type and mutant strains of *P. gingivalis* with host cells in multiple environmental conditions. The graphs in figures 17-18 depict the total interactions and intracellular invasions of V0214 (designated S1) and wild-type W83 strains into eukaryotic HUVEC cells. The HUVECs were grown to confluency while the V0214 and wild-type W83 were grown from overnight cultures and incubated until they reached mid-logarithmic growth. Half of the samples were treated with DP to create an iron-deficient environment. Cultures were washed, ODs checked, and were added to media containing the HUVEC cells at a MOI of 100:1 (bacteria: host). Antibiotics were added to the invasion samples to inhibit the survival of extracellular bacteria. The mixtures were then incubated and plated at dilutions of 1:100 and 1:1000. Plates were incubated for seven days followed by counting of the colony forming units (CFUs). This experiment was performed in biological triplicate on 5-29 and on 6-19. Figures 17 and 18 depict the average values of the triplicates for the 1:100 dilutions.

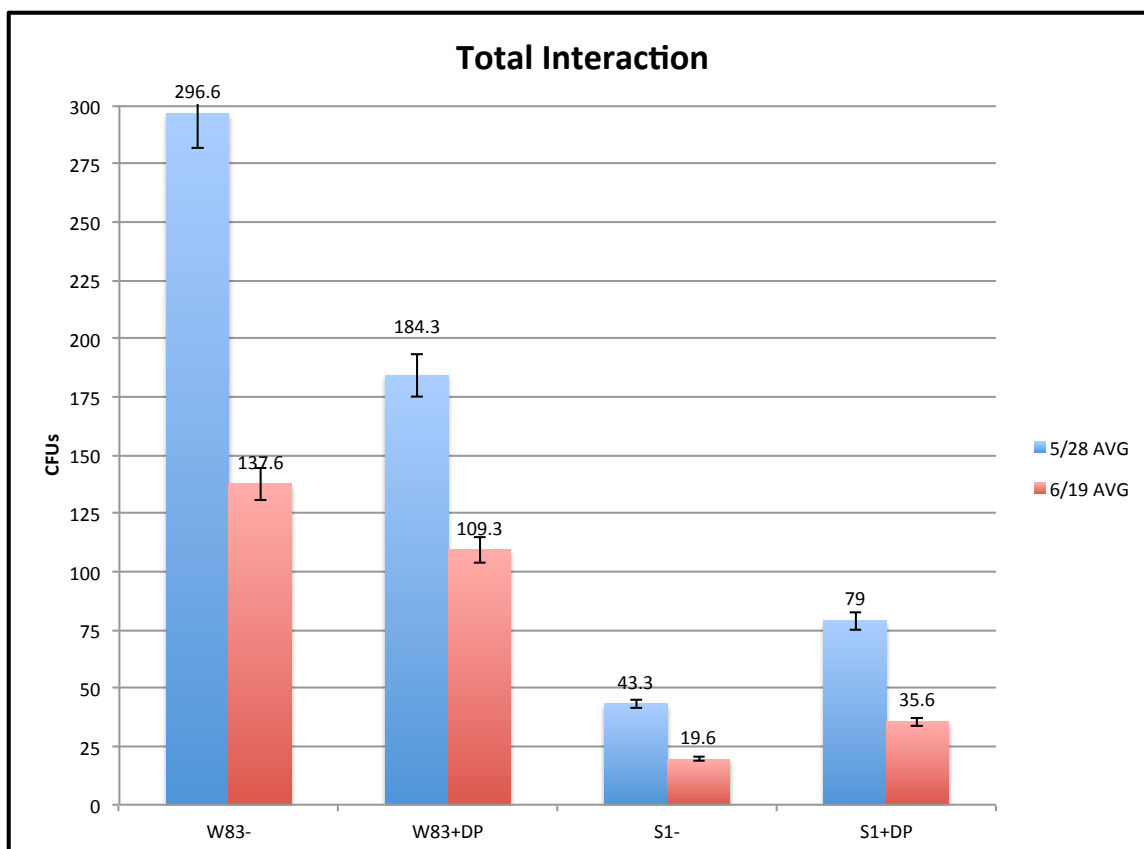


**Figure 17. Interaction of *P. gingivalis* W83 and V0214 Strains Into Eukaryotic HUVEC Cells.**

Colony forming units were counted to quantify the number of total interactions for the wild-type W83 and mutant V0214 strains under normal and iron-deficient conditions. Means and standard deviations for each experiment date are shown.

Analysis showed that the total interactions had 1.6-fold and 1.2-fold decrease comparing W83 to W83+DP (iron deficient) for the 5-28 and 6-19 experiments respectively. Surprisingly the V0214 strain displayed the opposite effect showing a 1.8-fold increase for V0214 under normal conditions versus V0214 in iron deficient conditions for both 5-28 and 6-19 experiments. Under normal conditions, a 6.88-fold and



7.2-fold decrease in CFUs can be seen when comparing W83 to V0214 for the 5-28 and 6-19 experiments respectively. In iron-deficient conditions, a 2.32-fold and 3.1-fold decrease in CFUs can be seen between W83 and V0214 for the 5-28 and 6-19 experiments respectively (Figure 17).

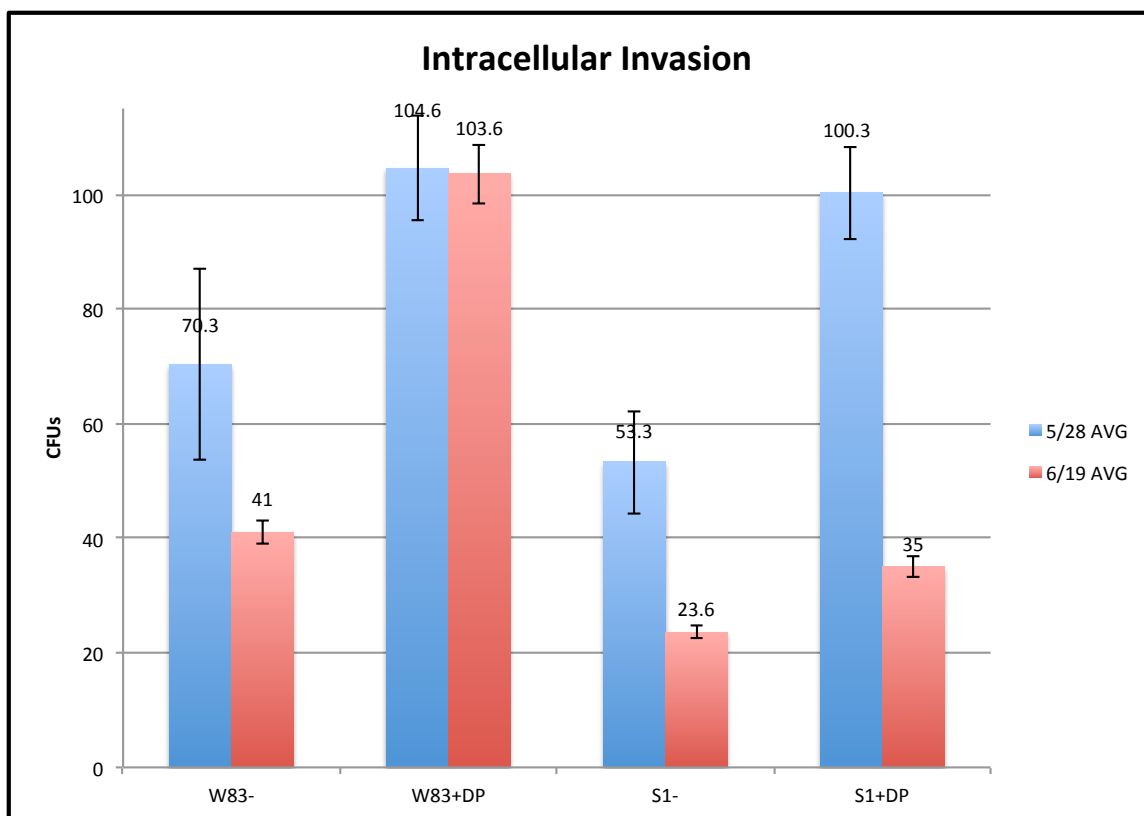


**Figure 18. Invasion of *P. gingivalis* W83 and V0214 Strains Into Eukaryotic HUVEC Cells.**

Colony forming units were counted to quantify the number of total intracellular invasions for the wild-type W83 and mutant V0214 strains under normal and iron-deficient conditions. Means and standard deviations for each experiment date are shown.

Analysis for the intracellular invasion (figure 18) showed a 1.5-fold and 2.5-fold increase in CFUs comparing W83 to W83+DP (iron deficient) for the 5-28 and 6-19 experiments respectively. The V0214 strain followed the same trend exhibiting a 1.8-fold and 1.5-fold increase in CFUs when comparing normal conditions to iron deficient conditions for the 5-28 and 6-19 experiments respectively. Under normal conditions, a 1.3-fold and 1.7-fold decrease in CFUs can be seen when comparing W83 to V0214 for

the 5-28 and 6-19 experiments respectively. In iron-deficient conditions, a 1.04-fold and 1.5-fold decrease in CFUs can be seen between W83 and V0214 for the 5-28 and 6-19 experiments respectively.

#### **Aim 4**

##### **4.5 Arg-X and Lys-X Protease Activity**

The fourth aim of this project was to determine the potential role of PG0214 in response to environmental stress by observing the protease activity. The graphs in figures 19-26 depict the protease activity of Arg-X and Lys-X in PG0214 (designated S1) versus wild-type W83 and wild-type ATCC 33277 (designated 77) in iron-excess and iron-limited conditions as well as anaerobic and microaerobic conditions. Means and standard deviations are shown for each.

In figures 19-22, the chromophore p-nitroaniline was released following the hydrolysis of the substrate DL-BAPNA reflecting the relative arginine protease activity for each sample. Samples begin to plateau at the 20-minute mark (T20) thus OD values at this time mark will be used for comparison.

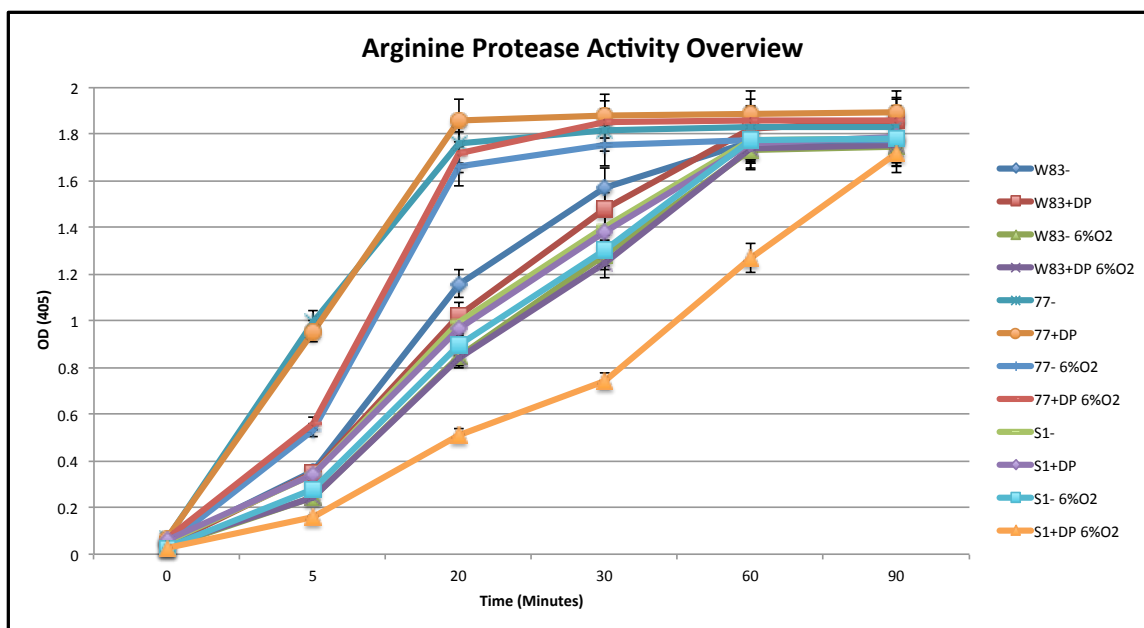


**Figure 19. Arginine Protease Activity Assay.**

Under normal conditions (iron-excess and anaerobic) strain S1 exhibits a 1.59-fold and 1.77-fold decrease in arginine protease activity compared to the wild-types W83 and 77 respectively (figure 19). This overview also shows a general trend that samples grown in iron-excess and oxygen-limited (anaerobic) conditions have increased protease activity versus those grown in iron-limited (+DP) and microaerobic (6% O<sub>2</sub>) conditions.

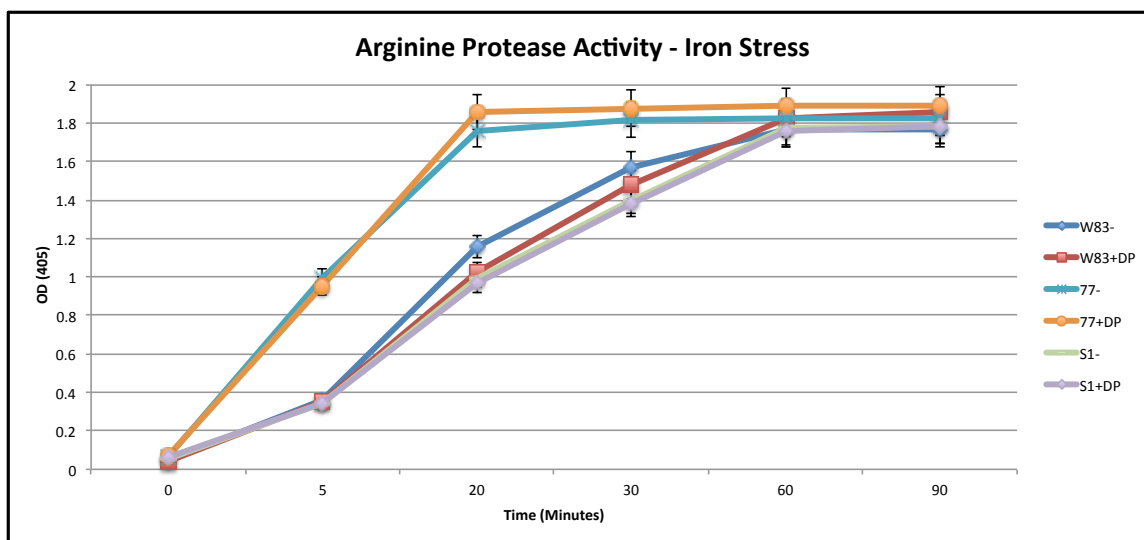


**Figure 20. Arginine Protease Activity Assay, Iron-Stress.**

In figure 20, the relative arginine protease activity is depicted comparing strains grown in iron-excess and iron-limited conditions. At T20 in iron-limited conditions (+DP), strain S1 exhibits a 1.06-fold and 1.92-fold decrease in arginine protease activity versus strains W83 and 77 respectively. Overall in iron-limited conditions, arginine protease activity is decreased for strains W83 and S1 but is increased for strain 77.

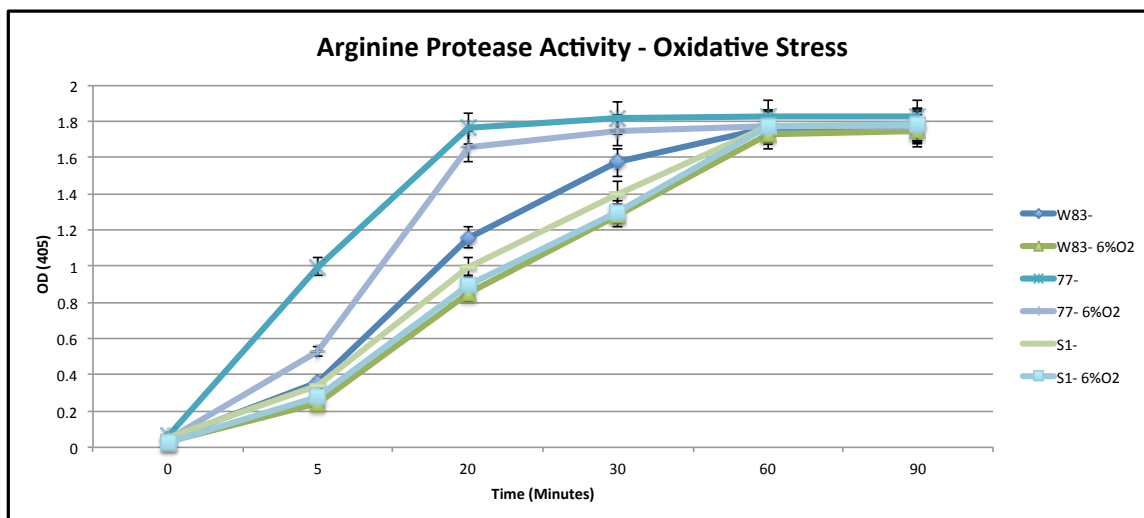


**Figure 21. Arginine Protease Activity Assay, Oxygen-Stress.**

Figure 21 illustrates the relative arginine protease activity for samples grown in anaerobic versus microaerobic conditions. At T20 in microaerobic conditions, strain S1 exhibits a 1.04-fold increase and a 1.85-fold decrease in arginine protease activity versus strains W83 and 77 respectively. Overall all three strains show a trend of increased arginine protease activity in anaerobic conditions versus microaerobic conditions.

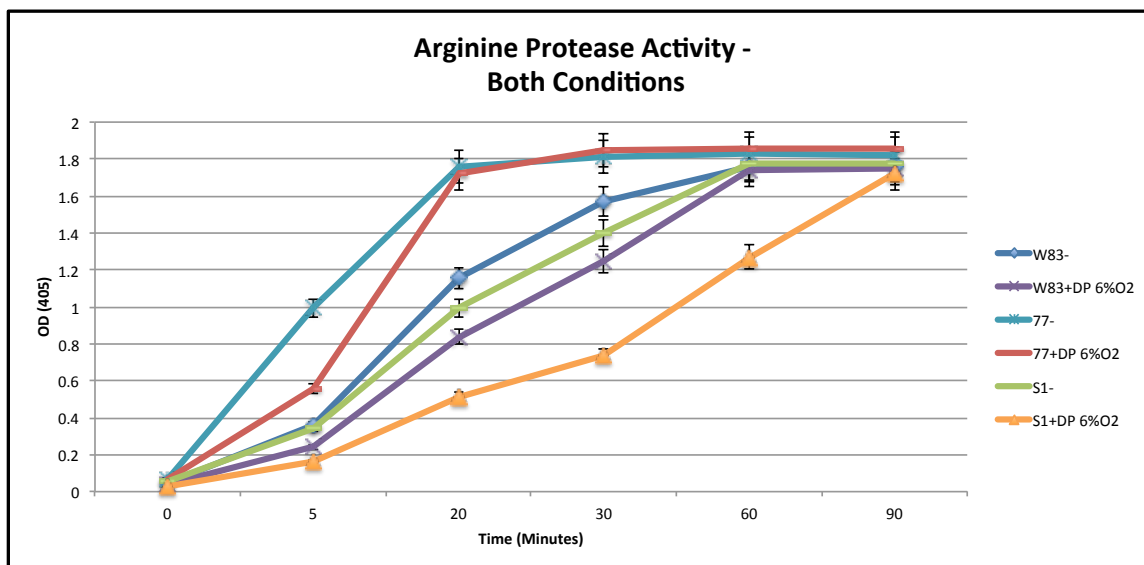


**Figure 22. Arginine Protease Activity Assay, Iron- and Oxygen-Stress.**

Figure 22 illustrates the relative arginine protease activity for samples grown in normal conditions (iron-excess and anaerobic) versus those grown in iron-limited and microaerobic conditions. At T20 in both stress conditions, strain S1 exhibits a 1.64-fold and 3.37-fold decrease in arginine protease activity versus strains W83 and 77 respectively. Overall each strain shows increased protease activity when grown in normal conditions versus iron-limited and microaerobic conditions.

Figures 23-26 depict the protease activity of Lys-X in PG0214 (designated S1) versus wild-type W83 and wild-type ATCC 33277 (designated 77) in iron-excess and iron-limited conditions as well as anaerobic and microaerobic conditions. In these figures, the chromophore p-nitroaniline was released following the hydrolysis of the substrate D-Phe-Pro-Lyz-pNA reflecting the relative lysine protease activity.



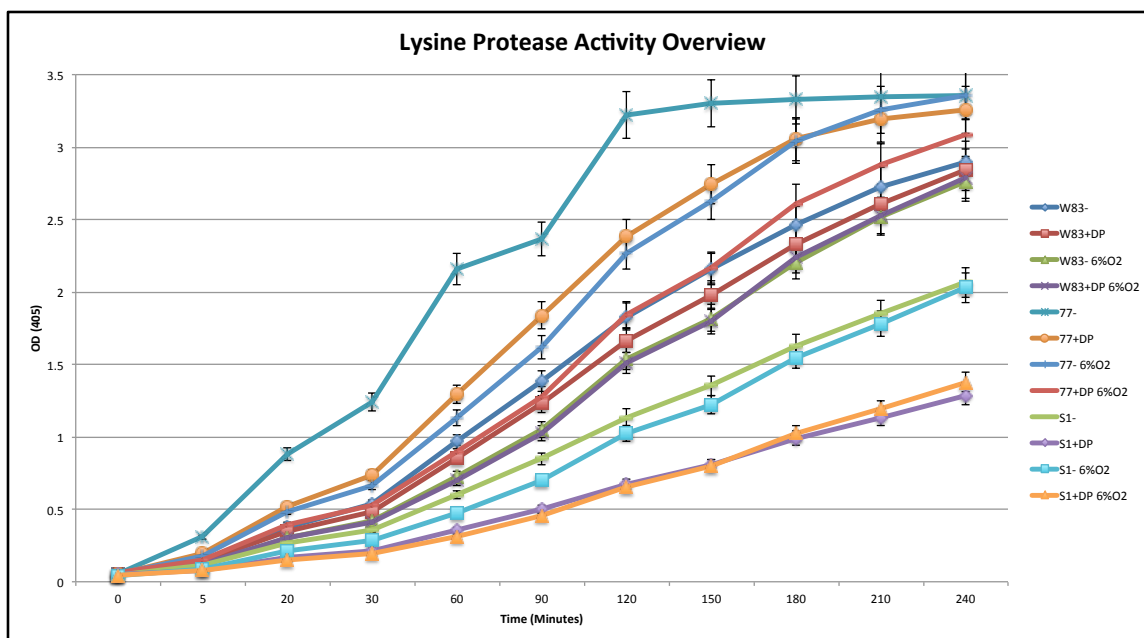


**Figure 23. Lysine Protease Activity Assay.**

In figure 23, an overview of all three strains grown in each condition can be seen. Samples begin to plateau at the 120-minute mark (T120) thus OD values at this time mark will be used for comparison. Under normal conditions (iron-excess and anaerobic) strain S1 exhibits a 1.60-fold and 2.82-fold decrease in lysine protease activity compared to wild-type strains W83 and 77 respectively. This overview figure also illustrates a general trend that samples grown in iron-excess and oxygen-limited (anaerobic) conditions have increased protease activity versus those grown in iron-limited (+DP) and microaerobic (6% O<sub>2</sub>) conditions.

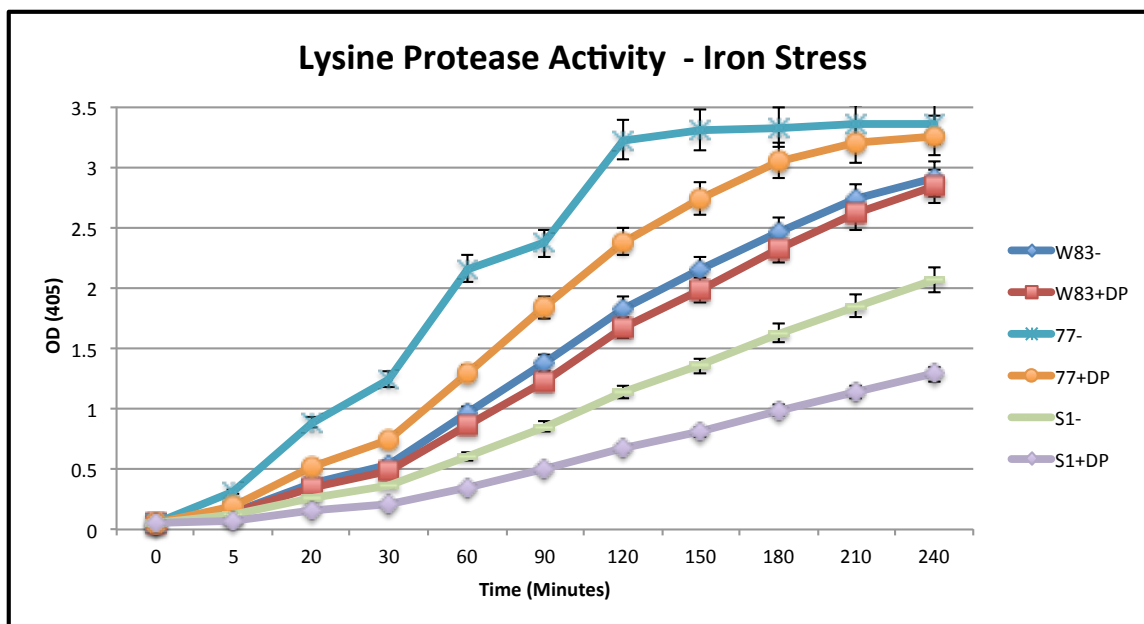


**Figure 24. Lysine Protease Activity Assay, Iron-Stress.**

In figure 24, the relative lysine protease activity is depicted comparing strains grown in iron-excess and iron-limited conditions. At T120 in iron-limited conditions (+DP), strain S1 exhibits a 2.47-fold and 3.55-fold decrease in lysine protease activity versus strains W83 and 77 respectively. Overall in iron-limited conditions, arginine protease activity is decreased for strains S1, W83, and 77 when compared to normal conditions.

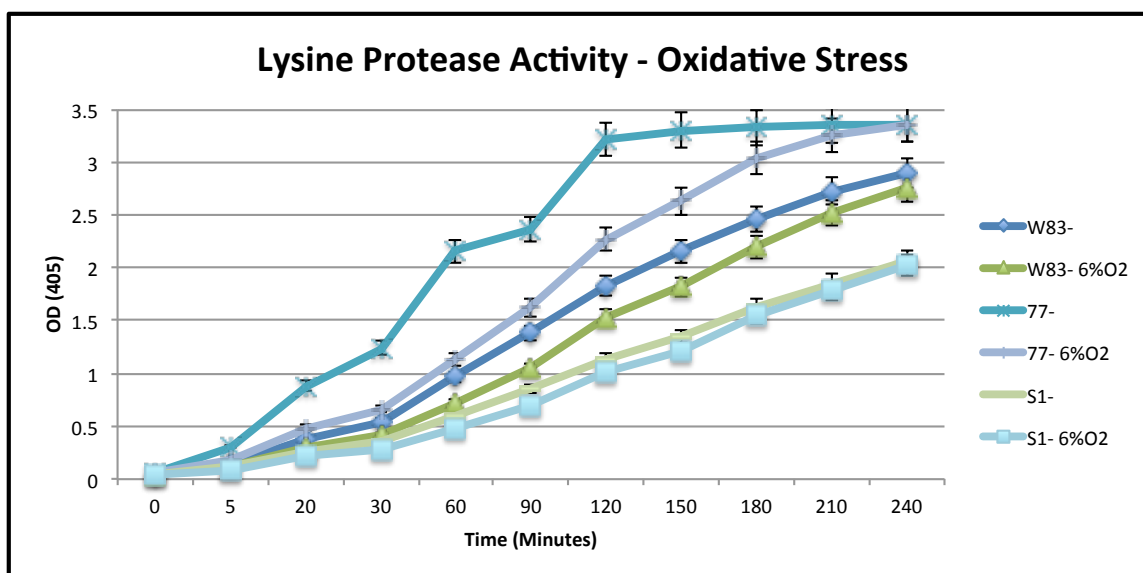


**Figure 25. Lysine Protease Activity Assay, Oxygen-Stress.**

Figure 25 illustrates the relative lysine protease activity for samples grown in anaerobic versus microaerobic conditions. At T120 in microaerobic conditions, strain S1 exhibits a 1.51-fold and a 2.23-fold decrease in lysine protease activity versus strains W83 and 77 respectively. Overall all three strains show a trend of increased lysine protease activity in anaerobic conditions versus microaerobic conditions.

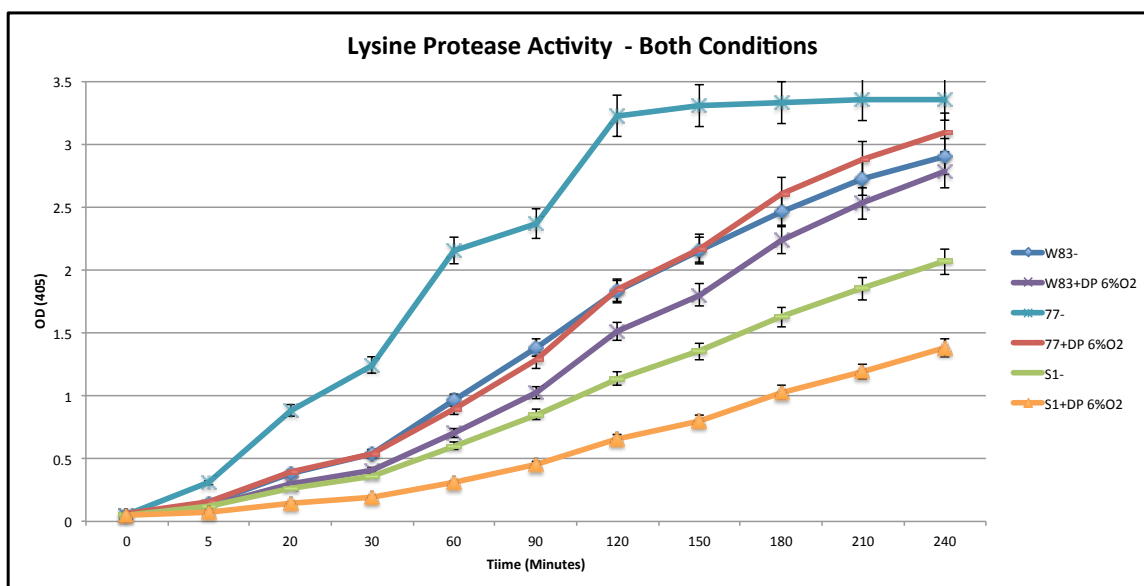


**Figure 26. Lysine Protease Activity Assay, Iron- and Oxygen-Stress.**

Figure 26 illustrates the relative lysine protease activity for samples grown in normal conditions (iron-excess and anaerobic) versus those grown in iron-limited and microaerobic conditions. At T120 in both stress conditions, strain S1 exhibits a 2.32-fold and 2.83-fold decrease in lysine protease activity versus strains W83 and 77 respectively. Overall each strain shows increased protease activity when grown in normal conditions versus iron-limited and microaerobic conditions.

Finally, lysine protease activity is significantly higher than arginine protease activity across all strains grown under either iron- and/or oxygen-stress conditions.

## CHAPTER 5: DISCUSSION

Bacterial response and adaptation to environmental stress is known to be mostly regulated at the level of transcription initiation (Dou et al., 2010). This gene regulation mainly involves alternative sigma factors, which recruit RNA polymerase and facilitate specific promoter recognition and transcription initiation (Paget and Helmann, 2003). The largest group of alternative sigma factors, known as extracytoplasmic function (ECF) sigma factors, plays a key role in bacterial response to environmental conditions as well as regulation of virulence factors (Staron et al., 2009).

Due to the ever-changing environment of the oral cavity, inhabitants like *Porphyromonas gingivalis* must possess the ability to adapt to changes in environmental conditions like pH, temperature, oxygen tension, and metal concentration. This ability to adjust is largely due to the presence of sigma factors, like the  $\sigma^{70}$ , extracytoplasmic function sigma factor (ECF- $\sigma$ ). The *P. gingivalis* W83 genome encodes around eight putative sigma factors; PG0162 (SigG), PG0194 (PG0214), PG0536 (RpoD), PG0879.1 (sigma-24 factor), PG0984 (RpoN), PG1158, PG1449 (SigG), and PG1827 (SigH), six of which belong to the extracytoplasmic function subfamily (Lewis, 2010 and Dou et al., 2010). Previous work from our lab, and others, has been done to characterize several of these genes, however little is known about the PG0194 (PG0214) sigma factor. Our goal was to analyze a PG0214-deficient strain of *Porphyromonas gingivalis* W83 (V0214) and observe its importance for survival of the bacteria as well as its response to changes in environmental conditions such as iron and oxygen.

In order to determine the effect of environmental stress on the various wild-type strains of *P. gingivalis*, high-throughput multiplex sequencing was performed on RNA isolated from strains grown under iron- and oxidative-stress conditions. RNA sequencing techniques have been used to generate and compare the transcriptomes of various bacterial species as well as explore biodiversity among oral species (Diaz et al., 2002). The database for annotation, visualization, and integrated discovery (DAVID) was used for sequencing analysis and to formulate functional annotation clustering. Using these functional clusters, we were able to see the most enriched functional groups for each comparison. Based on the gene hits and enrichment scores, pathways were created using the Kyoto encyclopedia of genes and genomes pathway database, known as KEGG.

The first aim of this project was to identify the changes in the transcriptome of *P. gingivalis* in response to environmental stress. For this aim the wild-type W83 and ATCC 33277 strains were grown in oxygen- and iron- stress conditions. The iron-stress condition was created by adding 2,2-dipyridil (DP), a high-affinity iron chelator, to cultures. DP limits the available extracellular iron for transport in the cell, and thus mimics an iron-deficient environment. Previous work from our lab on the iron- and hemin-dependent gene expression of *Porphyromonas gingivalis* used similar methods of whole-genome microarrays to compare the levels of gene expression in iron-replete and iron-depleted conditions (Anaya-Bergman *et al.*, 2015). This study found the *hmu* locus, and *tla*, *iht*, and *feoB1* genes to be drastically up-regulated in iron-depleted conditions. Our comparison of W83 in normal and iron-deficient conditions similarly exhibited two genes that showed highly altered expression; *hmuY* and *hmuR*, both of which play a major role in the hemin acquisition in *P. gingivalis* as shown by Lewis *et al.* (2006).

These results support the findings of Anaya-Bergman *et al.* (2015) that showed the *hmu* locus to be significantly up-regulated in *Porphyromonas gingivalis* grown in the presence of iron-stress. The iron-stress comparison for W83 also resulted in gene clusters mostly relating Ribosome, RNA binding, and translation at an enrichment score (ES) of 3.31 and DNA repair, cellular response to stress, and response to DNA damage at an enrichment score of 0.51. A KEGG ribosomal pathway was created for this comparison as it matched eleven of the fifty-seven genes in this pathway found in *P.gingivalis* W83. Similar to the W83 comparison, the ATCC 33277 strain comparison of normal and iron-deficient conditions also found *hmuY*, the *tonB*-dependent receptor gene that is essential for regulating the transport, binding, and uptake of hemin, to be highly regulated (Lewis *et al.*, 2006). The functional clustering for this condition exhibited the most affected groups to be DNA integration, metal-binding, and ATP/nucleotide-binding at enrichment scores of 2.33, 2.1, and 1.07 respectively. Similar to the W83 comparison, the ATCC 33277 comparison exhibited functional clusters such as DNA damage and repair at an enrichment score of 0.97. A KEGG thiamine metabolism pathway was created as all seven *P.gingivalis* genes found in the pathway were affected by iron-stress. Taken together these results reaffirm that iron is an essential nutrient for *P. gingivalis* that is acquired with the expression of *hmuY* and *hmuR* genes. Additionally, when the bacteria's ability to acquire iron is impaired, important processes like DNA repair as well as ribosomal and thiamine metabolism pathways are affected.

The next comparison was for oxidative-stress conditions in W83 and ATCC 33277. This stress condition was simulated by growing cultures in a 6 % O<sub>2</sub> atmosphere. A recent study by Lewis *et al.* (2009) involving the adaptation of *P. gingivalis* to

microaerobic conditions provides a basis of gene regulation using whole-genome microarrays for W83 in normal and microaerobic conditions. This study found genes encoding proteins involved in oxidative stress protection to be upregulated, including superoxide dismutase (*sodB*). Other genes up-regulated were those encoding proteins involved in mediating oxidative metabolism (*cydA and cydB*), as well as manganese transporter genes *feoB1* and *feoB2* (Lewis *et al.*, 2009). Our results also found the *sodB* and *feoB1* genes to be highly upregulated in the presence of oxygen for the W83 and ATCC 33277 comparisons. The W83 comparison found *cydA* and *cydB* to be highly upregulated, but these were not found in the ATCC 33277 comparison. This may be due to differing gene profiles of the strains, but could also be due to experimental error.

Affected gene clusters for W83 include Acyl-CoA dehydrogenase activity (ES1.29), cellular homeostasis processing (ES1.1), FAD and oxidoreductase (ES1.05), and ribosome (ES0.9). A KEGG ribosomal pathway was created as eight of the fifty-seven pathway genes found in *P.gingivalis* matched our data set of differentially regulated genes. The ATCC 33277 oxygen-stress comparison resulted in functional clusters relating to the ribosome and RNA binding (ES2.43), DNA integration (ES2.25), signal peptides (ES2.25), and DNA damage/ repair (ES0.92). A KEGG ribosomal pathway was created as thirty-three of the fifty-seven genes found in *P.g.* matched our data set of differentially regulated genes. Our gene regulation results for W83 are concurrent with the previous studies in our lab, and provide a view of similarities and differences between two wild-type strains of *P. gingivalis*, although further analysis is needed. Overall these results show that oxidative-stress causes a disruption in vital genes and functional groups, particularly the ribosomal pathway, which may negatively alter translational processes.



The second aim of this project was to analyze the PG0214 gene in response to environmental stress conditions. In order to better understand the role of the PG0214 gene in survival and adaptation we employed a variety of bioinformatic and sequence homology tools. Using databases like Oralgen and the bioinformatics resource for oral pathogens (BROP) we were able to find what is known about our gene of interest. Basic local alignment search tool (BLAST) was used to compare PG0214 against similar genes among different bacterial species. The BLAST analysis confirmed that the gene belongs to the RNA polymerase sigma ( $\sigma$ ) factor 70 family and that residues 14-161 share a 32% and 31% sequence similarity to an extracytoplasmic function alternative sigma factor in *Mycobacterium smegmatis* and *Mycobacterium avium* respectively. This analysis also identified a paralog of PG0214, found in *P. gingivalis*. This paralog, PG1449, designated SigG or SigW is a predicted RNA polymerase sigma factor subfamily gene, which further confirms PG0214 as an ECF- $\sigma$  gene. BLAST analysis also helped place PG0214 into regions 2 and 4 of the sigma factor 70 family (<http://blast.ncbi.nlm.nih.gov/Blast.cgi>). These regions are responsible for binding to the core RNA polymerase complex, recognition of the -10 and -35 promoter, and promoter melting (Paget and Helmann, 2003). These tools helped to verify PG0214 as an extracytoplasmic function sigma factor and place it in the sigma 70 family.

The next part of this aim was to identify the changes in the transcriptome of *P. gingivalis* in response to environmental stress. Since ECF sigma factor genes have been shown to be up-regulated in the presence of oxidative-stress we wanted to compare the transcriptomes of our sigma factor knockout mutant to wild-type W83 under stress. For this aim we compared wild-type W83 to the mutant PG0214 strain (V0214) grown in the

iron- and oxygen-stress conditions mentioned previously. The same high-throughput sequencing, clustering analysis, and KEGG pathway formation techniques mentioned above were performed for these comparisons. For the comparison of W83 to V0214 under normal conditions, several ribosomal genes were highly up-regulated. Functional clustering identified DNA integration (ES2.57), ribosome and translation (ES2.38), and biotin metabolism (ES0.83) as highly affected gene groups. A KEGG ribosomal pathway was created as thirty-five of the *P. gingivalis* genes found in this pathway matched our data set of differentially regulated genes. These results suggest that the PG0214 gene has a broad effect on various bacterial processes, but mostly affect the ribosome under normal conditions. Next, we compared W83 to V0214 in iron-deficient conditions (+DP). This comparison resulted in up-regulation of genes coding for ribosomal proteins (PG1710), DNA damage-inducible proteins (*dinF*), and ferrous iron acquisition proteins (*feoB1*). The most highly affected functional gene groups were found to be DNA binding, replication, repair, and transposition (ES2.96); coenzyme biosynthetic and metabolic processes (ES0.95); and acetyltransferase activity (ES0.92). These results show that the PG0214 gene likely plays a role in iron and nutrient acquisition and that an inhibited ability to uptake iron negatively impacts vital DNA processes. The next comparison was between W83 and V0214 in oxidative-stress conditions. Genes encoding ABC transporters and ATP-binding proteins (PG0496 and PG0844) were highly up-regulated while genes encoding rRNA (PG5SA-D) were highly down-regulated, contrary to the normal condition comparison. These results are similar to the findings of Lewis *et al.* (2009) that showed PG0258, an ABC transporter and ATP-binding encoding gene to be up-regulated in *Porphyromonas gingivalis* W83 grown in the presence of oxygen. The

most affected functional gene clusters for this comparison were DNA integration (ES3.96), DNA binding and recombination (ES2.44), and ubiquinone and other terpenoid-quinone biosynthesis (ES0.96). A KEGG ubiquinone and other terpenoid-quinone biosynthesis pathway was created as six of the genes found in *P.g.* matched our data set. Since reactive oxygen species have been shown to cause damage to cell membranes, nucleic acids, and proteins, the affected functional gene groups are not surprising (Imlay, J 2003). Several studies analyzing the growth of sigma factor deficient mutants of W83 in response to oxidative stress showed retarded growth among mutant strains when compared to the wild-type (Dou et al., 2010 and Yanamandra et al., 2012). Together with these findings, our results indicate that the PG0214 gene may play a role in the bacterial adaptation and resistance to oxidative stress, highlighting electron carriers for oxidative phosphorylation as the most affected processes. The final comparison used for this aim was W83 and V0214 grown under both iron- and oxygen-stress conditions. This comparison did not yield any statistically relevant functional clusters but did show a one gene match between our data set and the genes found in *Porphyromonas gingivalis* on the KEGG ribosomal pathway. Altogether the results for the W83 and V0214 transcriptome comparisons provide insight into which functional gene groups and pathways are most affected by environmental stress and offer a basis for the role of PG0214 in adaptive response and stress resistance, however further analysis is needed.

Proteomic studies were performed in order to determine which proteins were differentially regulated between the W83 and V0214 strains under normal and iron-deficient conditions. Proteomic experiments were performed on three separate occasions; however, of the three biological replicates only one data set came back from the VCU

Mass Spectrometry Core Lab with usable results. Of these results, the most regulated proteins for this comparison were found to be: PG0692, AbfD, which is a 4-hydroxybutyryl-CoA dehydratase; PG0393, RpIL, a ribosomal protein L7-L12; PG1232, Gdh, a glutamate dehydrogenase NAD-specific protein; and PG2117, Tuf, a translation elongation factor Tu protein. Conclusions for full proteomic analysis are limited due to quality of the results and the lack of biological replicates. Further proteomic studies should be performed with V0214 and compared to RNA sequencing results in order to bridge the gap between the transcriptional regulation and translational effects of the gene.

The next aim of this project was to observe the interaction and intracellular invasion efficiency of the wild-type W83 and mutant V0214 strains with host cells in various environmental conditions. This aim was addressed by performing an antibiotic protection assay on the two strains under normal and iron-deficient conditions. Bacteria was inoculated and combined with human umbilical vein endothelial cells (HUVEC) at an MOI of 100:1 (bacteria:host). Cultures were diluted, plated and colony forming units (CFUs) were counted to determine the total interaction, or number of bacteria that attach to and invade the endothelial cells, as well as the intracellular invasion of host endothelial cells. Results comparing normal and iron-deficient conditions exhibited a 1.2 and 1.6-fold decrease in total interactions for W83 and a 1.8-fold increase for the V0214 strain. Under normal conditions, a 6.88 and 7.2-fold decrease in CFUs can be seen when comparing the W83 to the V0214 strain. In Iron-deficient conditions a 2.32 and 3.1-fold decrease was observed between the W83 and V0214 strains.

Results for the intracellular invasion exhibited a 1.5 and 2.5 fold increase when comparing W83 under normal and iron-deficient conditions. Similarly, the V0214 strain

exhibited a 1.8 and 1.5-fold increase when compared under normal and iron-deficient conditions. Under normal conditions, a 1.3 and 1.7-fold decrease in CFUs was seen when comparing W83 to V0214. In iron-deficient conditions, a 1.04 and 1.5 fold decrease in CFUs was seen between the W83 and V0214 strains. The invasion results indicate that the wild-type strain invades better than the mutant and both strains have more successful invasion rates when grown under stress. These findings suggest the PG0214 gene may play a role in the invasion ability of *P. gingivalis* and that the bacterium may regulate gene pathways for invasion in order to survive in less than ideal conditions.

Altogether the results for total interaction and intracellular invasion were mostly as expected. Previous studies have shown higher interaction and survival rates for *P. gingivalis* grown in iron-stress conditions when compared to normal conditions (Anaya-Bergman *et al.*, 2015). Another comparable study from our lab looking at the interaction and invasion of a sigma factor gene (*sigH*) -deficient strain, resulted in 75% fewer colonies for interaction and 50% fewer colonies for invasion in the mutant strain when compared to the wild-type W83 (Yanamandra *et al.*, 2012). Similarly, our results demonstrated the wild-type samples to have many more CFUs than the V0214 strain under each condition and comparison. Samples grown in iron-deficient environment had a lower interaction rate in W83 but higher for V0214 when compared to normal conditions. Survival was notable higher for both strains in the iron-deficient conditions compared to normal conditions. The findings of Anaya-Bergman *et al.* (2015) also showed increased survival for *P. gingivalis* W83 grown in iron-stress conditions. Taken together these findings suggest the PG0214 gene plays a role in extracellular iron

acquisition in *P. gingivalis*, and without the gene, virulence processes for host cell interaction and invasion are more regulated, likely to enhance survival and gather iron by other means from the endothelial cells. While further work is needed to confirm this hypothesis, these results illustrate that the mutant has a reduced ability to survive inside and outside of the cell compared to the wild-type, suggesting the PG0214 gene may contribute to bacterial virulence and survival in this model.

The final aim of this project was to determine the potential role of PG0214 in response to environmental stress by observing the arginine and lysine protease activity. Three biological replicates of arginine- and lysine-specific assays were performed under normal, iron-deficient, and oxidative-stress conditions. For the arginine protease assay comparing normal and iron-stress conditions, several observations can be made. The first is that samples grown in the iron-deficient conditions had a lower overall protease activity than their normal condition counterparts, with the exception of the ATCC 33277 strain. The ATCC 33277 strain exhibited markedly higher arginine protease activity than the other two strains for either condition. In oxygen-stress conditions the three strains followed a similar trend. Each strain exhibited a higher protease activity when grown in normal conditions than its oxygen-stress counterpart. This supports the findings of Lewis *et al.* (2015) that *P. gingivalis* grown in oxidative-stress has reduced protease activity. When grown under both iron- and oxygen-stress conditions the three strains showed lower protease activity than their normal condition counterparts. Lysine-specific protease activity was also analyzed. Each comparison for this assay resulted in similar findings between the three strains. The ATCC 33277 strain showed a higher protease activity than the W83 and V0214 strains, with V0214 having the lowest lysine protease activity.

Additionally, samples grown under stress conditions; including iron-stress, oxygen-stress, as well as both stress conditions together, exhibited lower overall protease activity than their normal condition counterpart.

Overall the results for arginine and lysine protease activity were as expected. Samples show a general trend of higher activity when grown in ideal conditions than when grown under stress. The V0214 strain exhibited the lowest protease activity of the strains in each of the assays, reinforcing the findings of Dou *et al.*, (2006). Gingipain proteases are important virulence factors of *P. gingivalis* that have been shown to be essential for growth and to play a role in oxidative stress resistance (Sheets *et al.*, 2008). Specifically, the Lys-X (Lys-gingipain) and Arg-X (Arg-gingipain) cysteine proteases of *P. gingivalis* have been shown to bind and degrade erythrocytes, indicating their importance in iron acquisition processes of the bacteria (Lewis *et al.*, 1999). When taken together, our results suggest that the PG0214 gene may be involved in the post-transcriptional regulation of the Arg-X and Lys-X gingipain proteases, and thus may play a role in *P. gingivalis*' ability to acquire iron. These experiments provide a general understanding of the effect of the PG0214 gene on protease activity between *P. gingivalis* strains, however further work is needed to determine how these factors may be modulated by the gene.

## Conclusion

The results found in this project provide insight into the effect of environmental stress on several strains of *Porphyromonas gingivalis*. Results across all studies show that the wild-type strains of *P. gingivalis* have higher protease activity, survivability, and invasion potential than the PG0214-deficient strain, V0214, especially when responding to environmental stress. This suggests the PG0214 gene is important for adaptation to changes in the environment and for the virulence potential of the bacteria. The findings from RNA sequencing and proteomic studies show that there are many important functional gene clusters, pathways, and proteins affected between the mutant and wild-type strains. The most affected genes, clusters, and pathways across all conditions were related to ribosomal processes, signifying the importance this pathway for environmental stress adaptation of the bacteria. While these results do not provide a complete characterization of the gene of interest, many important bioinformatics and molecular techniques were learned in our attempt to identify the biological function of the bacterial gene.

Growing and passaging anaerobic bacteria and eukaryotic cells is an essential technique used in molecular biology that was utilized in this study. Additionally, using databases like Oralgen, DAVID, and KEGG we were able to identify functionally related genes, use bioinformatics software to generate functional gene clusters, and convert those clusters into visual pathways for analysis and interpretation. Proteomic, RNA isolation, and RNA sequencing techniques allowed us to observe changes in gene expression of the bacteria at transcriptional and translational levels. Antibiotic protection assays provided a



view of the interaction and invasion potential of the mutant V0214 strain, demonstrating the influence of the gene on survival and virulence factors in *P. gingivalis*. Our work has demonstrated that the PG0214 gene is a positive regulator of gene expression for the survival of the bacterium in the presence of oxidative- and iron-stress and virulence. Overall, our studies shed light on the potential roles of PG0214 in environmental stress responses as well as host cell colonization, however further work and analysis is needed in order to fully characterize this gene and determine its specific function.

### Literature Cited

1. Anaya-Bergman C, Rosato A, Lewis JP. Iron- and hemin-dependent gene expression of *Porphyromonas gingivalis*. *Molecular Oral Microbiology*. 2015;30:39-61.
2. Aruni, A, Y Dou, H Fletcher. The Biofilm Community-Rebels with a Cause. *Curr Oral Health Rep*. 2015; 2(1):48-56.
3. Bashyam MD, Hasnain SE. The extracytoplasmic function sigma factors: role in bacterial pathogenesis *Infect Genet Evol*. 2004;4:301-308.
4. Bostanci N, Belibasakis GN. *Porphyromonas gingivalis*: an invasive and evasive opportunistic oral pathogen *FEMS Microbiol Lett*. 2012;333:1-9.
5. Bramanti TE, Holt SC. Roles of porphyrins and host iron transport proteins in regulation of growth of *Porphyromonas gingivalis* W50 *J Bacteriol*. 1991;173:7330-7339.
6. Brooks BE, Buchanan SK. Signaling mechanisms for activation of extracytoplasmic function (ECF) sigma factors *Biochim Biophys Acta*. 2008;1778:1930-1945.
7. Coats SR, Do CT, Karimi-Naser LM, Braham PH, Darveau RP. Antagonistic lipopolysaccharides block E. coli lipopolysaccharide function at human TLR4 via interaction with the human MD-2 lipopolysaccharide binding site *Cell Microbiol*. 2007;9:1191-1202.

8. Dahlen G, Manji F, Baelum V, Fejerskov O. Putative periodontopathogens in "diseased" and "non-diseased" persons exhibiting poor oral hygiene *J Clin Periodontol.* 1992;19:35-42.
9. Darveau RP. Periodontitis: a polymicrobial disruption of host homeostasis *Nat Rev Microbiol.* 2010;8:481-490.
10. Darveau RP, Hsujishengallis G, Curtis M. *Porphyromonas gingivalis* as a Potential Community Activist for Disease. *J Dent Res.* 2012;91(9): 816-820.
11. Darveau RP, Pham TT, Lemley K, et al. *Porphyromonas gingivalis* lipopolysaccharide contains multiple lipid A species that functionally interact with both toll-like receptors 2 and 4 *Infect Immun.* 2004;72:5041-5051.
12. Dashper SG, Hendtlass A, Slakeski N, et al. Characterization of a novel outer membrane hemin-binding protein of *Porphyromonas gingivalis* *J Bacteriol.* 2000;182:6456-6462.
13. d'Empaire G, Baer MT, Gibson FC,3rd. The K1 serotype capsular polysaccharide of *Porphyromonas gingivalis* elicits chemokine production from murine macrophages that facilitates cell migration *Infect Immun.* 2006;74:6236-6243.
14. Diaz PI, Dupuy AK, Abusleme L, et al. Using high throughput sequencing to explore the biodiversity in oral bacterial communities *Mol Oral Microbiol.* 2012;27:182-201.
15. Diaz PI, Rogers AH. The effect of oxygen on the growth and physiology of *Porphyromonas gingivalis.* *Oral Microbiol Immunol.* 2004;19:88-94.

16. Dou Y, W Aruni, A Multhiah, F Roy, C Wang, H Fletcher. Studies of the extracytoplasmic function sigma factor PG0162 in *Porphyromonas gingivalis*. *Molecular Oral Microbiology*. 2015;10: 1111-1212.
17. Dou Y, Osbourne D, McKenzie R, Fletcher HM. Involvement of extracytoplasmic function sigma factors in virulence regulation in *Porphyromonas gingivalis* W83. *FEMS Microbiol Lett*. 2010;312:24-32.
18. Eke PI, Dye BA, Wei L, Thornton-Evans GO, Genco RJ. Prevalence of Periodontitis in Adults in the United States: 2009 and 2010 *J Dent Res*. 2012; 2012;91:914-920.
19. Evans RT, Klausen B, Sojar HT, et al. Immunization with *Porphyromonas (Bacteroides) gingivalis* fimbriae protects against periodontal destruction *Infect Immun*. 1992;60:2926-2935.
20. Hajishengallis G, Lamont RJ. Breaking bad: manipulation of the host response by *Porphyromonas gingivalis* *Eur J Immunol*. 2014;44:328-338.
21. Hajishengallis G, Liang S, Payne MA, et al. Low-abundance biofilm species orchestrates inflammatory periodontal disease through the commensal microbiota and complement *Cell Host Microbe*. 2011;10:497-506.
22. Heitz-Mayfield LJ. Disease progression: identification of high-risk groups and individuals for periodontitis *J Clin Periodontol*. 2005;32 Suppl 6:196-209.
23. Helmann JD. The extracytoplasmic function (ECF) sigma factors *Adv Microb Physiol*. 2002;46:47-110.

24. Henry LG, McKenzie RM, Robles A, Fletcher HM. Oxidative stress resistance in *Porphyromonas gingivalis* *Future Microbiol.* 2012;7:497-512.
25. Imlay JA. Pathways of oxidative damage. *Annu Rev Microbiol.* 2003; 57: 395-418.
26. Jandik KA, Belanger M, Low SL, Dorn BR, Yang MC, Progulsk-Fox A. Invasive differences among *Porphyromonas gingivalis* strains from healthy and diseased periodontal sites *J Periodontal Res.* 2008;43:524-530.
27. Jenkins S, Addy M, Wade W. The mechanism of action of chlorhexidine. A study of plaque growth on enamel inserts in vivo *J Clin Periodontol.* 1988;15:415-424.
28. Ji S, Kim Y, Min BM, Han SH, Choi Y. Innate immune responses of gingival epithelial cells to nonperiodontopathic and periodontopathic bacteria *J Periodontal Res.* 2007;42:503-510.
29. Kassebaum NJ, Bernabe E, Dahiya M, Bhandari B, Murray CJ, Marcenes W. Global burden of severe periodontitis in 1990-2010: a systematic review and meta-regression *J Dent Res.* 2014;93:1045-1053.
30. Kazmierczak MJ, Wiedmann M, Boor KJ. Alternative Sigma Factors and Their Roles in Bacterial Virulence *Microbiology and Molecular Biology Reviews.* 2005; 2005;69:527-543.
31. Kolenbrander PE, Andersen RN, Blehert DS, Eglund PG, Foster JS, Palmer RJ. Communication among Oral Bacteria *Microbiology and Molecular Biology Reviews.* 2002;66:486-505.

32. Laheij, A, C van Loveren, D Deng and J Johannes. The impact of virulence factors of *Porphyromonas gingivalis* on wound healing in vitro. *Journal of Oral Microbiology*. 2015;7: 27543.
33. Laine ML, van Winkelhoff AJ. Virulence of six capsular serotypes of *Porphyromonas gingivalis* in a mouse model *Oral Microbiol Immunol*. 1998;13:322-325.
34. Lamont R, Jenkinson H. Life Below the Gum Line: Pathogenic Mechanisms of *Porphyromonas gingivalis*. *Microbiol Mol Bio Rev*. 1998. 62: 1244-1263.
35. Lamont RJ, Jenkinson HF. Subgingival colonization by *Porphyromonas gingivalis* *Oral Microbiol Immunol*. 2000;15:341-349.
36. Lamont RJ, Yilmaz O. In or out: the invasiveness of oral bacteria *Periodontol 2000*. 2002. 30:61-69.
37. Lepine G, Progulske-Fox A. Duplication and differential expression of hemagglutinin genes in *Porphyromonas gingivalis* *Oral Microbiol Immunol*. 1996;11:65-78.
38. Lewis JP. Metal uptake in host-pathogen interactions: role of iron in *Porphyromonas gingivalis* interactions with host organisms *Periodontol 2000*. 2010;52:94-116.
39. Lewis JP, Dawson J, Hannis J, Muddiman D, Macrina F. Hemoglobinase activity of the lysine gingipane protease (Kgp) of *Porphyromonas gingivalis* W83. *J. Bacteriol*. 1999; 181(16): 4905-4913.

40. Lewis JP, Iyer D, Anaya-Bergman C. Adaptation of *Porphyromonas gingivalis* to microaerophilic conditions involves increased consumption of formate and reduced utilization of lactate. *Microbiology*. 2009;155:3758-3774.
41. Lewis JP, Plata K, Yu F, Rosato A, Anaya C. Transcriptional organization, regulation and role of the *Porphyromonas gingivalis* W83 hmu haemin-uptake locus *Microbiology*. 2006;152:3367-3382.
42. Li N, Collyer CA. Gingipains from *Porphyromonas gingivalis* - Complex domain structures confer diverse functions *Eur J Microbiol Immunol (Bp)*. 2011;1:41-58.
43. Loesche, W. Microbiology of Dental Decay and Periodontal Disease. *Medical Microbiology*. 1996; 99.
44. Marsh PD. Microbial ecology of dental plaque and its significance in health and disease *Adv Dent Res*. 1994;8:263-271.
45. Moore WE, Moore LV. The bacteria of periodontal diseases *Periodontol 2000*. 1994;5:66-77.
46. Murakami KS, Darst SA. Bacterial RNA polymerases: the whole story *Curr Opin Struct Biol*. 2003;13:31-39.
47. Mysak J, Podzimek S, Sommerova P, et al. *Porphyromonas gingivalis*: major periodontopathic pathogen overview *J Immunol Res*. 2014;2014:476068.

48. Nelson KE, Fleischmann RD, DeBoy RT, et al. Complete genome sequence of the oral pathogenic Bacterium *Porphyromonas gingivalis* strain W83 *J Bacteriol.* 2003;185:5591-5601.
49. Nishida E, Hara Y, Kaneko T, Ikeda Y, Ukai T, Kato I. Bone resorption and local interleukin-1alpha and interleukin-1beta synthesis induced by *Actinobacillus actinomycetemcomitans* and *Porphyromonas gingivalis* lipopolysaccharide *J Periodontal Res.* 2001;36:1-8.
50. Ohara N, Kikuchi Y, Shoji M, Naito M, Nakayama K. Superoxide dismutase-encoding gene of the obligate anaerobe *Porphyromonas gingivalis* is regulated by the redox-sensing transcription activator OxyR *Microbiology.* 2006;152:955-966.
51. Onozawa S, Kikuchi Y, Shibayama K, et al. Role of extracytoplasmic function sigma factors in biofilm formation of *Porphyromonas gingivalis* *BMC Oral Health.* 2015;15:4-6831-15-4.
52. Paget MS. Bacterial Sigma Factors and Anti-Sigma Factors: Structure, Function and Distribution *Biomolecules.* 2015;5:1245-1265.
53. Paget MS, Helmann JD. The sigma70 family of sigma factors *Genome Biol.* 2003;4:203.
54. Potempa J, Pike R, Travis J. Titration and mapping of the active site of cysteine proteinases from *Porphyromonas gingivalis* (gingipains) using peptidyl chloromethanes *Biol Chem.* 1997;378:223-230.



55. Seymour GJ, Ford PJ, Cullinan MP, Leishman S, Yamazaki K. Relationship between periodontal infections and systemic disease *Clinical Microbiology and Infection*. 2007;13:3-10.
56. Sheets SM, Robles-Price AG, McKenzie RM, Casiano CA, Fletcher HM. Gingipain-dependent interactions with their host are important for survival of *Porphyromonas gingivalis*. *Front Biosci*. 2008; 13: 3215-3238.
57. Shi B, Chang M, Martin J, et al. Dynamic changes in the subgingival microbiome and their potential for diagnosis and prognosis of periodontitis *MBio*. 2015;6:e01926-14.
58. Singh A, Wyant T, Anaya-Bergman C, et al. The capsule of *Porphyromonas gingivalis* leads to a reduction in the host inflammatory response, evasion of phagocytosis, and increase in virulence *Infect Immun*. 2011;79:4533-4542.
59. Slakeski N, Dashper SG, Cook P, Poon C, Moore C, Reynolds EC. A *Porphyromonas gingivalis* genetic locus encoding a heme transport system *Oral Microbiol Immunol*. 2000;15:388-392.
60. Socransky SS, Haffajee AD, Cugini MA, Smith C, Kent RL, Jr. Microbial complexes in subgingival plaque *J Clin Periodontol*. 1998;25:134-144.
61. Staron A, Sofia HJ, Dietrich S, Ulrich LE, Liesegang H, Mascher T. The third pillar of bacterial signal transduction: classification of the extracytoplasmic function (ECF) sigma factor protein family *Mol Microbiol*. 2009;74:557-581.

62. Stoodley P, Sauer K, Davies DG, Costerton JW. Biofilms as complex differentiated communities *Annu Rev Microbiol.* 2002;56:187-209.
63. Strand KR, Sun C, Li T, Jenney FE, Jr, Schut GJ, Adams MW. Oxidative stress protection and the repair response to hydrogen peroxide in the hyperthermophilic archaeon *Pyrococcus furiosus* and in related species *Arch Microbiol.* 2010;192:447-459.
64. Sundqvist G, Figdor D, Hanstrom L, Sorlin S, Sandstrom G. Phagocytosis and virulence of different strains of *Porphyromonas gingivalis* *Scand J Dent Res.* 1991;99:117-129.
65. Tazaki K, Inoshita E, Amano A, Hanioka T, Tamagawa H, Shizukuishi S. Interaction of *Porphyromonas gingivalis* with transferrin *FEMS Microbiol Lett.* 1995;131:161-166.
66. Tribble GD, Kerr JE, Wang BY. Genetic diversity in the oral pathogen *Porphyromonas gingivalis*: molecular mechanisms and biological consequences *Future Microbiol.* 2013;8:607-620.
67. Wang M, Shakhatreh MA, James D, et al. Fimbrial proteins of *Porphyromonas gingivalis* mediate in vivo virulence and exploit TLR2 and complement receptor 3 to persist in macrophages *J Immunol.* 2007;179:2349-2358.
68. Yanamandra SS, Sarrafee SS, Anaya-Bergman C, Jones K, Lewis JP. Role of the *Porphyromonas gingivalis* extracytoplasmic function sigma factor, SigH *Mol Oral Microbiol.* 2012;27:202-219.

69. Yang HW, Huang YF, Chou MY. Occurrence of *Porphyromonas gingivalis* and *Tannerella forsythensis* in periodontally diseased and healthy subjects *J Periodontol*. 2004;75:1077-1083.
70. Yilmaz O, Yao L, Maeda K, et al. ATP scavenging by the intracellular pathogen *Porphyromonas gingivalis* inhibits P2X7-mediated host-cell apoptosis *Cell Microbiol*. 2008;10:863-875.
71. Yost S, Duran-Pinedo AE, Teles R, Krishnan K, Frias-Lopez J. Functional signatures of oral dysbiosis during periodontitis progression revealed by microbial metatranscriptome analysis *Genome Med*. 2015;7:27-015-0153-3.

## Permissions for figures



RightsLink®

Home

Create Account

Help



AMERICAN  
SOCIETY FOR  
MICROBIOLOGY

**Title:** Communication among Oral Bacteria  
**Author:** Paul E. Kolenbrander, Roxanna N. Andersen, David S. Blehert et al.  
**Publication:** Microbiology and Molecular Biology Reviews  
**Publisher:** American Society for Microbiology  
**Date:** Sep 1, 2002

Copyright © 2002, American Society for Microbiology

LOGIN

If you're a [copyright.com user](#), you can login to RightsLink using your copyright.com credentials. Already a [RightsLink user](#) or want to [learn more?](#)

### Permissions Request

ASM authorizes an advanced degree candidate to republish the requested material in his/her doctoral thesis or dissertation. If your thesis, or dissertation, is to be published commercially, then you must reapply for permission.

BACK

CLOSE WINDOW

Copyright © 2015 [Copyright Clearance Center, Inc.](#) All Rights Reserved. [Privacy statement.](#) [Terms and Conditions.](#) Comments? We would like to hear from you. E-mail us at [customercare@copyright.com](mailto:customercare@copyright.com)



RightsLink®

Home

Create Account

Help



AMERICAN  
SOCIETY FOR  
MICROBIOLOGY

**Title:** Life Below the Gum Line:  
Pathogenic Mechanisms  
of Porphyromonas gingivalis

**Author:** Richard J. Lamont, Howard F.  
Jenkinson

**Publication:** Microbiology and Molecular  
Biology Reviews

**Publisher:** American Society for Microbiology

**Date:** Dec 1, 1998

Copyright © 1998, American Society for Microbiology

LOGIN

If you're a [copyright.com user](#), you can login to RightsLink using your copyright.com credentials. Already a [RightsLink user](#) or want to [learn more?](#)

### Permissions Request

ASM authorizes an advanced degree candidate to republish the requested material in his/her doctoral thesis or dissertation. If your thesis, or dissertation, is to be published commercially, then you must reapply for permission.

BACK

CLOSE WINDOW

Copyright © 2015 [Copyright Clearance Center, Inc.](#) All Rights Reserved. [Privacy statement.](#) [Terms and Conditions.](#) Comments? We would like to hear from you. E-mail us at [customercare@copyright.com](mailto:customercare@copyright.com)



RightsLink®

Home

Create Account

Help



AMERICAN  
SOCIETY FOR  
MICROBIOLOGY

**Title:** Life Below the Gum Line:  
Pathogenic Mechanisms  
of Porphyromonas gingivalis

**Author:** Richard J. Lamont, Howard F.  
Jenkinson

**Publication:** Microbiology and Molecular  
Biology Reviews

**Publisher:** American Society for Microbiology

**Date:** Dec 1, 1998

Copyright © 1998, American Society for Microbiology

LOGIN

If you're a [copyright.com user](#), you can login to RightsLink using your copyright.com credentials. Already a [RightsLink user](#) or want to [learn more?](#)

### Permissions Request

ASM authorizes an advanced degree candidate to republish the requested material in his/her doctoral thesis or dissertation. If your thesis, or dissertation, is to be published commercially, then you must reapply for permission.

BACK

CLOSE WINDOW

Copyright © 2015 [Copyright Clearance Center, Inc.](#) All Rights Reserved. [Privacy statement.](#) [Terms and Conditions.](#) Comments? We would like to hear from you. E-mail us at [customercare@copyright.com](mailto:customercare@copyright.com)

**JOHN WILEY AND SONS LICENSE  
TERMS AND CONDITIONS**

Dec 01, 2015

---

This Agreement between David Smith ("You") and John Wiley and Sons ("John Wiley and Sons") consists of your license details and the terms and conditions provided by John Wiley and Sons and Copyright Clearance Center.

License Number	3760270700097
License date	Dec 01, 2015
Licensed Content Publisher	John Wiley and Sons
Licensed Content Publication	Periodontology 2000
Licensed Content Title	Metal uptake in host-pathogen interactions: role of iron in Porphyromonas gingivalis interactions with host organisms
Licensed Content Author	Janina P. Lewis
Licensed Content Date	Dec 11, 2009
Pages	23
Type of use	Dissertation/Thesis
Requestor type	University/Academic
Format	Print and electronic
Portion	Figure/table
Number of figures/tables	1

[Print This Page](#)

Dear David

Thank you for your request.

Permission is granted for you to use the material requested for your thesis/dissertation subject to the usual acknowledgements (author, title of material, title of book/journal, ourselves as publisher) and on the understanding that you will reapply for permission if you wish to distribute or publish your thesis/dissertation commercially. You must also duplicate the copyright notice that appears in the Wiley publication in your use of the Material; this can be found on the copyright page if the material is a book or within the article if it is a journal.

Permission is granted solely for use in conjunction with the thesis, and the material may not be posted online separately.

Any third party material is expressly excluded from this permission. If any of the material you wish to use appears within our work with credit to another source, authorisation from that source must be obtained.

Best wishes,

Rebecca Cook

Permissions Assistant

John Wiley & Sons Ltd

The Atrium

Southern Gate, Chichester

West Sussex, PO19 8SQ

UK

**From:** David Smith [mailto:[smithdm28@mymail.vcu.edu](mailto:smithdm28@mymail.vcu.edu)]

**Sent:** 01 December 2015 16:50

**To:** Wiley Global Permissions

**Subject:** figure permission

Hello,

I would like to request permission to use a figure for the introduction section of my masters thesis. It is on the role of sigma factors in *Porphyromonas gingivalis* and the response to environmental stress. The thesis will be used for academic purposed only and will be published in our university library archives at Virginia Commonwealth University. The figure I would like to use is Figure 1. in Chandrangs, Pete, and Helmann, John D(Mar 2014) Sigma Factors in Gene Expression. In: eLS. John Wiley &



Sons Ltd, Chichester. <http://www.els.net> [doi: 10.1002/9780470015902.a0000854.pub3].  
I will cite properly in my thesis to give the proper credit to the authors. Please let me know if this would be possible. Thanks and have a great day!

Best,

David

## **Vita**

David Michael Smith was born in Forest, Virginia. After completing his schoolwork at Virginia Episcopal School in Lynchburg, Virginia in 2007, David entered Christopher Newport University in Newport News, Virginia. He received a Bachelor of Science in Biology from Christopher Newport University in 2011. After college, David attended Virginia Commonwealth University in Richmond, Virginia for the Pre-medical Graduate Health Sciences Certificate program. Following the program, in August of 2013 David entered the Physiology and Biophysics graduate program at Virginia Commonwealth University.